

**Impact of increased atmospheric CO₂
concentration on photosynthesis, growth and
productivity in a field grown tree species,
Gmelina arborea Roxb.**

*A thesis submitted to the University of Hyderabad
for the award of a Ph.D. degree in
Plant Sciences*

By

Girish Kumar R



Department of Plant Sciences
School of Life Science
University of Hyderabad
Hyderabad-500 046
India.

Regd. No: 05LPPH08
November 2010



University of Hyderabad
School of Life Sciences
Department of Plant Sciences
Hyderabad-500 046

DECLARATION

I, Girish Kumar R, hereby declare that this thesis entitled “**Impact of increased atmospheric CO₂ concentration on photosynthesis, growth and productivity in a field grown tree species, *Gmelina arborea* Roxb.**” submitted by me under the guidance and supervision of Professor Attipalli R. Reddy is an original and independent research work. I also declare that it has not been submitted previously in part or in full to this University or any other University or Institution for the award of any degree or diploma.

Date:

Name: Girish Kumar R

Signature:

Regd. No.: 05LPPH08



University of Hyderabad
School of Life Sciences
Department of Plant Sciences
Hyderabad-500 046

CERTIFICATE

This is to certify that this thesis entitled “**Impact of increased atmospheric CO₂ concentration on photosynthesis, growth and productivity in a field grown tree species, *Gmelina arborea* Roxb.**” is a record of bonafide work done by Mr. Girish Kumar R, a research scholar for Ph.D. programme in Plant Sciences, Department of Plant Sciences, School of Life Sciences, University of Hyderabad under my guidance and supervision. The thesis has not been submitted previously in part or in full to this or any other University or Institution for the award of any degree or diploma.

Professor Attipalli R. Reddy
(Supervisor)

(Head of the Department)

(Dean of the School)

*This thesis is dedicated to my parents and brother
Hari, for their love, endless support
and encouragement.*

ACKNOWLEDGEMENTS

I owe a deep sense of gratitude towards my research supervisor **Professor Attipalli R. Reddy**, for providing me the opportunity to work under his invaluable guidance and for his constant encouragement, support and helping attitude.

My sincere thanks to **Prof. Atipalli R. Reddy**, Head, Department of Plant Sciences and **Prof. M. Ramanadham**, Dean, School of Life Sciences, for providing the facilities necessary for my research. In this regard I would also like to thank former Heads **Prof. P. B. Kirti**, **Prof. Appa Rao Podile** and former Dean **Prof. A. S. Raghavendra**.

I am grateful to **Prof. A.S. Raghavendra** and **Dr. K.P.M.S.V. Padmasri**, Doctoral committee members for their valuable suggestions and kind help.

I am thankful to **Prof. A.S. Raghavendra**, **Prof. S. Dayananda** and **Dr. Rajagopal** for their kind suggestions whenever I approached them with my work problems and for kindly providing their lab facilities to carry out few of my experiments.

My special thanks to **Prof. Prasanna Mohanty** for his kind suggestions and help whenever I approached him.

I am thankful to my former lab mates and seniors **Dr. Sundar**, **Dr. Chaitanya**, **Dr. Pavan**, **Dr. Sumitra**, **Mr. Dalton**, **Dr. Asha**, **Dr. Ramesh** and **Dr. Sreedhar** for their encouraging, helping and caring attitude. My present lab mates **Mr. Chalapathi**, **Mr. Anirban Guha**, **Ms. Debashree**, **Mr. Chaitanya**, **Mr. Madan**, **Ms. Shalini** and **Mr. Sumit** for their kind help and also maintaining a cheerful environment in the laboratory. I specially thank **Mr. Guha** and **Ms. Debashree** for their timely help and support.

I also thank **Mr. David**, **Mr. Jaffer** and **Mrs Vedavathi** for their assistance in admin block works. I am also thankful to **Mr. Pandu**, **Mr. Vinodh** and **Mr. Lakshman** for their assistance in the lab and in maintaining the plants in the field that were regularly needed for my research work.

I am grateful to my friends **Mr. Anumodh**, **Mr. Sreedhar**, **Mr. Balu**, **Mrs. Ratna**, **Mr. Sunil**, **Mr. Uday**, **Mr. Paul**, **Mr. Aravind**, **Mr. Naveen**, **Ms. Sirisha**, **Mr. Harshal**, **Mr. Bhanu** and **Ms. Mahasweta** for being a constant support during my ups and down. Life would not have been this good without them. They always provided a healing touch. I specially thank **Mr. Anumodh** and **Mr. Sreedhar** for readily helping me whenever I am in need.

I am grateful to my brother **Hari** for his ceaseless love, guidance and being my greatest strength and support. My sister in-law for her support and niece **Hariketana** for adding colours to our lives.

I thank **Jalaja madam** and **Latha madam** for their generosity and kindness.

I am thankful to my parents (**Amma**, **Nanna**) for their love, patience, support and absolute confidence in me.

Funding from **CSIR**, **DBT** and **DST** to Prof. Attipalli R. Reddy as well as **DST-FIST**, **DBT** and **UGC** (for funding to Department and School) are acknowledged.

The financial support from **DBT** and **CSIR**, New Delhi for **JRF** and **SRF** is gratefully acknowledged.

Girish Kumar R

ABBREVIATIONS

[CO ₂]	=	Atmospheric CO ₂
2-DE	=	Two- dimensional electrophoresis
ABS/CS _M	=	Absorption flux per excited leaf cross-section
ABS/RC	=	Absorption flux per reaction centre
ACN	=	Acetonitrile
AGR	=	Absolute growth rate
<i>Ca</i>	=	Ambient CO ₂ concentration
CA	=	Carbonic anhydrase
<i>Ci</i>	=	Internal CO ₂ concentration
DI0/ CS _M	=	Dissipated energy flux per excited leaf cross-section
DI0/RC	=	Dissipated energy flux per reaction centre
DTT	=	Dithiotheritol
<i>E</i>	=	Transpiration rates
EDTA	=	Ethylenediaminetetraacetic acid
EGTA	=	Ethylene glycol-bis- (β – aminoethy ether) N, N, N', N' tetra acetic acid
ET0/ CS _M	=	Electron transport flux per excited leaf cross-section
ET0/RC	=	Electron transport flux per reaction centre
F ₀	=	Mimimal florescence
FBPase	=	Fructose 1,6 bisphosphatase
F _m	=	Maximum fluorescence
F _V /F _M or Φ _{P0}	=	Maximum quantum yield of primary photochemistry at t=0
<i>gs</i>	=	Stomatal conductance
HCCA	=	α- cyano-4-hydroxy trans-cinnamic acid
MALDI-TOF-TOF	=	Matrix assisted laser desorption/ionization time of flight
OTC	=	Open top Chambers
PAR	=	Photosynthetic active radiation
PI _{ABS}	=	Performance index on absorption basis
PMF	=	Peptide mass finger printing
<i>Pn</i>	=	Photosynthetic rate

PRUE	=	Photosynthetic radiation use efficiency
PVPP	=	Polyvinylpolypyrrolidone
RC/ABS	=	Density of reaction centres
RHGR	=	Relative height growth rate
Rubisco	=	Ribulose-1,5- biphosphate carboxylase/ oxygenase
RUBP	=	Ribulose-1,5- biphosphate
RUBPcase	=	Ribulose- 1,5- biphosphate carboxylase
SDGR	=	Stem basal diameter growth rate
<i>Sm</i>	=	Multiple turnover Q_A reduction events
SPsynthase	=	Sucrose phosphate synthase
TAGDB	=	Total above ground dry biomass
TAGFB	=	Total above ground fresh biomass
TDB	=	Total dry biomass
TFA	=	Trifluoro acetic acid
TFB	=	Total fresh biomass
TR0/ CS_M	=	Trapped energy flux per excited leaf cross-section
TR0/RC	=	Trapped energy flux per reaction centre
<i>WUE_i</i>	=	Instantaneous water use efficiency
Ψ_o ,	=	The probability at $t=0$ that a trapped exciton moves an electron into the electron transport chain beyond Q_A^-

CONTENTS

Chapter 1. Introduction and Experimental Design

Introduction	1-6
Plant Material and Experimental Design	7-12

Chapter 2. Photosynthetic physiology of *Gmelina* grown under ambient and elevated CO₂ atmosphere

Introduction	13-15
Methods	16-20
Results	21-34
Discussion	35-40

Chapter 3. Studies on biochemical responses of *Gmelina* under ambient and elevated CO₂ atmosphere

Introduction	41-43
Methods	44-48
Results	49-57
Discussion	58-61

Chapter 4. Growth, biomass and carbon sequestration efficacy in *Gmelina* under ambient and elevated CO₂ concentrations

Introduction	62-63
Methods	64-66
Results	67-77
Discussion	78-81

Chapter 5. Foliar proteomic changes in photosynthetic protein profile in response to elevated CO₂ concentrations

Introduction	82-83
Methods	84-86
Results	87-108
Discussion	109-113

Chapter 6. Summary and Conclusions

114-118

Chapter 7. Literature Cited

119-135

Appendix : List of publications

Chapter 1

Introduction and Experimental Design

Chapter 1

Introduction and Experimental Design

Introduction

Climate change is widely recognized as one of the most critical challenges the world has ever faced. Warming of the global climate system is unequivocal, as is now evident from observations of increased average air and ocean temperatures, widespread melting of snow and ice, and rising average sea level (IPCC, 2007). This scenario mainly depends on the concentrations of greenhouse gases (GHG's). GHG's have been injected into the lower atmosphere in increasing amounts through the burning of fossil fuels for industry, transportation, and residential uses. Modern global warming is widely believed to be the result of an increase in magnitude of the greenhouse effect- a warming of earth's surface and lower atmosphere caused by the presence of water vapour, carbon dioxide, methane, and other GHG's. Of all these gases, carbon dioxide (CO₂) is the most important, both for its role in the greenhouse effect and for its role in the human economy. It has been estimated that at the beginning of the industrial age, the concentration of CO₂ in the atmosphere was roughly ~280 $\mu\text{mol mol}^{-1}$. By the end of the twentieth century, the concentration reached ~369 $\mu\text{mol mol}^{-1}$ (possibly the highest concentration in at least 650,000 years) and by the mid-twenty century, if fossil fuels continue to be burned at current rates, it is projected to reach ~560 $\mu\text{mol mol}^{-1}$, essentially a doubling of atmospheric carbon dioxide in 300 years (IPCC, 2007).

Natural sources of atmospheric CO₂ [CO₂] include outgassing (the slow release of absorbed or trapped gases) from volcanoes, the combustion and natural decay of organic matter, and respiration by aerobic organisms. These sources are balanced on an average, by a set of physical, chemical or biological processes called "sinks" that tend to remove CO₂ from the atmosphere.

Significant natural sinks include terrestrial vegetation, which takes up CO₂ through photosynthesis (Prentice *et al.*, 2001; Solomon *et al.*, 2007). Human activities, increasing atmospheric CO₂ levels primarily through the burning of fossil fuels (principally oil and coal, and also natural gas, for use in transportation, heating and the generation of electrical power) and other anthropogenic sources, include the burning of forests and the clearing of land. Anthropogenic emissions currently account for the annual release of about 7 gigatons (7 billion tons) of carbon into the atmosphere (IPCC, 2001). Anthropogenic emissions are equal to approximately 3 percent of the total emissions of CO₂ by natural resources and this amplified carbon load from human activities far exceeds the offsetting capacity of natural sinks (by perhaps as much as 2-3 gigatons per year) (Dyson, 2005). Consequently, CO₂ has accumulated in the atmosphere at an average rate of 1.4 $\mu\text{mol mol}^{-1}$ by volume per year between 1959 and 2009, and this rate of accumulation has been linear. Now the global CO₂ concentration is at 384 $\mu\text{mol mol}^{-1}$, ~40% higher than at any time in the least 20 million years and it is increasing significantly faster than anticipated by the Intergovernmental panel on climate change (IPCC) (Canadell *et al.*, 2007; Leakey *et al.*, 2009).

The drastic increase in [CO₂] has put in question the use of fossil fuels which constitute the most abundant and most reliable energy resource ever known to mankind. There is an urgent need to reduce CO₂ emissions and at the same time have to provide energy sources for the growing energy demand of the world. None of the competing energy resources, including nuclear energy, appear to be in a position to fill the gap should fossil energy consumption need to be substantially reduced. Therefore, meeting the ever growing world demand for cheap energy, while simultaneously achieving the required drastic reduction in CO₂ emissions can only be accomplished by carbon sequestration and energy cropping (Lemus and Lal, 2005).

The Kyoto protocol of 1997 had a focus on reducing carbon dioxide emission and stabilization of [CO₂] by a combination of limitation on the use of fossil fuel and creation of carbon sinks within a specified time frame. CO₂ is constantly exchanged between the atmosphere and terrestrial ecosystems. Vegetation and soils can accumulate carbon and thus can reduce the rate of CO₂ build-up in the atmosphere that is responsible for climate change (Streck and Scholz, 2006). Forest ecosystems contain the majority (approximately 60%) of the carbon stored in terrestrial ecosystems and thus the world's forests sequester and conserve more carbon than all other terrestrial ecosystems and account for 90% of the annual carbon flux between atmosphere and the earth's land surface (Winjum and Lewis, 1993; IPCC, 2000; Streck and Scholz, 2006).

Globally, forest area has been reduced by almost 20 percent in the last 140 years and the greatest sources of forestry-related emissions were clear-cutting and logging in forests accounting to about 20 percent of human-induced emissions (IPCC, 2001). Planting forests (afforestation and reforestation), clearly provide an opportunity to sequester carbon in vegetation and soils. Among the desired means to stabilize the GHG concentrations in the atmosphere at a level that would prevent dangerous anthropogenic interference with the climate system is use of potential sinks to reduce the concentrations of GHG's in the atmosphere (Lemus and Lal, 2005). Afforestation and reforestation are the only means of carbon sequestration under Clean Development Mechanism (CDM) of the Kyoto protocol in developing countries (IPCC, 2001).

Trees have potential to capture and retain large volumes of carbon over long periods as they absorb carbon through photosynthesis process (Gunderson *et al.*, 2002; Long *et al.*, 2004). Young rapidly growing trees can sequester relatively large volumes of additional carbon which is roughly proportional to the tree growth in biomass (Bernacchi *et al.*, 2003). Mature trees acts as a reservoir, holding large volumes of carbon, even if it is not experiencing net growth (Korner *et*

al., 2006). Present estimates indicate that with appropriate policies, the carbon pool in the terrestrial system could increase by up to 100 GtC by the year 2050 compared to the level of carbon that would be sequestered without such policies (IPCC, 2001). This is equivalent to about 10 to 20% of projected GHG emissions from fossil fuel consumption during the same period. Reducing deforestation, expanding forest cover, expanding forest biomass per unit area, and expanding the inventory of long-lived wood products are some of the activities that could help global community from global warming (Streck and Scholz, 2006). Carbon sequestration as a climate change mitigation policy option had received significant attention over the past several years. Planting young fast growing trees species to absorb excess atmospheric CO₂, an idea of carbon offset plantings (Dyson, 1977), has recently gained potentiality leading to identification of tree species with high CO₂ sequestration capacity. In this context, young fast growing tree species could conceptually be considered as terrestrial carbon sinks and hence studies on carbon sequestration potentials of these tree species is of profound significance (Davey *et al.*, 2006).

Many predictions of greater tree productivity with increasing CO₂ depends on a sustained increase in the photosynthetic capacity of leaves (Reynolds *et al.*, 1996; Herrick and Thomas, 2001). Understanding the photosynthetic responses of trees to CO₂-enrichment is essential in assessing the potential of forests to store carbon. Certain C₃ plants were found to show acclimatory down regulation in photosynthesis under elevated CO₂ atmosphere (Long *et al.*, 2004; Uprety *et al.*, 2006). Important factors that led to photosynthetic acclimation were the ability to store carbon in storage pools (Ammerlaan and de Visser, 1993; Schapendonk *et al.*, 2000) and the efficient use of stored carbohydrates as energy source. Light intensity is another important factor in determining whether or not photosynthetic down-regulation to CO₂ will occur, as light attenuation through the canopy plays a strong role in developmental,

morphological, and physiological characteristics of leaves; all have a significant influence on productivity response to climate change.

The initial stimulation of photosynthesis has been predicted to be reduced by direct feedback inhibition due to accumulation of intermediates, by decrease of certain transcripts that encode for ribulose- 1,5 bis phosphate carboxylase/ oxygenase (rubisco; EC 4.1.1.39) and other proteins involved in photosynthesis (Van Oosten and Besford, 1994). Increased levels of soluble sugars have also been shown to down-regulate photosynthetic gene transcription. In addition, factors such as sink strength and carbohydrate accumulation have also been implicated for decreasing photosynthetic potential. Although some studies have shown the tree responses under elevated CO₂ (Liu *et al.*, 2002; Rogers and Ellsworth, 2002; Greenep *et al.*, 2003; Ainsworth and Long, 2005), there is little information on either photosynthetic productivity or expression of photosynthetic proteins in tropical tree species grown under elevated CO₂ atmosphere. With this background we framed the following objectives to investigate the effects of elevated CO₂ on a fast growing tropical tree species, *Gmelina arborea* Roxb.

Objectives of my research

- 1) To study photosynthetic physiology of a fast growing tree species under ambient and elevated CO₂ atmosphere.
- 2) To determine the biochemical responses of the tree species with emphasis on photosynthetic potential under ambient and elevated CO₂ atmosphere.
- 3) To estimate the growth, biomass and carbon sequestration efficacy in the tree species under ambient and elevated CO₂ atmosphere.
- 4) Foliar proteomic changes in photosynthetic protein profile in response to elevated CO₂.

Plant material

***Gmelina arborea* (Roxb.)**

Taxonomy

Gmelina arborea belongs to Kingdom- *Plantae*; Division- *Magnoliophyta*; Class- *Magnoliopsida*; Order- *Lamiales*; Family-*Verbenaceae*; Genus- *Gmelina* and Species-*Gmelina arborea* Roxb.

Common name: Yemane; *Gmelina*; Melina

Description

Gmelina arborea is a tropical deciduous tree which has a very remarkable growth rate. In a reasonably good site, it takes only three years to attain a merchantable timber size of 5.8 m – 8.3 m with 20 cm – 25 cm diameter. The average yield of *Gmelina* is approximately 21m³/ha/yr (Swamy *et al.*, 2003). It is considered a drought and fire resistant species. Leaves are opposite; deciduous; entire and have waxy bloom on the underside.

Economic Uses

Gmelina is primarily used for pulpwood production because of its relatively high yield of kraft pulp and low chlorine requirement. Its wood is sawn for general carpentry, joinery, furniture components, and other household fixtures. The round timbers are used for posts, house timbers and poles while rotary cut veneers are utilized for plywood. It can also be used as fuelwood.

Distribution

Gmelina is native to India, Pakistan, Northern Rhodesia, and Malaysia. It thrives well on sites with an elevation of up to 525 m (1,750 ft) above sea level (MASL). It can tolerate acidic,

calcareous (soil containing sufficient calcium carbonate), and lateritic soil. However, the species prefers loamy, well drained, moderately fertile soil. Vigorous growth can be observed in sites under monsoonal climate with distinct dry period.

Experimental design

Structure of Open-top chambers (OTCs)

The OTCs are of square type structure having 4x4x4m dimension with a closing door facility (Fig.1B). The basic structure of the OTCs was fabricated with galvanized iron (GI) pipe and installed in the botanical gardens of University of Hyderabad, India located between 17.3° 10' N and 78° 23' E at an altitude of 542.6 m above MSL. The OTCs were covered with polycarbonate sheet (Polygal plastic industries Ltd. Israel) of 4 mm thickness and with 90 % transmittance of light. At 3.4 m height of the each chamber a frustum with an angle, 0.6 m towards inside, was maintained to reduce the dilution effect of the air current within the chamber. The upper portion of the chamber was kept open to maintain the near-natural conditions of temperature and relative humidity. OTCs were equipped with temperature and humidity sensors.

CO₂ supply to OTCs and air sampling

The plenum at the base (0.3 m) was provided for carbon dioxide circulation in the OTCs. The 100% CO₂ gas of commercial grade was used to elevate CO₂ levels within the chambers. The normal air from the air compressor was mixed with this pure CO₂ to maintain uniformity of the CO₂ and to dilute the concentration of pure CO₂ to required CO₂ concentration. Two CO₂ gas cylinders of 45 kg capacity each were used and the gas was released to the chambers through manifold fitted with copper tubing. Within each chamber the copper tubing was again fitted with

solenoid valve and rotameters to regulate the gas supply. The air is sampled from the centre point of the chamber through a coiled copper tube.

CO₂ control and monitoring system

The equipment for monitoring and controlling the CO₂ in OTCs is fully automatic and the desired CO₂ level can be maintained throughout the experimental period in the OTCs with the help of this system. The system basically consists of non-dispersion infra ray (NDIR) CO₂ gas analyzer (Fuji Electric systems Co. Ltd., Japan), pumps to draw the sample from OTCs, the valves and meters to control and regulate the CO₂ and air flow, Program Logic Control (PLC) and Supervisory Control And Data Acquisition (SCADA) platform were used for data acquisition.

Plantation and Experimental CO₂ conditions

In each OTC, four *Gmelina* plants were planted in four pits with a spacing of 2x2 m. Plantation was undertaken at the onset of spring (February), saplings were allowed to establish inside the OTCs for 10 days and thereafter, CO₂ pumping was started. The mean CO₂ concentrations in the ambient CO₂ chamber was ~ 360 $\mu\text{mol mol}^{-1}$ and ranged from 340-390 $\mu\text{mol mol}^{-1}$ depending on ambient weather conditions whereas the mean CO₂ concentration in elevated CO₂ chamber was maintained ~ 460 $\mu\text{mol mol}^{-1}$.

Phenology of *Gmelina* and Experimentation

Gmelina has a phenology of a tropical deciduous plant. It starts leaf flushing with the advent of the spring, grows luxuriantly throughout late spring and summer seasons and undergoes senescence in winter. In our experiment, measurements and data collection were confined to

these two marked growth seasons: spring (Feb-April) and summer (May-July) for all the experimental years (2006-2010). Figure 2 illustrates the average climatic conditions of these growth seasons as monitored during the experimentation. The climatic conditions of years 2006, 2007 and 2008 were depicted in the figure 2, whereas the experimental years of 2009 and 2010 also showed almost same pattern. Throughout the experiment, the soil beneath the trees was uniformly maintained in both ambient and elevated CO₂ OTC's at optimum moisture and nutrient levels by means of surface irrigation and organic manure application. All the data were recorded periodically at an interval of 25-30 days.



Fig. 1A *Gmelina arborea* Roxb (Verbenaceae)



Fig. 1B Square type Open Top Chambers (OTC's) with 4 x 4 x 4 m dimensions. The OTC's were covered with polycarbonate sheet and were equipped with temperature, humidity and rainfall sensors. The CO₂ concentration in the ambient CO₂ chamber was ~ 360 $\mu\text{mol mol}^{-1}$ whereas the CO₂ concentration in elevated CO₂ chamber was maintained ~ 460 $\mu\text{mol mol}^{-1}$.

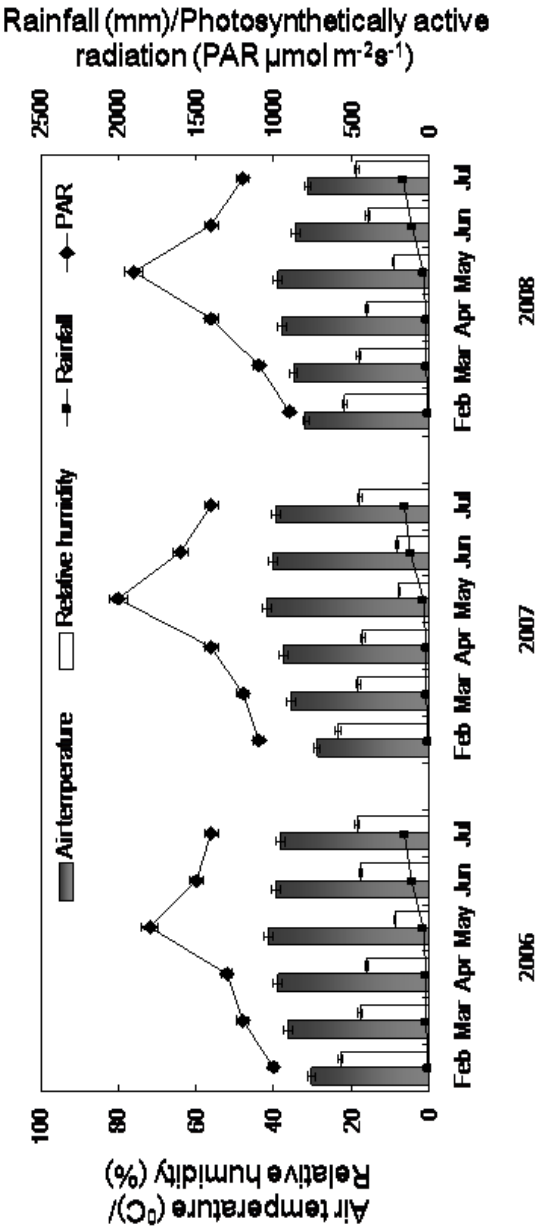


Fig. 2. Monthly averages of air temperature ($^{\circ}\text{C}$), rainfall (mm), relative humidity (%) and photosynthetically active radiation (PAR $\mu\text{mol m}^{-2}\text{s}^{-1}$) at the study site for two growing seasons; spring (Feb-Apr) and summer (May-Jul) during three consecutive years (2006-2008). The same pattern was observed for experimental years 2009 and 2010.

Chapter 2
**Photosynthetic physiology of *Gmelina* grown under
ambient and elevated CO₂ atmosphere**

Chapter 2

Photosynthetic physiology of *Gmelina* grown under ambient and elevated CO₂ atmosphere

Introduction

Trees form a critical component of the global carbon budget accounting for over half of the total net carbon uptake into terrestrial vegetation (Geider *et al.*, 2001). Therefore, it is important to understand how photosynthesis of tree species will respond to changes of CO₂. Photosynthesis is the primary process by which carbon enters into the biosphere and by which plants sense rising atmospheric CO₂ concentrations (Spunda *et al.*, 2005). The current [CO₂] limits the photosynthetic capability, growth and productivity of many plants, among which the C₃ species showed a potential response to rising CO₂ (Upreti *et al.*, 2000; Vu *et al.*, 2001). The initial interaction between a terrestrial plant and atmospheric CO₂ is the diffusion of CO₂ into the sub-stomatal cavity of leaf tissues and its subsequent fixation by carboxylation in the chloroplast stroma (Flexas *et al.*, 2008). Plants are known to sense and respond to rising CO₂ concentrations through increased photosynthesis and reduced stomatal conductance (Upreti *et al.*, 2002; Ainsworth and Rogers, 2007). The exponential increase of CO₂ in the atmosphere should theoretically stimulate photosynthesis due to enhanced rubisco carboxylation and reduction in photorespiration (Long *et al.*, 2004). However, many plant species grown at elevated CO₂ exhibit an acclimatory down regulation, associated with decreased photosynthetic potential (Davey *et al.*, 2006). The photosynthetic down regulation at physiological level are mainly observed due to rise in *C_i*, imbalance in *C_i/C_a* ratio and decrease in stomatal conductance (Long *et al.*, 2004). The decrease in photosynthetic potential in plants has also been attributed to high light-conditions because photosynthetic apparatus exposed to variable photosynthetically active radiation (PAR) may result in a typical photoinhibition of actual CO₂ assimilation (Spunda *et al.*, 2005).

Many predictions of greater productivity with increasing CO₂ depend on a sustained increase in photosynthetic capacity of leaves (Reynolds *et al.*, 1996). Photosynthetic physiology under elevated CO₂ modulates mainly through rise in *C_i*. Stomata respond to rising [CO₂] in-order to maintain a constant *C_i/C_a*, through decreasing the stomatal conductance and causing an offset in photosynthetic rates (Long *et al.*, 2004). High light environments also have significant impact on photosynthetic apparatus in plants. Excess light limits photosynthesis by photoinhibition, resulting in reduced carbon gain and also causing photo-damage (Öquist and Huner, 2003; Pastenes *et al.*, 2003). Plants grown in tropical climate usually experiences significantly high irradiance, leading to strong midday depression of photosynthesis (Hymus *et al.*, 2001; Aranjuelo *et al.*, 2008). Studies on photosynthetic physiology and PSII photochemistry in trees are significant to understand how elevated CO₂ affects plant growth and in-turn carbon sequestration efficacy (Wang *et al.*, 2003).

Chlorophyll *a* fluorescence transients have been widely used to probe the activity and integrity of photosynthetic apparatus. Chl *a* fluorescence of dark adapted leaf follows characteristic changes with time after the onset of illumination, a process popularly known as “Kautsky effect” (Kautsky and Hirsch, 1931). A poly-phasic fluorescence rise, consisting of a sequence of phases denoted as O, J, I and P were observed after the illumination of dark adapted leaves. In this fluorescence induction curve all the reaction centers are open at the minimal fluorescence (F_o) while all the reaction centres are closed at maximum fluorescence (F_m). A JIP test has been developed for the quantification of these OJIP fluorescence transients by which several phenomenological and biophysical expressions of PSII were conceived (Strasser *et al.*, 2000). Thus JIP test has been a powerful tool for *in vivo* investigations of PSII functions, including the fluxes of absorption, trapping and electron transport (Mehta *et al.*, 2009). Fluorescence emanates from only the top few layers of chlorenchyma (Maxwell and Johnson, 2000), whereas gas exchange is integrated across the thickness of the leaf and hence

simultaneous measurements of photosynthesis and chlorophyll *a* fluorescence have emerged as potential tools for investigating the relationship between light use efficiency and CO₂ fixation.

Our main objective in this chapter was to investigate effects of elevated CO₂ concentrations on photosynthetic physiology and primary photochemistry of PSII in leaves of *Gmelina arborea* Roxb., (*Verbanaceae*), a fast growing tropical tree species grown under natural light. We have further compared the characteristics of PSII photochemistry during midday depression in elevated CO₂-grown plants with those grown under ambient CO₂ to gain a critical understanding of the influence of increased CO₂ atmosphere on photoinhibition in tree species. Correlation studies between photosynthetic rates, stomatal conductance, water use efficiency and *Ci/Ca* were also done in-order to identify the effect of increased [CO₂] on photosynthetic rates.

Methods

Photosynthetic gas exchange measurements

The rate of leaf gas exchange was measured using a portable infrared CO₂/H₂O gas analyzer (IRGA) (LC Pro+, ADC Bioscientific Ltd. U.K.) equipped with a broad leaf chamber. The instrument allows determination of gaseous exchange by individual leaf enclosed in leaf chamber over time. The gas analyzer was used to measure instantaneous net photosynthetic rates (P_n ; $\mu\text{mol m}^{-2} \text{s}^{-1}$), stomatal conductance (g_s ; $\text{mol m}^{-2} \text{s}^{-1}$) and transpiration rates (E ; $\text{mmol m}^{-2} \text{s}^{-1}$), periodically during each growing season between 10:00 -11:00 h solar time. The instant water use efficiency (WUE_i) was also calculated ($WUE_i = P_n/E$; $\text{mmol CO}_2 \text{mol}^{-1} \text{H}_2\text{O}$). The plants were also analyzed for internal CO₂ concentrations (C_i) and internal to ambient CO₂ ratios (C_i/C_a). Both P_n and g_s were expressed on a projected leaf area basis which was measured with an automatic image analyzer. Leaf temperature (T_L) was measured by an integral leaf thermistor probe (ADC. M.PLC-011. LICOR) mounted on the lower jaw of leaf chamber that touches the underside of the leaf. Once a leaf was enclosed in the chamber, an incubation time of 2 min was given to the leaf to re-adjust to its new microclimate and the measurements were recorded thereafter. All photosynthetic measurements were performed *in-situ* on young, well-expanded and light-exposed leaves randomly chosen from the upper half of the plant canopy. The approach was adopted to avoid variation in photosynthetic characteristics between leaves of different age. The leaves were tagged to allow repeated measurements.

Scanning electron microscopy (SEM)

Leaf samples of 3×3 and 3×1 mm sizes were fixed for 4 h in FAA (10% formalin: 0.5 % acetic acid: 50 % ethyl alcohol: 35 % H₂O) dehydrated in ethyl alcohol – acetone series, dried in critical point drier (EMS 850) and mounted on to copper stubs using double stick

cellophane tape. The mounted samples were coated with gold in a sputter coater (FC-1100, Jeol) and observed under scanning electron microscope (EDAX, Philips XL 30 ESEM). The behavioural changes in stomata were observed and stomatal density in the leaf samples was determined using a photomicroscope system (MPS 60, Leica, Wetzlar, Germany). Stomatal size was defined as the length in micrometres (μm) between the junctions of the guard cells at each end of the stomata which may indicate the maximum potential opening of the stomatal pore (Malone *et al.*, 1993; Maherali *et al.*, 2002).

Diurnal measurements of photosynthetic rates and photosynthetic radiation use efficiency (PRUE)

Diurnal courses of leaf photosynthetic rates (P_n ; $\mu\text{mol m}^{-2} \text{s}^{-1}$) were measured on clear days for every 30 min from 06:00 to 18:00 h., measurements were made on light exposed fully developed leaves of *Gmelina* using a portable infrared $\text{CO}_2/\text{H}_2\text{O}$ gas analyzer (IRGA) (LC Pro+, ADC Bioscientific Ltd. U.K.) equipped with a broad leaf chamber. The leaves were incubated for 2 min in the leaf chamber until photosynthetic rates (P_n) were stabilized and thereafter data were recorded. PAR ($\mu\text{mol mol}^{-1}$ photons) on leaf canopy was measured with a silicon-based PAR sensor mounted on the radiation shield above the leaf chamber window and corrected for chamber light attenuation. PAR readings were periodically compared to values obtained with a quantum sensor (LI-190 SA, LI-COR) mounted in the plane of upper plant canopy. Photosynthetic radiation use efficiency (*PRUE*) [$\text{mmol (CO}_2\text{) mol}^{-1}$ (photons)] was calculated according to Ma *et al.*, (2004) [$PRUE = \text{Net photosynthetic rate } (P_n) / \text{incident PAR}$]. All the above measurements were made under the prevailing light conditions on at least four sun-exposed, upper canopy leaves belonging to four different trees in each ambient and elevated OTC's. The leaves were tagged and measured in sequence. To avoid ontogenetic effects, measurements were limited to the third or fourth leaf on each shoot.

Diurnal measurements of chlorophyll a fluorescence

All measurements of chlorophyll fluorescence were made with the Plant Efficiency Analyser, PEA (Hansatech Instruments Ltd., King's Lynn, Norfolk, England). Measurements were performed on healthy top intact leaves of plants grown under ambient and elevated CO₂ treatments. For possible comparison of fluorescence and gas exchange parameters, the fluorescence recordings were initiated approximately at the same time and at the same canopy level as photosynthetic rates were measured. The leaves were pre-darkened with clips for 20 min prior to measurements and later chlorophyll *a* fluorescence transients of dark-adapted leaves were measured. The transients were induced by 1 s illumination with an array of three light emitting diodes providing a maximum light intensity of 3000 μ mol (photon) m⁻² s⁻¹ and a homogenous irradiation over a 4-mm diameter leaf area. The fast fluorescence kinetics (f_0 to f_M) were recorded from 50 μ s to 1s. The fluorescence intensity at 50 μ s was considered as f_0 (Strasser and Strasser, 1995). The maximum quantum yield of primary photochemistry (at t=0) of dark adapted leaves was calculated as $F_V/F_M \equiv \Phi_{P0} \equiv TR_0/ABS = [1-(f_0/f_M)]$.

Analysis of the fluorescence transients using the JIP-test

Raw fluorescence OJIP transients were transferred with WINPEA 32 software and BiolyzeP3 to a spreadsheet (Strasser and Govindjee, 1992; Albert *et al.*, 2005). The translation of the measured parameters into JIP-test parameters provided information on the stepwise flow of energy through PS II at different levels such as specific fluxes on the level per reaction centre (RC) [absorption flux per RC (ABS/RC), trapped energy flux per RC (TR₀/RC), dissipated energy flux per RC (DI₀/RC) and electron transport flux per RC (ET₀/RC)] and phenomenological fluxes on the level of the excited leaf cross-section (CS)[absorption flux per CS_M (ABS/CS_M), trapped energy flux per CS_M (TR₀/CS_M), dissipated energy flux per

CS_M (DI_0/CS_M) and electron transport flux per CS_M (ET_0/CS_M)]. The efficiency of light reaction was calculated as $\Phi_{P_0}/(1 - \Phi_{P_0})$ (Φ_{P_0} , maximum quantum yield of primary photochemistry (at $t = 0$) and the efficiency of biochemical reaction was calculated as $\Psi_o/(1 - \Psi_o)$ (Ψ_o , is the probability that an electron can move further than Q_A^-). Ψ_o was calculated according to formula: $(F_P - F_J)/(F_P - F_{50\mu s})$ where F_P = Fluorescence maximum in OJIP transient, F_J and $F_{50\mu s}$ = Fluorescence yield at point J and at $50\mu s$. Normalized total complementary area above the O-J-I-P transient (reflecting multiple turnover Q_A reduction events) was calculated as S_m [$S_m = (\text{Area})/(F_P - F_{50\mu s})$]. The performance index (PI) was calculated as combined measurement of the amount of photosynthetic reaction centers (RC/ABS), the maximal energy flux which reaches to the PS II reaction centers and the electron transport at the onset of illumination using the formula: $PI_{ABS} = RC/ABS \cdot \Phi_{P_0} / (1 - \Phi_{P_0}) \cdot \Psi_o / (1 - \Psi_o)$.

Chlorophyll contents

For chlorophyll analysis, circular discs were cut with 16 mm diameter punch (approx. 200 mm² surface) from the leaves used for determining photosynthetic rates and chlorophyll *a* fluorescence during 10:00h-11:00h. The discs were extracted with N, N'-dimethylformamide by grinding with 2ml of solvent in mortar with pestle. The homogenate, combined with a further three washings of the pestle and mortar (each of 1.5 ml) was centrifuged at 2500 rpm for 10 min. Absorbance of the clear extract at 646.8 and 663.8 nm were recorded and concentrations of chlorophylls *a*, *b* and *a/b* were computed after Porra *et al.*, (1989). Chlorophyll concentration of the extract and the total disk surface area of 1m² were used to compute chlorophyll concentrations per unit leaf area.

Statistical analysis

Results were represented as mean \pm SE. The significance of the difference between mean

values of ambient and elevated CO₂ plants, was determined using Paired *t*-tests. Correlation coefficient (*r*) and coefficient of determination (*r*²) of linear relationships between the investigated parameters were established by using linear regression. The linear regression slopes were analysed using bivariate correlation significance tests. Data were analyzed by multivariate analysis of variance (ANOVA). All the statistical analysis was performed using statistical package Sigma Plot 11.0.

Results

Photosynthetic leaf gas exchange

CO₂ enrichment had a profound influence on the leaf gas exchange in young *Gmelina* when compared to its counterparts grown at ambient CO₂ concentration (Table I). The P_n of *Gmelina* under ambient and elevated CO₂ atmosphere at 30 DAP showed no significant differences and the average P_n was 10.4 $\mu\text{mol m}^{-2}\text{s}^{-1}$. However, by the end of 120 DAP, a significant increase in P_n ($p < 0.05$) of 32 % was observed in elevated CO₂ - grown plants (35.17 $\mu\text{mol m}^{-2}\text{s}^{-1}$), compared to ambient CO₂-grown plants. The stomatal conductance (g_s) and transpiration rates (E) showed a decreasing trend in the plants under elevated CO₂. An initial value of $\sim 0.35 \text{ mol m}^{-2} \text{ s}^{-1}$ in g_s was recorded in elevated CO₂-grown plants at 30 DAP, which decreased to 0.25 $\text{mol m}^{-2} \text{ s}^{-1}$ in elevated CO₂ grown plants at 120 DAP which is a reduction of 30% ($p < 0.001$) compared to ambient CO₂- grown plants. The rates of E in CO₂ - enriched plants also showed a significant ($p < 0.001$) reduction of 50% at 120 DAP compared to those grown in ambient CO₂. The internal CO₂ concentration (C_i) in the leaves of elevated CO₂-grown plants was significantly high compared to ambient grown plants but the C_i/C_a ratio was maintained almost constant during the growth at elevated CO₂ and ambient atmosphere (Table 1).

Photosynthetic rates in relation to stomatal conductance, transpiration and internal carbon dioxide concentrations

Under ambient CO₂ atmosphere, P_n values were positively correlated with g_s ($r^2=0.49$; $p < 0.10$) as shown in Figure 3A. However, the values of P_n vs. g_s as obtained in plants grown under elevated CO₂ atmosphere showed negative correlation ($r^2= 0.75$; $p < 0.10$) when plotted together. The relationship between the P_n and C_i/C_a for the ambient and elevated CO₂ grown plants were shown in Figure 3B. The nearly constant C_i/C_a throughout the growth seasons

had no influence on photosynthetic rates as evidenced by a weak correlation in *Gmelina*, grown under elevated CO₂ atmosphere ($r^2 = 0.04$ $p < 0.001$). Compared to elevated CO₂-grown plants, plants grown under ambient CO₂ showed a weak but significant correlation ($r^2=0.46$ $p < 0.001$) (Fig. 3B). The relationship between g_s and C_i/C_a also showed no correlation under elevated CO₂ atmosphere ($r^2 = 0.02$ $p < 0.001$) but a weak correlation under ambient conditions ($r^2 = 0.23$ $p < 0.001$) (Fig. 3D). In both the conditions of ambient and elevated CO₂, Instantaneous Water Use Efficiency (WUE_i) and P_n shared positive linear correlation. However, the correlation was stronger ($r^2=0.93$; $p < 0.001$) under elevated CO₂ conditions, compared to ambient ($r^2=0.89$; $p < 0.18$) (Fig. 3C).

Distribution of Stomata on the leaf surfaces

Stomatal density in *Gmelina* leaves grown under elevated CO₂ was significantly reduced (~36.5% $P < 0.05$) compared to that in the leaves of ambient grown plants (Fig4, Table 2). Further, most of the stomata in leaves under elevated CO₂ were closed (~ 44 % $p < 0.001$), while only 13 % of the total stomata in the ambient leaves were found to be closed. Partially closed stomata constituted ~ 29 % ($p < 0.05$) of total stomata in the CO₂ - enriched plants while only 26 % ($p < 0.05$) were fully opened (Table 2). Even the stomatal length (~ 12 % $p < 0.05$) and stomatal width (~22 % $p < 0.001$) decreased in the leaves of plants grown under elevated CO₂ compared to those grown under ambient CO₂ (Fig. 4 A and B). Figure 4C depicts the behavioural changes in stomatal opening due to elevated CO₂ treatment. A typical patchiness of stomata was observed in the leaves of plants grown under elevated CO₂ (Fig. 4C).

Diurnal dynamics of P_n and PRUE

Diurnal trends of photosynthetically active radiation (PAR), photosynthetic rates (P_n) and photosynthetic radiation use efficiency (PRUE) were presented in Figure 5. During early

Table 1 Photosynthetic characteristics as influenced by CO₂ (ambient, 360 $\mu\text{mol mol}^{-1}$; elevated, 460 $\mu\text{mol mol}^{-1}$) in young *Gmelina arborea* recorded during two growth seasons (spring and summer) at periodic intervals (days after plantation, DAP) for three consecutive years (2006 to 2008). Photosynthetic rate (P_n , $\mu\text{mol m}^{-2} \text{s}^{-1}$), stomatal conductance (g_s , $\text{mol m}^{-2} \text{s}^{-1}$), transpiration rate (E , $\text{m mol m}^{-2} \text{s}^{-1}$) and C_i/C_a ratio. Values are mean \pm standard deviation. Effects of CO₂ were tested by paired t -test. *** $p < 0.001$, ** $p < 0.01$, * $p < 0.05$, n.s. not significant.

Year	DAP	P_n			g_s			E			C_i/C_a		
		Ambient	Elevated		Ambient	Elevated		Ambient	Elevated		Ambient	Elevated	
2006	30	10.90	10.80	n.s.	0.34	0.36	**	4.90	5.15	***	0.79	0.73	n.s.
	60	17.91	18.72	**	0.37	0.32	**	5.10	4.90	**	0.76	0.76	n.s.
	90	24.91	28.63	*	0.38	0.29	***	5.20	4.43	n.s.	0.70	0.75	n.s.
	120	25.32	34.96	**	0.39	0.26	***	5.40	4.02	***	0.67	0.75	*
2007	30	10.60	9.20	**	0.28	0.36	***	4.90	5.00	n.s.	0.81	0.75	n.s.
	60	16.91	19.19	**	0.35	0.34	n.s.	5.50	4.12	**	0.78	0.74	n.s.
	90	25.42	26.97	*	0.38	0.27	***	5.00	3.92	***	0.72	0.78	n.s.
	120	24.16	35.42	*	0.36	0.24	**	5.20	3.77	***	0.69	0.72	*
2008	30	9.80	11.20	**	0.31	0.34	**	4.6	4.9	n.s.	0.79	0.72	n.s.
	60	18.16	19.72	n.s.	0.33	0.31	n.s.	5.0	4.7	**	0.75	0.69	*
	90	25.42	26.63	*	0.36	0.28	***	5.3	4.5	***	0.70	0.75	n.s.
	120	26.12	35.14	***	0.38	0.26	***	5.5	4.1	***	0.65	0.77	n.s.

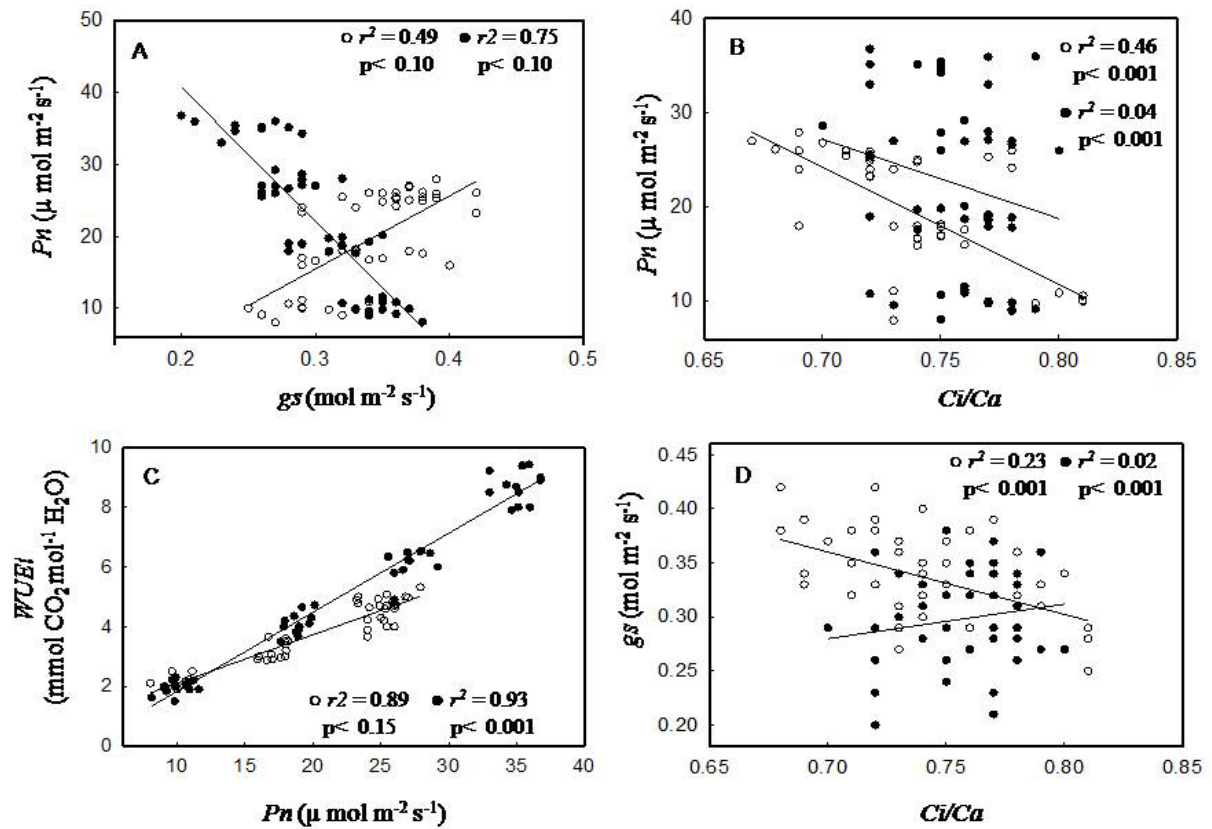


Fig 3. Relationship between photosynthetic rates (P_n) and stomatal conductance (g_s) (A), rates of photosynthesis (P_n) and C_i/C_a ratios (B), instantaneous water use efficiency (WUE_i) and photosynthetic rates (P_n) (C) and stomatal conductance (g_s) and C_i/C_a ratios (D) in young *Gmelina arborea* grown under ambient and elevated CO_2 concentrations (○ ambient; ● elevated).

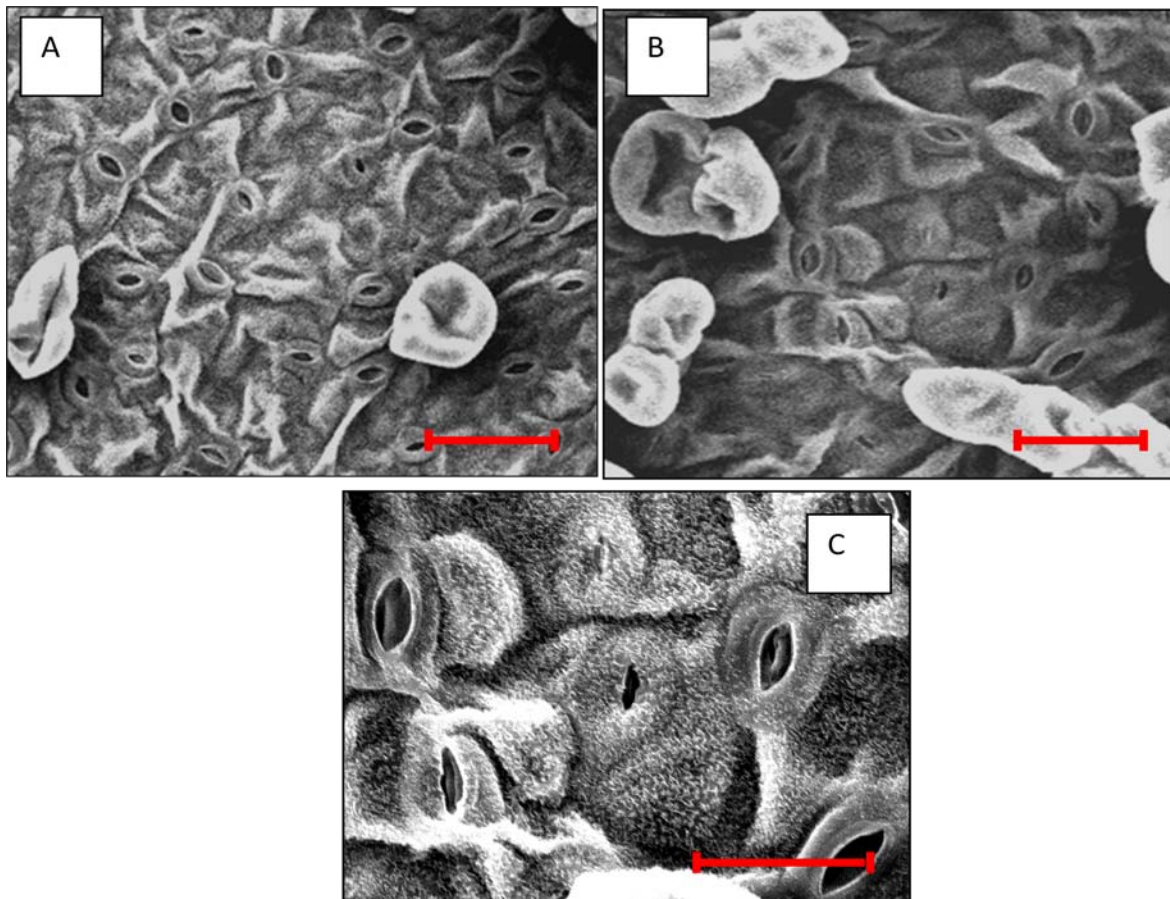


Fig 4. Scanning electron micrographs of stomata on abaxial surface of young *Gmelina* leaves. Note the comparative difference in stomatal number between the ambient (A) and elevated CO₂ (B) grown *Gmelina*. Scale bar = 100 μm. (C) Microphotograph of the behavioural response of stomata in *Gmelina* exposed to elevated CO₂ concentration. Variation in the degree of stomatal opening showing a typical stomatal patchiness was induced by enriched CO₂ atmosphere. Scale bar = 50 μm.

Table 2 Stomatal characteristics in young *Gmelina* leaves grown under ambient and elevated CO₂ concentrations.Values are mean \pm standard deviations.

Variables	Ambient	Elevated
Stomatal density (mm ⁻²)	1024 \pm 55.53	750 \pm 21.60
Stomatal length (μ m)	12.0 \pm 1.29	10.6 \pm 0.60
Stomatal width (μ m)	6.91 \pm 0.46	5.41 \pm 0.23
Number of fully opened stomata (mm ⁻²)	652 \pm 25.05	192 \pm 5.43
Number of partially opened stomata (mm ⁻²)	238 \pm 19.36	216 \pm 9.98
Number of closed stomata (mm ⁻²)	134 \pm 9.93	344 \pm 13.30

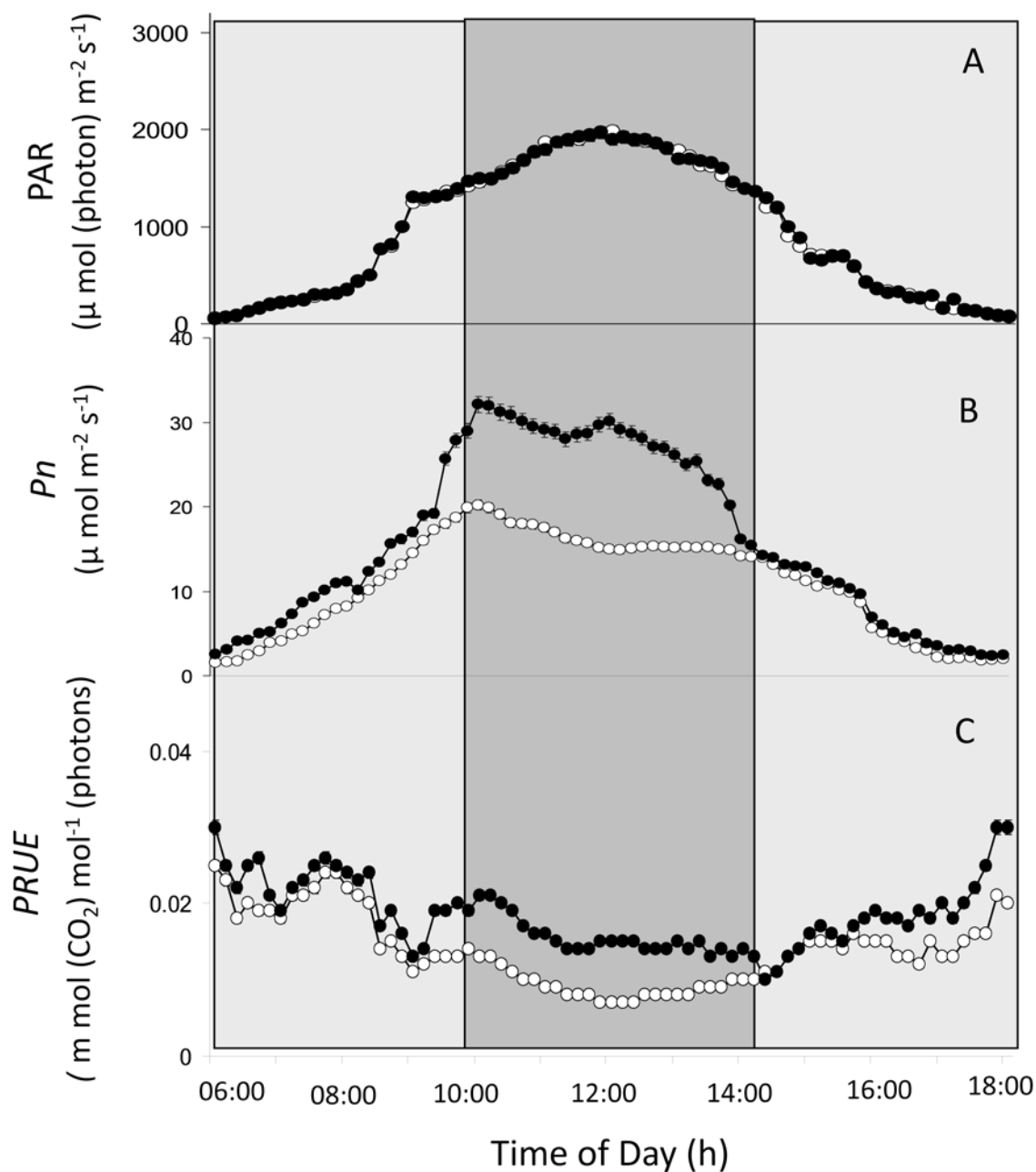


Fig.5. Diurnal courses of photosynthetically active radiation (PAR) (A), photosynthetic rates (P_n) (B) and photosynthetically active radiation use efficiency (PRUE)(C) in the leaves of *Gmelina arborea* grown under ambient and elevated CO_2 concentrations (\circ ambient; \bullet elevated). Values are mean \pm standard deviations.

(08:00-11:00 h) and late (13:00-16:00 h) daylight hours, PAR in OTCs ranged between 500 to 1700 $\mu\text{mol m}^{-2} \text{s}^{-1}$ whereas a peak irradiance of 1800-2000 $\mu\text{mol m}^{-2} \text{s}^{-1}$ was observed during midday hours (11:00-13:00 h) (Fig. 5A). Diurnal photosynthesis typically maximized between 09:00 h and 10:00 h in both ambient and elevated CO_2 -grown plants (20 and 32.5 $\mu\text{mol m}^{-2} \text{s}^{-1}$ respectively) and decreased there after (Fig. 5B). During the midday hours (11:00-13:00), P_n in elevated CO_2 -grown plants was much higher (~37%, $p < 0.001$) compared to ambient CO_2 -grown plants. A recovery phase was also observed between 12:00 to 13:00 h in the leaves of elevated CO_2 grown plants, where P_n increased from ~27.00 $\mu\text{mol m}^{-2} \text{s}^{-1}$ (12:00 h) to ~30.12 $\mu\text{mol m}^{-2} \text{s}^{-1}$ (13:00 h). The recovery phase was not noticed in ambient CO_2 -grown plants and P_n decreased from ~16.23 $\mu\text{mol m}^{-2} \text{s}^{-1}$ (12:00 h) to ~15.20 $\mu\text{mol m}^{-2} \text{s}^{-1}$ (13:00 h). The diurnal lowest values of P_n were observed between 15:00 – 18:00 h in both ambient and elevated CO_2 -grown plants (Fig. 5B). The $PRUE$ varied from 0.008 to 0.025 $\text{mmol CO}_2 \text{mol}^{-1} \text{photons}$ in both the variants and it was significantly high (~38%, $p < 0.001$) in elevated CO_2 grown plants during 09:00-10:00 h compared to ambient CO_2 -grown plants. Even during the peak irradiance (11:00-13:00), $PRUE$ was much higher in elevated CO_2 -grown plants (~0.015 $\text{mmol CO}_2 \text{mol}^{-1} \text{photons}$) compared to ambient CO_2 -grown plants (~0.08 $\text{mmol CO}_2 \text{mol}^{-1} \text{photons}$) (Fig. 5 C).

Chlorophyll a fluorescence

There was no significant change in the average predawn F_v/F_m values in ambient (~ 0.83) and elevated CO_2 -grown (~ 0.84) plants. However, as incident PAR increased (08:00-12:00 h), the F_v/F_m values decreased in both ambient and elevated CO_2 -grown plants. During midday (12:00 h), F_v/F_m value was significantly high (~19%, $p < 0.01$) in elevated CO_2 -grown plants. Between 14:00 -18:00 h, recovery of F_v/F_m was observed in elevated CO_2 -grown plants reaching ~ 0.82

by 18:00 h. This progressive recovery was not recorded in the ambient CO₂-grown plants, where the values were consistent at ~ 0.7 even after 16:00h (Fig. 6).

The probability of electron transfer from PSII to PQ pool (Ψ_o) was significantly high ($p < 0.001$) in elevated CO₂-grown plants during the peak irradiance (10:00 h to 14:00 h) when compared with ambient CO₂-grown plants (Fig. 7A). Ψ_o was ~ 35% more in elevated CO₂-grown *Gmelina* during 10:00 h when compared with ambient CO₂-grown plants. Interestingly the S_m (multiple turnover of Q_A reduction events) was also significantly ($p < 0.001$) high during 10:00 h in elevated CO₂-grown plants when compared to ambient CO₂-grown plants (Fig. 7 A). S_m and Ψ_o are proportional to the photosynthetic rates. The efficiency of light reaction [$\Phi_{P_0}/(1 - \Phi_{P_0})$] during early hours showed no significant difference in both elevated and ambient CO₂-grown plants. At peak irradiance (12:00 h), the efficiency of light reaction was significantly high ($p < 0.001$, ~54%) in plants grown under increased CO₂ atmosphere (Fig. 8A). The efficiency of biochemical reaction [$\Psi_o/(1 - \Psi_o)$] was also not significantly (n.s) different in elevated CO₂-grown plants compared to ambient CO₂-grown plants (Fig. 5B). Though there was decrease in the efficiency during the peak irradiance (12:00 h), a ~ 49% more efficiency was observed in plants grown under elevated CO₂ atmosphere compared to ambient CO₂-grown plants (Fig. 8B).

The derived parameters can be visualized by means of dynamic energy pipeline leaf model of the photosynthetic apparatus which deals with the phenomenological energy fluxes per cross-section. Interestingly, plants grown under ambient CO₂ conditions showed a high ABS/CS_M , TR_0/CS_M and DI_0/CS_M compared to those grown under elevated CO₂, whereas electron transport in PSII cross-section (ET_0/CS_M) was significantly high ($p < 0.001$) in elevated CO₂-grown plants compared to ambient CO₂-grown plants (Fig. 9 and 10).

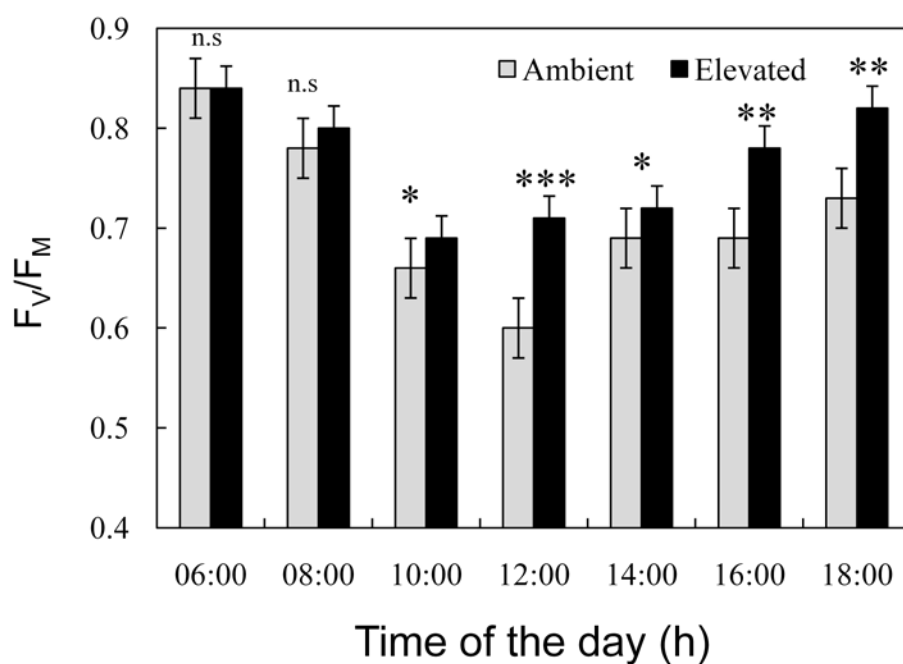


Fig.6. Diurnal patterns of potential quantum yield of PSII primary photochemistry (F_v/F_m) in *Gmelina arborea* leaves grown under ambient and elevated CO_2 concentrations. Values are mean \pm standard deviations. Effects of CO_2 were tested by paired t -test. *** $p < 0.001$, ** $p < 0.01$, * $p < 0.05$, n.s. not significant.

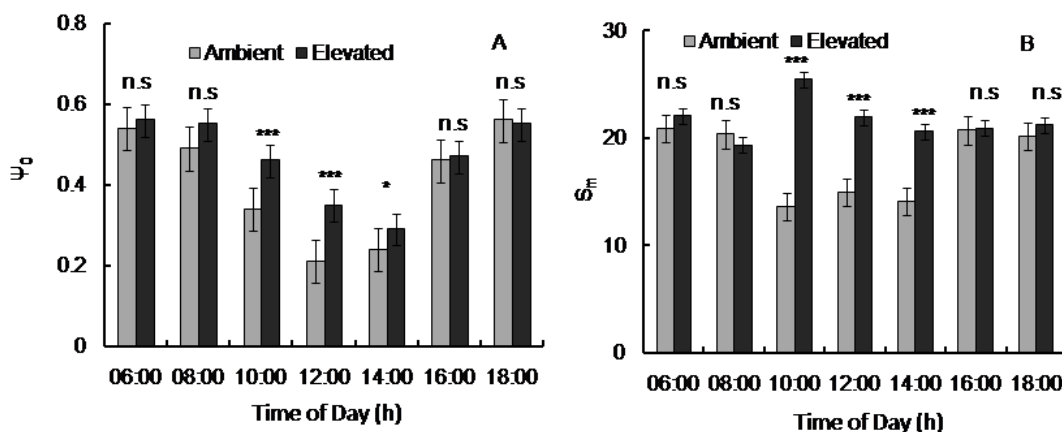


Fig.7. Diurnal patterns of changes in the JIP-test parameters, the probability of electron transfer from PSII to PQ pool (Ψ_0) (A) and normalized area between OJIP curve and F_P value (S_m) (B) in leaves of *Gmelina arborea* grown under ambient and elevated CO_2 concentrations (\circ ambient; \bullet elevated). Values are mean \pm standard deviations. Effects of CO_2 were tested by paired t -test. *** $p < 0.001$, ** $p < 0.01$, * $p < 0.05$, n.s. not significant.

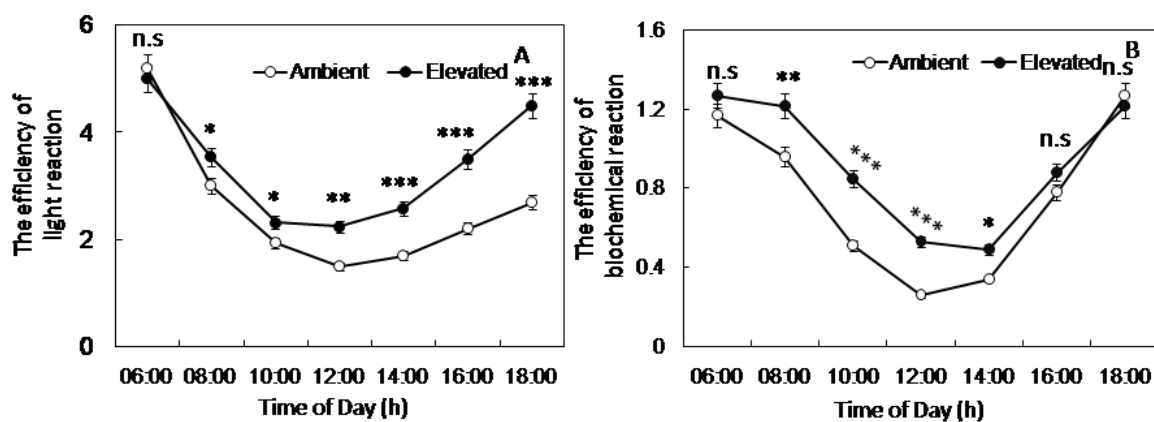


Fig.8. Diurnal patterns of the efficiency of light (A) and biochemical reaction (B) in *Gmelina arborea* leaves grown under ambient and elevated CO_2 concentrations (\circ ambient; \bullet elevated). Values are mean \pm standard deviations. Effects of CO_2 were tested by paired t -test. *** $p < 0.001$, ** $p < 0.01$, * $p < 0.05$, n.s. not significant.

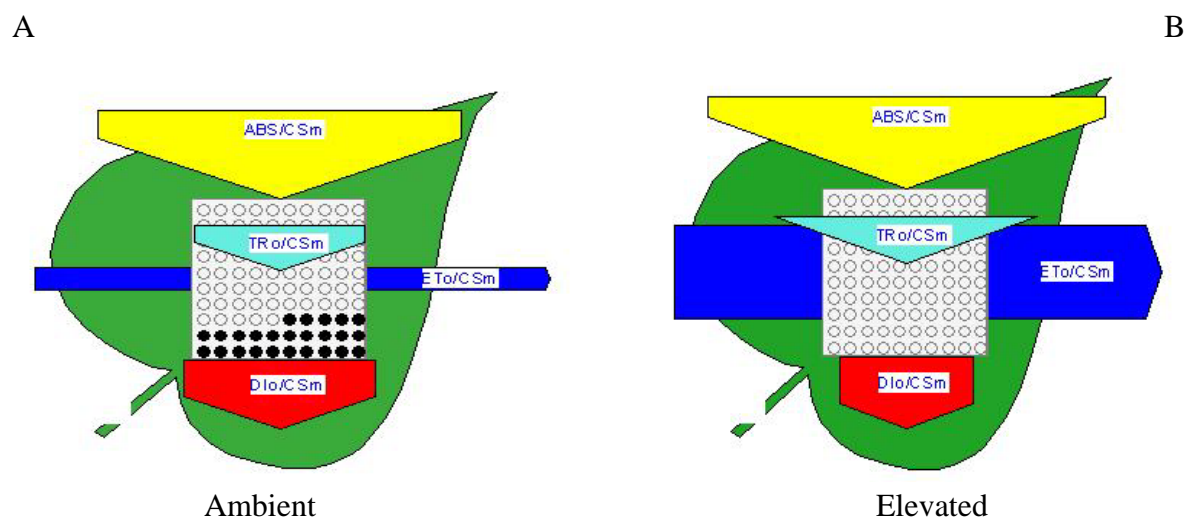


Fig.9. Energy pipeline models of phenomenological fluxes (per cross-section) during the peak irradiance (12:00 h) in leaves of *Gmelina arborea* grown under ambient (A) and elevated CO₂ (B) concentrations.

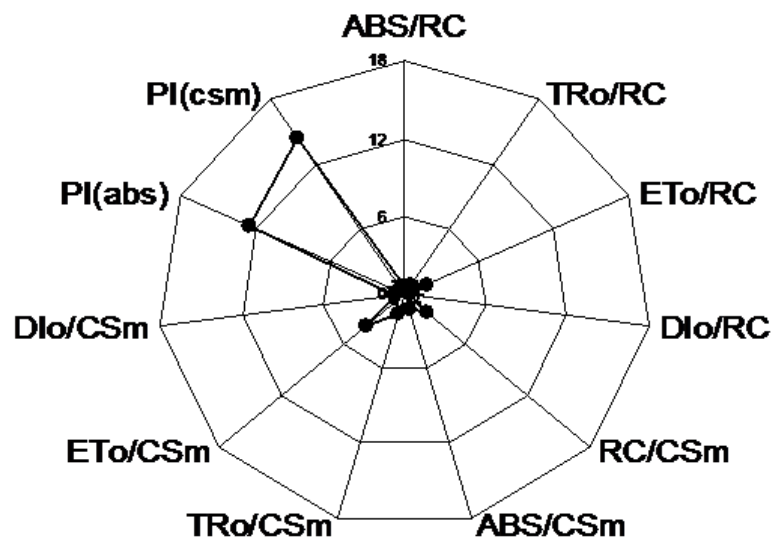


Fig.10. Radar plot of fluorescence parameters during the peak irradiance (12:00 h) with ambient values as reference level.

During the midday (12:00 h), density of the active reaction centers (RC/CS_M) (indicated as open circles) were significantly high in elevated CO₂-grown plants (Fig. 9B) compared to those in ambient CO₂ grown plants (Fig. 9A). During peak irradiance (12:00 h) a significant number of active RCs were converted into inactive RCs (indicated as dark circles) in ambient CO₂-grown plants, (Fig. 9A). The overall performance of PSII assessed by performance indices (PI_{Abs} and PI_{CSm}) showed significant ($p < 0.001$) increase in plants grown under elevated CO₂ atmosphere compared to those grown under ambient CO₂-grown plants (Fig. 10).

Chlorophyll content

The chl *a*, *b* and total chlorophyll contents per unit leaf area (Table 3) were high in ambient CO₂-grown plants compared to elevated CO₂-grown plants. Ambient CO₂-grown plants showed a 22% ($p < 0.05$) increase in the total chlorophyll content and 23 % ($p < 0.05$) increase in the chl *a* content compared to elevated CO₂-grown plants, where as Chl *b* and Chl *a/b* ratio showed no significant differences between ambient and elevated CO₂-grown plants (Table 3).

Table 3. Leaf chlorophyll content in ambient and elevated CO₂ grown *Gmelina* leaves.

Parameters	Ambient ^a	Elevated ^{a,b}	
Chl a (mg m ⁻²)	0.21±0.06	0.16±0.07	*
Chl b (mg m ⁻²)	0.06±0.002	0.05±0.005	n.s
Chl a/b	3.5±0.9	3.2±0.7	n.s
Total chlorophylls (mg m ⁻²)	0.27±0.09	0.21±0.02	*

^a Values are mean ± standard deviation.

^b Effects of CO₂ were tested by paired *t*-test.* p<0.05, n.s. not significant.

Discussion

Young *Gmelina* plants showed a significant upsurge in P_n in the interim enriched CO₂ exposure and same trend of enhancement was discerned for all the consecutive experimental years. Increased CO₂ concentrations can boost the rates of carboxylation sites of rubisco and concomitantly increase the P_n of C₃ plants. Copious models elucidated greater photosynthetic enhancement under increasing CO₂ atmosphere (Herrick and Thomas, 2001; Possell and Hewitt, 2009). Synchronously, a time dependent photosynthetic down regulation under elevated CO₂ has also been observed in many plants, on account of diffusion limitation of CO₂, internal CO₂ concentration (C_i), availability of light and sink capacity for photosynthates resulting in curtailment of CO₂ assimilation (von Caemmerer and Farquhar, 1981; Guderson and Wullschleger, 1994; Stylinski *et al.*, 2000; Norby *et al.*, 2001; Oren *et al.*, 2001; Delucia *et al.*, 2002; Ainsworth *et al.*, 2004; Warren and Adams, 2004).

The CO₂ exchange between the plants and its atmosphere mainly occurs through the stomata and g_s is one of the major limitations in carbon assimilation, particularly when plants were grown under elevated CO₂ (Jensen, 2000; Anderson *et al.*, 2001; Beedlow *et al.*, 2004; Ainsworth and Rogers, 2007). A down drop in the g_s was observed under elevated CO₂ atmosphere mainly due to escalation in the C_i as the stomata respond to C_i through the guard cells (Paoletti and Grulke, 2005). Another major effect of elevated CO₂ on g_s was due to repercussion in stomatal density (Hetherington and Woodward, 2003). There was a mean abatement in the stomatal density and the existence of the patchy stomata in the plants grown under CO₂ enriched atmosphere. *Gmelina* showed significantly less number of stomata with varying degree of stomatal opening and a pertinent patchiness in stomata under CO₂ enriched atmosphere. Stomatal response to elevated CO₂ was assumed to maintain a constant C_i/C_a ratio (Long *et al.*, 2004) and this was clearly

observed in *Gmelina*, where C_i/C_a ratio was unchanged with growth under elevated CO_2 atmosphere. The subsidence in photosynthetic acclimation despite the decrement in g_s was believed to be due to the maintenance of a constant C_i/C_a ratio and through accelerated internal photosynthetic activity as stomata were found to limit the P_n particularly when C_i was saturating (Farquhar and Sharkey, 1982; Rey and Jarvis, 1998; Assmann, 1999; Noormets *et al.*, 2001; Sage, 2002; Herrick *et al.*, 2004; Paoletti and Grulke, 2005). Elevated CO_2 increased photosynthetic rates in *Gmelina* leaves but greatly decreased transpiration and which significantly increased water use efficiency. In sum, *Gmelina* appeared to sense and respond to rising CO_2 exclusively through direct effects of increased carboxylation and decreased stomatal opening.

The present study also suggests that under high irradiance, exposure of *Gmelina* to elevated CO_2 atmosphere led to significant increase in the photosynthetic activity and also maintained efficient PSII photochemistry compared to the ambient CO_2 -grown plants. Our results showed that there were no significant differences in CO_2 assimilation rates during early hours (06:00 h) in both ambient and elevated CO_2 grown plants which could be due to limited absorption of photons at low irradiance (Špunda, 2005). Photoinhibition of photosynthesis observed during midday in both ambient and elevated CO_2 -grown *Gmelina* suggests that irradiance levels were in excess of that used in photosynthesis, leading to chronic deactivation of the reactions associated with photosystem II (Werner *et al.*, 2003; Allakhverdiev *et al.*, 2008). However, significantly high rates of photosynthesis during peak irradiance in elevated CO_2 -grown *Gmelina* demonstrate that increased atmospheric CO_2 stimulated light-saturated photosynthesis through increased absorption of photosynthetically active photon flux density used for photochemistry (Hymus *et al.*, 2001). The recovery of carbon assimilation during midday hours (12:00-13:00 h) and high

PRUE in elevated CO₂-grown *Gmelina* suggests that CO₂ atmosphere could play a significant role in the rate of energy absorption and associated light reactions in *Gmelina* (Fig. 5C).

The sensitivity of photoinhibition was lower in plants grown under elevated CO₂ atmosphere compared to ambient CO₂ grown plants as reflected by the F_V/F_M in our study. It is well known that changes in F_V/F_M values were due to changes in efficiency of photochemical quenching which is a sensitive indicator of photosynthetic performance (Mehta *et al.*, 2009). The decrease in F_V/F_M values in ambient and elevated CO₂ grown plants from morning to midday reflects protective mechanism to avoid photodamage to the photosynthetic apparatus under excess light energy (Escobar-Gutiérrez *et al.*, 2009). During midday, the significantly high ($p < 0.001$) F_V/F_M values under high irradiance in elevated CO₂ grown plants suggest that plant growth under elevated CO₂ significantly increases the photochemical efficiency of PSII. The recovery of F_V/F_M values during 13:00 -18:00 h in *Gmelina* grown under elevated CO₂ depicts the efficiency of PSII photosynthetic machinery under increased CO₂ atmosphere.

Data on JIP-test in our study reveal biophysical and biochemical performance of photosynthetic apparatus as well as performance index of PSII photosynthetic machinery (Clark *et al.*, 2000; van Heerden *et al.*, 2004; Albert *et al.*, 2005). The reduced absorption flux per RC in elevated CO₂-grown plants suggest that RCs were not converted into heat sinks while the antennae formed an active RCs group as ABS/RC was influenced by ratio of active and inactive RCs (Strasser and Strasser, 1995). Changes in the total chlorophyll and Chl a/b ratios could be related to the balance of light absorption capacity of the photosystems (Kitajima and Hogan, 2003). Typically, elevated CO₂-grown plants had lower chlorophyll content than ambient CO₂-grown plants with slightly lower Chl a/b ratios associated with an increase in the size of the PSII light harvesting antenna (Evans and Poorter, 2001). The effective increase in the size of the PSII light harvesting

antenna and also a significant increase in the active RCs in elevated CO₂-grown *Gmelina* compared to the ambient CO₂-grown plants indicate that elevated CO₂ atmosphere also increased the linear electron flow in leaves of *Gmelina* even under high irradiance.

The efficiency of light reaction was significantly high ($p < 0.001$) in elevated CO₂-grown plants suggesting an effective increase in the number of quanta absorbed per unit leaf area compared to those grown under ambient CO₂. Since F_v/F_m was also significantly high in elevated CO₂-grown plants, it is conceivable that these plants possessed more efficient light reaction systems compared to ambient CO₂-grown plants. The efficiency of biochemical reactions were also substantially high in elevated CO₂-grown plants suggesting that the efficiency of the forward electron transport rates were increased in these plants. The mechanistic model of C₃ photosynthesis also supports our findings that elevated CO₂ increased photosynthesis, photochemistry and linear electron flow through photosystem II (Farquhar *et al.*, 1980; Hymus *et al.*, 1999). Concomitantly, significantly high efficient light reactions and biochemical reactions in elevated CO₂-grown plants provide evidence that elevated CO₂ protects PSII from photoinhibition and also enhances the photochemical quenching in *Gmelina*.

The increase in electron transport per excited cross section (ET_0/CS_M) in elevated CO₂-grown *Gmelina* as observed in dynamic leaf models suggests that the elevated CO₂ atmosphere increased electron transport through increased number of active RCs in PSII cross section of *Gmelina* leaf. However, the significant decrease in the dissipation of the untrapped excitons (DI_0/RC) in elevated CO₂-grown plants depicts that effective electron transport and carbon assimilation decreased the energy dissipation non-photochemically but increased the photochemical quenching. All JIP characteristics were positively correlated with rates of CO₂ assimilation as shown in Fig. 5 (B). Significantly high ET_0/CS_M and low DI_0/CS_M in elevated

CO₂-grown plants led to an increase in performance indices like PI_{ABS} and PI_{CSM}, which were the integrated responses of specific fluxes per active PSII RC and phenomenological fluxes per leaf CS. The significantly high performance indices in elevated CO₂ grown plants also suggest an efficient overall performance of PSII photosynthetic machinery in these plants (Clark *et al.*, 2000; Strasser *et al.*, 2000). In conclusion, our data demonstrate that future increase in atmospheric CO₂ may have positive effects on photochemical efficiency in tree species like *Gmelina arborea*. High CO₂ can also mitigate the photoinhibition caused due to high irradiation through enhanced electron transport rates and through efficient biochemical reactions.

Conclusions

1. Young *Gmelina* plants showed a significant upsurge in photosynthetic rates in the enriched CO₂ atmosphere and same trend of enhancement was discerned for all the experimental years.
2. A drop in the g_s as observed in this study under elevated CO₂ atmosphere was believed mainly due to escalation in the C_i , as the fact that the stomata respond to C_i through the guard cells. Another major effect of elevated CO₂ on g_s might be due to repercussion in stomatal density.
3. The subsidence in photosynthetic acclimation, despite the decrement in g_s was believed to be due to the maintenance of a constant C_i/C_a ratio and through accelerated internal photosynthetic activity as stomata were found to limit the P_n particularly when C_i is saturating.
4. High rates of photosynthesis at peak irradiance in elevated CO₂-grown *Gmelina*, indicate the efficacy of photosynthetic carbon assimilation under elevated CO₂ atmosphere even under high irradiance.
5. CO₂ atmosphere could play a significant role in the rate of energy absorption and partitioning in the light reactions of photosynthesis.
6. The significantly high F_v/F_m values in elevated CO₂ grown plants under high irradiance and an effective recovery from midday depression strongly suggest that growth in elevated CO₂ increases the photochemical efficiency of PSII.
7. The pertinent high performance indices in elevated CO₂ grown plants suggest an efficient processing of light energy per RC and CS, as PI indices accentuate PSII performance.
8. Our results suggest that effective carbon assimilation decreased the energy dissipation non-photochemically but increased the photochemical quenching in elevated CO₂-grown plants.

Chapter 3

Studies on biochemical responses of *Gmelina* under ambient and elevated CO₂ atmosphere

Chapter 3

Studies on biochemical responses of *Gmelina* under ambient and elevated CO₂ atmosphere

Introduction

As atmospheric CO₂ continue to increase, there is considerable research interest in mechanisms by which plants respond to these changes with special reference to elevated CO₂ effects on photosynthetic machinery (Bowes, 1991; Stitt, 1991; Sage, 1994; Webber *et al.*, 1994). The increase in atmospheric CO₂ should result in an effective photosynthetic carbon fixation, primarily due to a reduction in photorespiration as the rubisco carboxylation reaction is favoured under elevated CO₂ (Farquhar *et al.*, 1980; von Caemmerer and Farquhar, 1981; Long *et al.*, 2004). However, many studies have shown a decline in photosynthetic rates after exposure to high-CO₂ (Stitt, 1991; Webber *et al.*, 1994; Rogers and Ellesworth, 2002). This decline in photosynthesis was often correlated with reduction in stomatal conductance, increase in *Ci*, reduction in rubisco activity and also decrease in associated photosynthetic enzyme activities (Ainsworth and Long, 2005). Significantly increased *Ci* and decreased stomatal conductance were found to limit the photosynthetic activity by influencing the key photosynthetic enzymes (Herrick *et al.*, 2004).

The primary biochemical effect of high CO₂ was on the carboxylating enzyme rubisco. The activity of rubisco was dependent *inter alia* on the partial pressure of CO₂ at the active site and the diffusion of CO₂ from air outside the leaf boundary layer to the site of CO₂ fixation. However, another key enzyme carbonic anhydrase (CA; EC 4. 2. 1. 1), which was localized primarily in the chloroplast stroma was thought to play a major role in photosynthesis by facilitating diffusion of CO₂ into and across the chloroplast, as well as by catalyzing HCO₃⁻

dehydration to supply CO_2 for rubisco carboxylation (Majeau and Coleman, 1996). The unanalyzed rate of CO_2 generation from HCO_3^- is relatively slow limiting rubisco catalytic activity and thus CA has been considered as rate limiting enzyme in photosynthesis (Hoang and Chapman, 2002). Efficient supply of inorganic carbon species to the cell surface is the primary step in the CO_2 capture and this active capture of CO_2 into an intermediate pool is a crucial step in carbon concentrating mechanisms (Badger and Price, 1994). Therefore, it is anticipated that CA would respond to changes in the atmospheric CO_2 and it might be playing a crucial role in efficient capture of C_i in the plants exposed to elevated CO_2 .

Increased levels of soluble sugars were also shown to down-regulate photosynthesis, through decreasing photosynthetic gene transcription via hexose-cycling (Pego *et al.*, 2000; Long *et al.*, 2004). Although a correlation between carbohydrate accumulation and down regulation of photosynthesis at elevated CO_2 has been observed, the extent and the nature of acclimatory responses mainly depends on species and growth conditions (Herrick and Thomas, 2001; Ainsworth *et al.*, 2003). In addition, factors such as sink strength and sink-source transition have also been implicated for effective photosynthesis (Ainsworth *et al.*, 2002; Li *et al.*, 2008). The net productivity enhancement in trees, compared to other crop plants under elevated CO_2 has been attributed to the source-sink carbohydrate relations or sinks strength conferring effective utilization of the available photosynthates (Ainsworth and Rogers, 2007). Although a number of studies have been undertaken to investigate the tree responses to elevated CO_2 , there is little information on either carbohydrate status or the activities of photosynthetic enzymes in trees grown under elevated CO_2 (Ainsworth and Long, 2005). In this study, we examined whether *Gmelina* leaves grown under elevated CO_2 show any evidence of biochemical acclimation in terms of accumulation of leaf starch and any decrease in expression of key photosynthetic

enzymes. We have studied the CA and RUBPcase activities along with the levels of foliar total carbohydrates, starch and key enzymes of photosynthetic metabolism like hexokinase (EC 2.7.1.1), sucrose-phosphate synthase (SPsynthase) (EC 2.4.1.14) and fructose biphosphatase (FBPase) (EC 3.1.3.11).

Methods

RUBPcase activity

Extraction of RUBPcase and activity measurements were performed according to Cheng and Fuchigami (2000). Fresh leaf tissue (2g) was homogenised in 3 ml extraction buffer containing 100 mM bicine (pH 7.8), 5 mM EDTA, 0.75% (w/v) polyethylene glycol (20000), 14 mM β -mercaptoethanol, 1% (v/v) Tween 80, and 1.5 % (w/v) insoluble PVPP. The homogenate was centrifuged at 18,000 g for 5 min and the supernatant was used immediately for assaying RUBPcase activity. Activity of RUBPcase was measured at 25 °C by enzymatically coupling RUBP carboxylation to NADH oxidation which was monitored at 340 nm in a Shimadzu UV-160 spectrophotometer. For initial RUBPcase activity, a 50 μ l sample extract was added to a semi-microcuvette containing 900 μ l of an assay solution, followed by immediate addition of 50 μ l of 0.5 mM RUBP. For total rubisco activity, 50 μ l of 0.5 mM RUBP was added 15 min later, after a sample extract was combined with the assay solution to fully activate RUBPcase. The assay solution for both initial and total activity measurements contained : 100 mM Bicine (pH 8.0), 25 mM KHCO₃, 20mM MgCl₂, 3.5 mM ATP, 5 mM phosphocreatine, 80 nkat glyceraldehyde-3-phosphate dehydrogenase, 80 nkat 3-phosphoglycerate kinase, 80 nkat creatine phosphokinase, and 0.25 mM NADH.

CA activity

Fresh leaf tissue (1gm) were homogenized in liquid nitrogen and then extracted in 10 ml of 60 mM phosphate buffer (pH 8.3) containing 5 mM cysteine and 1mM EDTA. The homogenate was centrifuged at 8000 g for 20 min and the supernatant was used for enzyme assay. The activity of CA in the leaf extracts was determined by following the time-dependent decrease in pH from 8.3

to 7.3 at 4 °C (Wilbur and Anderson, 1948; Li *et al.*, 2004). Assay mixture containing 25 µl of enzyme extract and 2 ml of extraction buffer (pH 8.3) was stirred at a constant rate in a small cuvette, and the reaction was initiated by the addition of 1 ml of a CO₂ solution (distilled water saturated with CO₂ at 0 °C, approximately 76 mM). The units (U) of enzyme activity were calculated according to the formula: $U = 10 (t_o / t - 1)$, where t and t_o represent the time required to change the pH of buffer from 8.3 to 7.3 with and without the enzyme extract respectively. Protein content in the leaf extract was quantified according to Bradford (1976). The enzyme activity was expressed as U mg⁻¹ protein.

Ingel assay of CA

Fresh leaf tissue was homogenized at 0 °C with 2 ml electrophoresis buffer (pH 8.3) containing tris (hydroxymethyl) methylamine (10.75 gm), disodium ethylenediaminetetraacetic acid (0.93 gm), boric acid (5.04 gm) and 10 mM dithiothreitol. The homogenate was centrifuged at 14,000 g for 20 min. The supernatant was collected and sucrose was added to the supernatants to give a concentration of 5 % (w/v). 10 µl of sample was added to 6 % native PAGE gel and the gel was run for 12 h at 5 °C and 35V (Patterson *et al.*, 1971). Thereafter, the gel was kept at 0 °C on an aluminium plate and flooded with a cold solution of bromocresol purple (0.1 %) in electrophoresis buffer containing 10 mM DTT. After 1 min, the gel was blotted free of all excess liquid and covered for 0.5 to 2 min with an inverted filter funnel attached to a source of pure CO₂. Immediately after CO₂ treatment the gel was frozen in dry ice and examined under UV light (λ max = 366 nm). The yellow form of the bromocresol purple in the zones of carbonic anhydrase activity fluoresced bright yellow against a pink back ground. The gels were photographed using the fluorescence, UV-visible gel documentation and analysis system

(Alphaimager EC system, Alpha Innotech USA).

Hexokinase activity

Hexokinase activity was estimated according to the method of Martinez-Barajas and Randall (1998) with slight modification. Fresh leaf tissue (5 g) was homogenised in 8 ml of 50 mM Tris-HCl (pH 6.8) containing 5 mM MgCl₂, 5mM β-mercaptoethanol, 15% glycerol, 1 mM EDTA and 1 mM EGTA, centrifuged at 15000 g for 15 min at 4 °C and the supernatant was used for the enzyme assay. The reaction mixture (200μl) contained: 50 mM Tris-HCl (pH 8.0), 50 mM KCl, 5 mM MgCl₂, 5 mM DTT, 0.3 mM NAD⁺, 1 mM ATP, 1.4 U/ml glucose-6-phosphate dehydrogenase and 5mM of glucose. Assay was initiated by the addition of enzyme preparation and the reduction of NAD was followed at 340 nm at 30°C.

Fructose-1, 6-bisphosphatase (FBPase) activity

FBPase activity was assayed according to Zimmerman *et al.*, (1978). Fresh leaf tissue (10g) was homogenized with 100mM Tris-HCl buffer (pH 7.8) containing 5mM DTT, 10mM MgCl₂, 1mM EDTA, 5mM magnesium acetate and 1.5 % PVP-40. The homogenate was filtered through Wattman filter paper and centrifuged at 10000 g for 10 min. 25 g of DEAE-cellulose was added to the supernatant and the solution was stirred well for 15 min, filtered to remove cellulose and washed thrice with the extraction medium. Protein was precipitated with 75 % (m/v) ammonium sulphate, spun at 30000 g for 30 min and the precipitate was dissolved in 50 mM Tris-HCl buffer (pH 8.0) containing 1 mM DTT and 0.2 mM NADPH. FBPase was assayed in a reaction mixture containing 50 mM Tris-HCl (pH 8.0); 10mM MgCl₂; 5 mM DTT; 1 mM EDTA; 0.5 mM NADP; 1 mM fructose-1, 6-bisphosphate; 10 units each of glucose phosphate isomerase and

glucose-6-phosphate dehydrogenase and the enzyme extract. The reaction was started by adding 0.06 μ mol of fructose-1, 6-bisphosphate and the absorbance at 366 nm was recorded.

Sucrose phosphate synthase (SPsynthase) activity

SPsynthase was assayed by the method described by Huber (1981). The leaf tissue (5 g) was homogenised using a mortar and pestle in 5 ml of the extraction buffer containing 100 mM HEPES (pH 7.5), 5 mM MgCl_2 , 1 mM EDTA, 25 mM β -mercaptoethanol, 1 mM PMSF and 0.02 % Triton-X-100. The homogenate was filtered through Whatman filter paper and the filtrate was centrifuged at 13000 g for 10 min. The supernatant was desalted using the sephadex G-25 column and equilibrated with the extraction buffer containing Triton-X-100. The elute was centrifuged at 2500 g for 5 min and the supernatant was used for the assay. 50 μ l of the enzyme extract was added to 100 μ l of assay buffer containing 50 mM HEPES (pH 7.5), 5 mM MgCl_2 , 4 mM fructose-6-phosphate, 5mM UDP-glucose and 20mM glucose-6-phosphate and incubated at 25 $^{\circ}\text{C}$ for 20 min. The reaction was terminated by adding 100 μ l of 30 % potassium hydroxide. The reaction mixture was incubated at 40 $^{\circ}\text{C}$ for 20 min on a water bath and the absorbance of the solution was read at 620 nm.

Leaf starch and total carbohydrates measurements

Starch and total carbohydrates were estimated according to Hodge and Hofreiter (1962). Leaf disks (3 cm^2) were collected from the plants, immediately frozen in liquid nitrogen and stored at -80 $^{\circ}\text{C}$. Starch was extracted from the leaf tissues using 32% (v/v) perchloric acid and the total carbohydrates from the leaf sample were hydrolysed using dilute hydrochloric acid.

Transmission electron microscopy (TEM)

Leaf samples were fixed in 2.5 % glutaraldehyde in 0.05 M phosphate buffer (pH 7.2) for 24 hrs at 4 °C and post fixed in 0.5 % aqueous osmium tetroxide in the same buffer for 2 hrs. After the post fixation, samples were dehydrated in a series of graded alcohol, infiltrated and embedded in Araldite 6005 resin. Sections were taken using Leica Ultra cut microtome (UCT-GA-D/E-1/00). Ultra thin sections (50-70 nm) were mounted on grids for staining with saturated aqueous uranyl acetate and counter stained with 4% lead acetate and observed under transmission electron microscope (Hitachi H-7500, Japan).

Statistical analysis

Results were represented as mean \pm SE. The significance of the difference between mean values of ambient and elevated CO₂ plants was determined using paired *t*-tests. Correlation coefficient (*r*) and coefficient of determination (*r*²) of linear relationships between the investigated parameters were established by using linear regression. The linear regression slopes were analysed using bivariate correlation significance tests. Data were analyzed by multivariate analysis of variance (ANOVA). All the statistical analysis was performed using statistical package Sigma Plot 11.0.

Results

RUBPcase and CA activities

Changes in biochemical indices were recorded at regular intervals during 120 days of exposure to elevated CO₂. Initial and total RUBPcase activity of the leaf samples at midday for *Gmelina* grown under ambient and elevated CO₂ were shown in Figures 11. Initial and total RUBPcase activity showed a progressive increase during 120 days of treatment. *Gmelina* plants grown under elevated CO₂, showed 48% ($p < 0.05$) and 44% ($p < 0.05$) higher initial and total activity, respectively, compared to the plants grown under ambient CO₂ (Fig. 11 A and B). In the initial days of experiments (60 DAP), no significant changes (only 8.6 %) in CA activity were recorded in *Gmelina* leaves grown under ambient and elevated CO₂. Thereafter, a progressive increase in the CA was recorded in leaves and the enzyme activity was significantly higher (61 % $p < 0.05$) on 120 DAP in plants under elevated CO₂ (Fig. 12 A). This increase in the enzyme activity was also depicted the in-gel assay of CA which showed a high intensity of fluorescence compared to ambient grown plant leaf extracts (Fig. 12 C).

P_n in relation to activities of RUBPcase and CA

The values of P_n and RUBPcase initial activities when plotted together showed a strong positive correlation ($r^2=0.95$ $p < 0.001$) under elevated CO₂ (Fig. 13A). Strong positive correlation ($r^2=0.95$ $p < 0.001$) was also recorded between P_n and total activity of RUBPcase under elevated CO₂-grown *Gmelina* (Fig. 13B). Figure 13 shows the linear relationships between CA vs. P_n (Fig. 13C) and CA vs. RUBPcase activity (Fig. 13D). P_n was strongly correlated with the CA activity ($r^2=0.94$ $p < 0.001$) in the young *Gmelina* plants grown under elevated CO₂ when compared with ambient CO₂ grown plants ($r^2=0.86$ $p < 0.001$). The activities of CA and

RUBPcase shared a positive linear correlation under ambient conditions ($r^2=0.84$ $p<0.15$). However, the correlation was found to be much stronger in case of elevated CO₂-grown plants ($r^2=0.95$ $p<0.001$).

Photosynthetic rate as a function of carbonic anhydrase activity and stomatal conductance

P_n in *Gmelina* leaves were intimately linked to CA activity and g_s . The combined effects of these processes were illustrated in Figure 14 A and B for ambient and elevated CO₂ conditions respectively. The plants grown under ambient CO₂ conditions showed an increase in P_n with a slight increase in g_s and CA activity (Figure 14A). P_n significantly increased even when the g_s was reduced in the plants grown under elevated CO₂ and concomitantly a progressive increase in the activity of the CA was also recorded (Fig. 14 B).

FBPase, SPsynthase and Hexokinase activities

The activities of fructose 1,6-bisphosphatase, sucrose phosphate synthase and hexokinase in the elevated CO₂ -grown plants were significantly high when compared to plants under ambient CO₂ (Fig. 15). Similar to RUBPcase and CA activities, in the initial days of experiments (60 DAP), no significant changes (only 0.8 %) in activities of hexokinase, FBPase and SPsynthase were recorded in *Gmelina* leaves grown under ambient and elevated CO₂. Thereafter, a progressive increase in the hexokinase was recorded in leaves and the enzyme activity was significantly higher (37.5 % $p<0.05$) on 120 DAP in plants under elevated CO₂ (Fig. 15 A). FBPase was ~ 75 % higher in elevated CO₂-grown plants, a significant increase ($P<0.001$) when compared to ambient CO₂-grown plants (Fig. 15 B). Elevated CO₂ -grown plants showed ~30% higher activity of SPsynthase compared to ambient CO₂ -grown plants (Fig. 15 C).

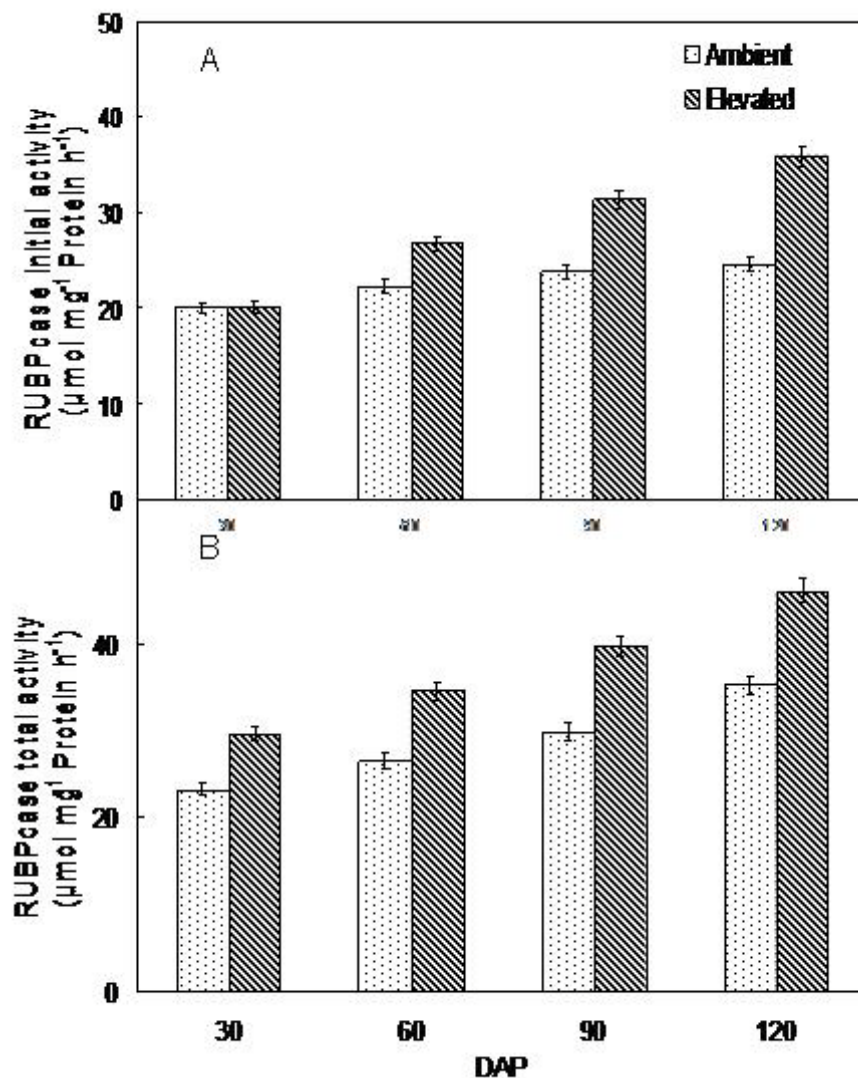


Fig. 11. Initial (A) and total activity (B) of RUBPcase in leaves of young *Gmelina* grown at ambient and elevated CO₂ concentrations. Activities were determined at regular intervals during 120 days of CO₂ treatment for three consecutive years. Values are mean \pm standard deviations.

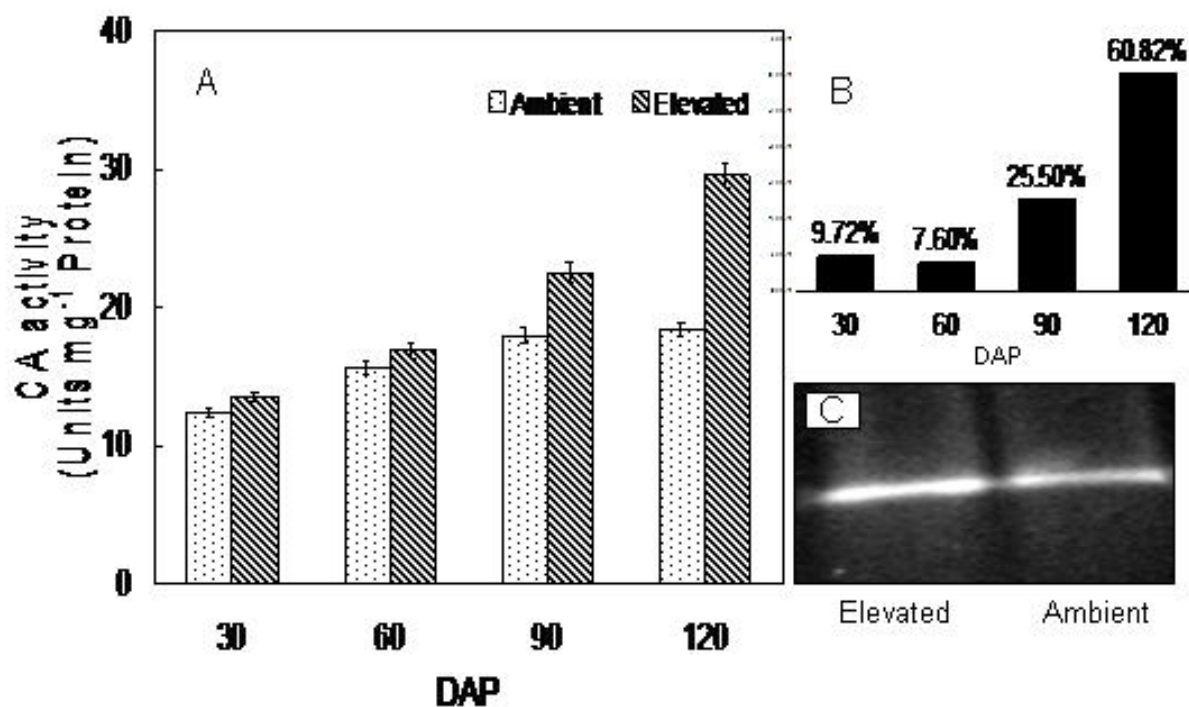


Fig 12. (A) Carbonic anhydrase (CA) activity in the leaves of young *Gmelina* grown at ambient and elevated CO₂ concentrations. Activity was measured at regular intervals during 120 days of experiment for consecutive three years. Values are mean \pm standard deviations. (B) Time dependent increase (in terms of percentage) in carbonic anhydrase (CA) activity as observed in elevated CO₂- grown *Gmelina* compared to ambient-grown counterparts. Values are mean \pm standard deviations. (C) In-gel assay depicting carbonic anhydrase activity. The band corresponding to CA from the leaf extracts of elevated CO₂-grown plants showed high intensity of fluorescence.

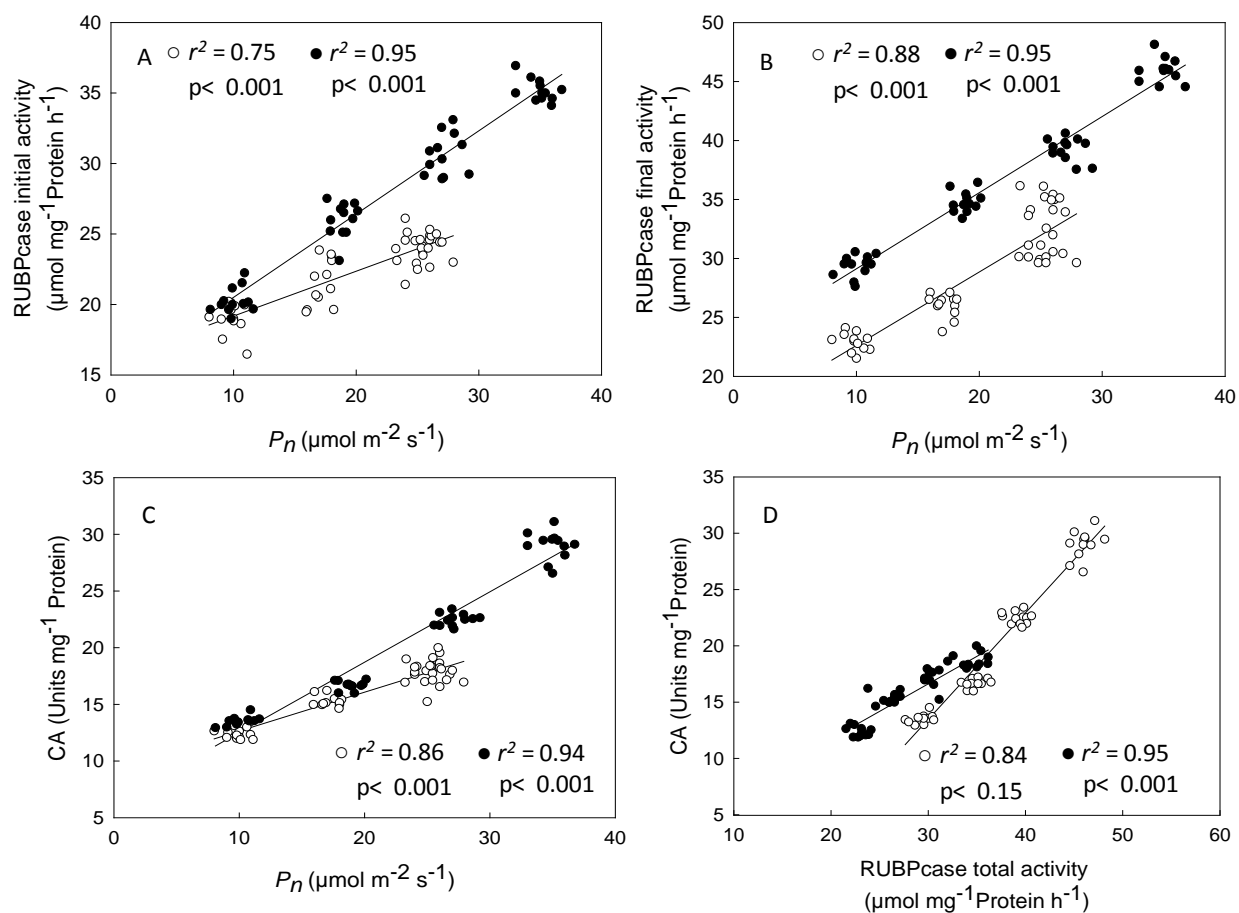


Fig 13. Correlation analysis between (A) RUBPcase initial activity and photosynthetic rates P_n , (B) RUBPcase total activity and photosynthetic rates P_n , (C) CA activity and photosynthetic rates P_n , (D) carbonic anhydrase (CA) activity and RUBPcase total activity in young *Gmelina* under ambient and elevated CO₂ conditions (○ ambient; ● elevated).

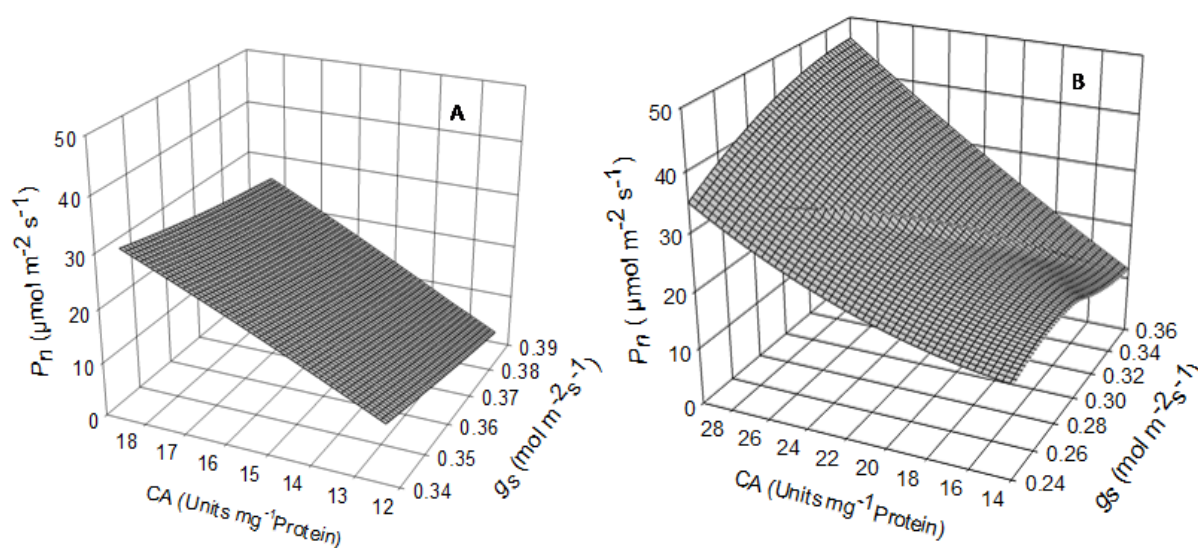


Fig 14. Three dimensional plot analysis showing photosynthetic rates (P_n) as a function of carbonic anhydrase (CA) activity and stomatal conductance (g_s) in young *Gmelina* grown under ambient (A) and elevated CO_2 (B).

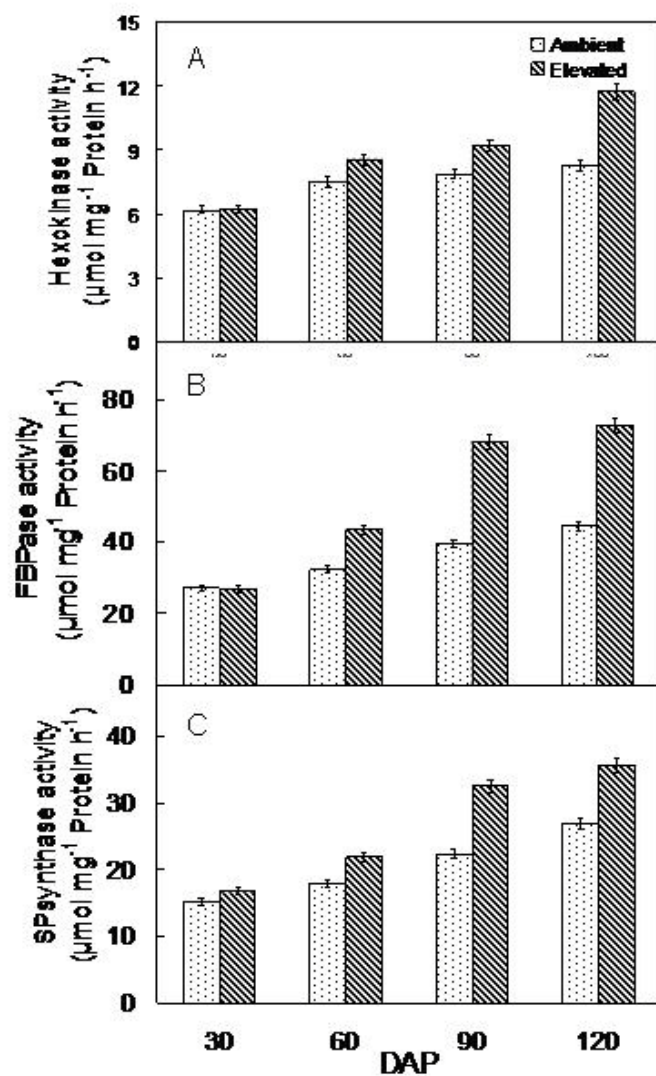


Fig. 15. Activities of hexokinase (A), Fructose-1, 6-bisphosphatase (FBPase) (B) and sucrose phosphate synthase (SPsynthase) (C) in leaves of *Gmelina* grown under ambient and elevated CO_2 atmosphere. Values are mean \pm standard deviations.

Total carbohydrates and Starch content

The starch content in the leaves grown under elevated CO₂ increased up to ~54 % ($p < 0.01$) and total carbohydrates up to ~ 17 % ($p < 0.05$) (Fig. 16 A and B). Figure 16 C and E shows the leaves of *Gmelina* harvested at 15:00 h from ambient and elevated CO₂ chambers. Figure 16 F represents transmission electron micrograph picture of *Gmelina* leaves grown under elevated CO₂ depicting conspicuous starch granule, filling the whole chloroplast, compared to their counterparts grown under ambient conditions (Fig. 16 D).

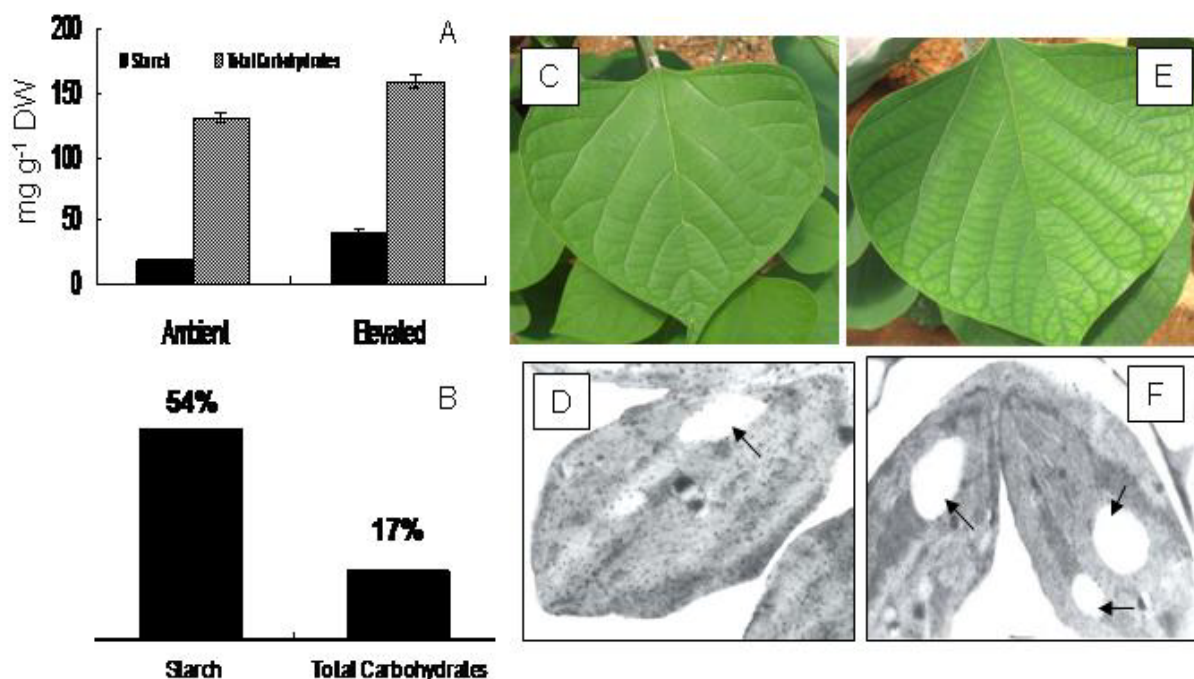


Fig 16. (A) Starch and total carbohydrate concentrations in leaves of *Gmelina* grown under ambient and elevated CO₂ atmosphere. Values are mean \pm standard deviations. (B) Percentage increment in starch and total carbohydrates concentrations in the leaves of elevated CO₂ grown *Gmelina*. Single leaf morphology of *Gmelina* grown under ambient (C) and elevated CO₂ atmosphere (E). Note the yellowish tint observed in *Gmelina* leaf grown under elevated CO₂ due to accumulation of copious starch granules. Transmission electron micrograph of chloroplasts of *Gmelina* grown under ambient and elevated CO₂ atmosphere, showing conspicuous starch granules in *Gmelina* grown under elevated CO₂ atmosphere (F) compared to ambient (D).

Discussion

The effective increase in photosynthetic rates in elevated CO₂-grown *Gmelina* was mainly believed to be due to accelerated internal photosynthetic biochemistry. The increase in photosynthetic rates under elevated CO₂, despite the decrease in *g_s* was also believed to be due to the maintenance of a constant *C_i/C_a* and effective capture and assimilation of *C_i* (Farquhar and Sharkey, 1982; Assmann, 1999; Herrick *et al.*, 2004). It has been propounded that enzymatic processes like modulation of rubisco activity and expression of certain other key photosynthetic enzymes probably play an important role in influencing the guard cell responses to *C_i* saturation and prevention of down regulation of *P_n* in young tree species under elevated CO₂ atmosphere (Coleman, 2000; von Caemmerer and Quick 2000; Warren and Adams, 2004; Messinger *et al.*, 2006). Although internal CO₂ concentration (*C_i*) influences the rate of CO₂ fixation in chloroplasts, the initial assimilation of CO₂ is known to occur in mesophyll cells (Li *et al.*, 2004). This initial assimilation of *C_i* is catalysed by CA, which plays an important role in accelerating carbon assimilation by catalyzing the reversible interconversion of CO₂ and HCO₃⁻ and preventing the *C_i* saturation (Coleman, 2000).

CA rapidly interconverts the major form of *C_i* and maintains the supply of CO₂ for rubisco by speeding the dehydration of HCO₃⁻ in the stroma. In this study, *Gmelina* showed a dynamic increase in the activity of the CA in elevated CO₂ atmosphere. Very little is known about any increase in CA activity in plants grown under elevated CO₂ (Sicher, 1994). In the initial days of CO₂ exposure, no significant changes in CA activity was observed and later, progressive increase in the activity was recorded in our study (Fig. 12A) which was well related to *C_i* concentrations in *Gmelina*. The increase in the *C_i* concomitant with radical increase in CA activity might lead

an upsurge in the rubisco activity. The activity of RUBPcase in *Gmelina* grown under enriched CO₂ was significantly high at 120 DAP, associated in an absonant increase in P_n (~35 $\mu\text{mol m}^{-2} \text{s}^{-1}$), when compared to the plants grown under ambient CO₂. The significant linear correlations between CA activity and P_n as well as between CA and RUBPcase activities indicate that CA might regulate the photosynthetic capacity under elevated CO₂. P_n as a function of CA and g_s as observed in our study suggests that despite decrease in the stomatal conductance under elevated CO₂, the plants showed high photosynthetic activity which could be attributed to the efficacy of CA in maintaining supply of CO₂ to RUBPcase (Fig. 14). These observations indicate that CA in *Gmelina* plants grown under elevated CO₂ concentrations might play a pivotal role in preventing the acclimation of photosynthesis due to the limitation in the stomatal conductance and C_i saturation.

Our results also demonstrate that photosynthetic down regulation was not observed in *Gmelina* plants grown under elevated CO₂. We believe that this lack of down regulation should be due to greater sink demand. In spite of increase in starch and sucrose concentrations in the leaves of plants grown at elevated CO₂, the high CO₂-grown plants showed significantly high P_n . The carbohydrate-derived signals were usually observed to down regulate photosynthetic machinery (Long *et al.*, 2004), but rapidly growing young tree species were considered to be 'source-limited' which can utilize the additional carbohydrates resulting from enhanced CO₂ for growth (Davey *et al.*, 2006; Ainsworth and Rogers, 2007). Starch content was significantly higher in elevated CO₂-grown *Gmelina* plants at 15:00 h compared with the ambient CO₂-grown plants. An increase in the total carbohydrates and sucrose was also observed during the mid day. The activities of key carbohydrate metabolising enzymes like FBPase, SPsynthase and hexokinase were also significantly high in the plants grown under elevated CO₂ atmosphere compared to

those grown under ambient CO₂. These enzymes could play a major role in preventing the accumulation of carbohydrates including starch, leading to effective growth and development (Lee *et al.*, 2008). Our results clearly suggest that significantly high rates of photosynthesis in *Gmelina* under elevated CO₂ resulted in greater accumulation of carbohydrates which in-turn could result in significantly high photosynthetic productivity.

Conclusions

1. *Gmelina* grown under the elevated CO₂ atmosphere showed a dynamic increase in the activity of the CA.
2. In the initial days of CO₂ exposure, no significant changes in CA activity were observed. Later on, progressive increase in the CA activity was recorded which was well related to *Ci* concentrations in *Gmelina* under elevated CO₂.
3. The significant increase in the activities of CA associated with *Ci* was believed to increase the activities of RUBPcase.
4. The significant linear correlation between CA vs. P_n and CA vs. RUBPcase activity indicates that CA regulates the photosynthetic capacity in *Gmelina* grown under elevated CO₂.
5. The increase in starch and sucrose concentrations in the leaves of *Gmelina* grown at elevated CO₂ atmosphere was due to increased photosynthetic rates.
6. The activities of key carbohydrate metabolising enzymes including FBPase, SPsynthase and hexokinase were also significantly high in plants grown under elevated CO₂.
7. Photosynthetic down regulation was not observed in *Gmelina* plants grown under elevated CO₂ probably due to high sink demand.

Chapter 4
Growth, biomass and carbon sequestration efficacy in
***Gmelina* under ambient and elevated CO₂ concentrations**

Chapter 4

Growth, biomass and carbon sequestration efficacy in *Gmelina* under ambient and elevated CO₂ concentrations

Introduction

The rising CO₂ levels affects plant growth and development primarily due to changes in photosynthetic carbon assimilation patterns. Studies under elevated CO₂ showed substantial increase in net leaf photosynthetic CO₂ uptake in plants because the rubisco is not CO₂-saturated with the present atmospheric CO₂ (Drake *et al.*, 1997; Ainsworth *et al.*, 2004). However, this increased photosynthetic potential was realized to be down-regulated in many crop plants due inadequate “sink” capacity. “Sink” is defined as the parts of the plant that at a given stage of development are utilizing photosynthate in storage, construction, or respiration. Changes in photosynthetic rates and acclimatory responses in plants grown under elevated CO₂ concentration could also be attributed to the feedback metabolic control wherein large accumulation of foliar starch and other carbohydrates could inhibit CO₂ assimilation rates (Gunderson *et al.*, 2002). The plants with potential sinks for carbohydrate translocation and accumulation showed no down regulation of photosynthetic capacity, suggesting that imbalances in source–sink could be attributed to the variations in the photosynthetic acclimation in plants (Ainsworth and Rogers, 2007).

The possible occurrence of photosynthetic acclimation in plants can be explained by studying plant source-sink relationships. The degree to which plants exhibit photosynthetic down regulation when grown under elevated CO₂ may be related to physiological growth level and to resource allocation within the plant (Sholtis *et al.*, 2004). In plants, resources must be partitioned between light-harvesting and non-harvesting components, which can explain at a broader scale that resources must be allocated between the net exporters of photosynthate (sources) and net

importers (sinks), characterized as new roots, shoots and leaves. Maintenance of active sinks is necessary for the effective stimulation of photosynthesis (Stitt, 1991). The increased production of carbohydrates induced by higher photosynthetic rates in elevated CO₂ can be sustained only with continued translocation of photosynthates to active sink material (Wolfe *et al.*, 1998). An imbalance in the source –sink relationship can result in an accumulation of leaf carbohydrates which may trigger feedback mechanism that reduces photosynthetic capacity (Sholtis *et al.*, 2004).

Among the C₃ plants, photosynthetic rates of trees grown under elevated CO₂ have been shown to increase by up to 50% (Gunderson *et al.*, 2002; Long *et al.*, 2004) especially, fast growing tree species were found to utilize the accumulated carbohydrates and starch for enhancement in growth, primarily, as they are source-limited (Ainsworth and Rogers, 2007, Davey *et al.*, 2006, Korner, 2006). This chapter of our study elucidates the physiological basis of high biomass production of fast growing tree species, *Gmelina* grown under elevated CO₂. To determine the relation between the plant growth characteristics and photosynthesis, we correlated the biomass parameters of ambient and elevated CO₂-grown *Gmelina* with respective photosynthetic rates. The information about yield-defining traits is needed to provide silvicultural recommendations for producing high biomass from the fast growing tree species under future fast changing climate conditions and for future energy source.

Methods

Non-destructive measurements

Non-destructive measurements were made on the developing shoots at approximately 25-30 days intervals. The height of the main stem (measured vertically from substrate surface till apical meristem [cm]) of each tree was measured with a paper ruler to avoid damage to the stem and leaves. The number of braches was calculated and the length of all the branches of a plant was added to obtain the total shoot length (TSL). In addition, the main stem diameter was measured at a consistent point 0.5cm above the base of the stem using the callipers.

Destructive harvest and Biomass determination

Total plant biomass was determined destructively on four successive harvest dates (30,60,90 and 120 days from the start of the experiment) using four trees per chamber which were selected at random from within the four plants in each chamber. At each harvest, plants were separated into leaves and stems. Fresh weight was measured immediately. The dry weights of individual plant stems and leaves were obtained after oven drying for 48h at 85 °C. Soil was then excavated so that roots could be separated from soil and collected from a 1m x 1m x 1m volume around the plant base. The roots were then air dried in the laboratory to enable adhered soil particles to be removed by hand and was then oven dried. The above-ground and root biomass were added to derive total plant biomass. Absolute growth rate (AGR), the rate of increase in dry matter per plant per unit time was calculated according to Radford, (1967). AGR was expressed in $\text{g plant}^{-1} \text{day}^{-1}$. $\text{AGR} = (W_2 - W_1) / (t_2 - t_1)$ where W_1 = Dry weight (mass) of plant in g at time t_1 ; and W_2 = Dry weight (mass) of plant in g at time t_2 . Relative height growth rate (RHGR) and stem basal diameter growth rate (SDGR) were calculated every month as; $\text{RHGR} = (H_2 - H_1) / (t_2 - t_1)$ where H_1

= Height of the plant in cm at time t_1 and H_2 = Height of the plant in cm at time t_2 ; $SDGR = (D_2 - D_1) / (t_2 - t_1)$ where D_1 = Basal diameter in cm at time t_1 and D_2 = Basal diameter in cm at time t_2 .

Biomass allocation

Biomass allocation to leaves, stem and roots was calculated as the proportion of the total fresh and dry biomass invested in these plants. The leaf biomass used to calculate the allocation to leaves excluding that of leaves shed before the end of the experiment.

Carbon content in above ground biomass

The estimation of the biomass and carbon content in the stem were determined using the tree height, diameter and basal girth of the tree. The volume of individual trees was estimated according to Newbould, (1967): Volume = basal area x total height x 0.5. Specific gravity (SG) of the wood was calculated using the oven dry weight and the volume of the wood ($SG = \text{Oven dry weight} / \text{volume}$) (Negi *et al.*, 2003). The above ground biomass stock and above ground carbon of the trees was calculated using volume of biomass and specific gravity of the trees as per Rajput *et al.*, (1996) and Negi *et al.*, (2003). Biomass (g) = Volume of biomass (m^3) x Specific gravity (SG). The average carbon content was generally 50% of the tree's biomass and the carbon dioxide sequestered by tree was calculated as the weight of carbon in the tree x 3.663.

Statistical analysis

The data on height, biomass parameters and absolute growth rates were analyzed by two-way analysis of variance (ANOVA) with CO_2 and time of treatment as the main factors. The significance of the difference between mean values of ambient and elevated CO_2 plants was

determined using Paired *t*-tests. Correlation coefficient (*r*) and coefficient of determination (r^2) of linear relationships between the investigated parameters were established by using linear regression. The linear regression slopes were analysed using bivariate correlation significance tests. All the statistical analysis was performed using statistical package Sigma Plot 11.0.

Results

Non-destructive measurements

Plant height was significantly ($p < 0.001$) increased after 90 days of growth in elevated CO_2 atmosphere (Table 4; Fig. 17A) which continued until harvest (120 DAP), when trees were ~42% taller than those grown in ambient CO_2 concentrations (Fig. 17A). Concurrent with this was an enhancement of main stem basal diameter (Fig. 17B) which was again significantly ($p < 0.001$) high at 90 DAP and 120 DAP in plants grown under elevated CO_2 compared to ambient CO_2 -grown plants. The basal stem diameter at 120 DAP in elevated CO_2 -grown plants was ~ 28cm which was ~ 52% high compared to ambient CO_2 -grown plants (Fig. 17B). The PHGR depicts typically that the significant ($p < 0.001$) growth rate was observed after 90 DAP in plants grown under elevated CO_2 compared to ambient CO_2 - grown plants (Fig. 17C). After 120 DAP, plants grown under elevated CO_2 atmosphere showed significantly greater plant height growth rate (~40%, $p < 0.001$) when compared to ambient CO_2 - grown plants. SDGR showed significant ($p < 0.001$) increase after 60 DAP in plants grown under elevated CO_2 (Fig. 17D). SDGR was ~ 0.3 $\text{cm day}^{-1} \text{ plant}^{-1}$ at 120 DAP in elevated CO_2 -grown plants which was ~46 % high when compared to ambient CO_2 -grown plants. Figure 17E and F depicts data on *Gmelina* grown under ambient and elevated CO_2 conditions respectively at 120DAP. The plants grown under ambient CO_2 conditions have grown to a height of ~210 cm after 120 DAP whereas, elevated CO_2 -grown plants were much taller (~ 360 cm after 120 DAP). More number of branches were also observed in elevated CO_2 -grown plants when compared to ambient CO_2 -grown plants. The plants in inset (Fig. 17G and H) depict 30DAP condition where ambient and elevated CO_2 concentration showed no-significant (n.s) differences in height and number of branches. Single leaf morphology of *Gmelina* grown under ambient (Fig. 17I) and elevated CO_2

atmosphere was shown in figure 17J. Note the significant leaf size increase observed in the leaf of *Gmelina* grown under elevated CO₂ compared to ambient CO₂-grown plants. Figure 17K and L portray the basal stem diameter of ambient and elevated CO₂-grown plants. The basal diameter was significantly ($p < 0.001$) high in elevated CO₂-grown plants compared to ambient CO₂-grown plants.

Destructive harvest and Biomass determination

Elevated CO₂ had significant effects on the total biomass per tree and the biomass of individual organs ($p < 0.001$, Table 4; Fig. 18). Fresh weights of leaf (Fig. 18 A), stem (Fig. 18 B) and root (Fig. 18 C) were significantly high in elevated CO₂-grown plants compared to ambient CO₂ grown plants. A distinctive difference was not observed until 90 DAP in fresh weights under both ambient and elevated CO₂-grown plants. After 90 DAP plants under elevated CO₂ showed a ~40% increase in fresh weight (Fig. 18 A). The total stem fresh weight was ~23kg during 120 DAP in elevated CO₂-grown plants, which was ~42% more compared to ambient CO₂-grown plants (Fig. 18 B). Root fresh weight was also significantly ($p < 0.001$) increased by 90 days of treatment under elevated CO₂ (Table 4; Fig. 18 C). Plants grown under elevated CO₂ atmosphere showed ~40% more fresh root weight compared to ambient CO₂-grown plants after 120 days of treatment (Fig. 18 C). The dry weights of individual organs also showed the typical pattern as of fresh weights. A significant ($p < 0.001$) increase in dry weights were observed after 90 DAP (Table 4; Fig 18). Interestingly, leaf dry weight was ~ 45% high in elevated CO₂ atmosphere after 120 days of treatment when compared with the corresponding ambient CO₂-grown plants (Fig. 18 D). During initial 30 days of treatment there was no significant difference in the total stem dry weight in both ambient and elevated CO₂-grown plants (Fig. 18 E). After 120 days of

treatment, the elevated CO₂-grown plants showed a significant ($p < 0.001$) increase in dry weights (~40.6%) compared to ambient CO₂-grown plants. At 30 DAP, the root dry weight was ~0.3kg in both ambient and elevated CO₂ grown plants, a statistically non-significant difference but by 90 DAP the increase in the root dry weights was significantly ($p < 0.001$) high in elevated CO₂-grown plants compared to ambient CO₂-grown plants (Fig. 18 F). Total above ground fresh biomass also showed same trend as of fresh and dry weights of individual organs. TAGFB started to increase after 90 days of treatment in elevated and ambient CO₂-grown plants (Fig.18 G). After 120 days of treatment TAGFB was highest in elevated CO₂ grown plants accounting for ~32% more when compared to ambient CO₂-grown plants (Table 4; Fig. 18 G). The TAGDB was ~45% high in elevated CO₂-grown plants when compared with ambient CO₂-grown plants (Table 4; Fig. 18 H). Figure 18 I and J depicts the total fresh and dry biomass in plants grown under ambient and elevated CO₂ atmosphere. TFB was significantly ($p < 0.001$) high in elevated CO₂-grown plants after 120 days of treatment when compared to ambient CO₂-grown plants (Table 4; Fig. 18 I). TDB was ~13 kg in elevated CO₂- grown plants which was ~53% more when compared to ambient CO₂-grown plants (Table 4; Fig. 18 J).

Absolute growth rate, above ground biomass and carbon sequestration potential

The plants grown under elevated CO₂ showed a significant ($p < 0.001$) effect on absolute growth rate (Table 4; Fig. 19A). After 90 days of treatment, the absolute growth rate in elevated CO₂-grown plants was ~150 g plant⁻¹ day⁻¹, which was ~65% high when compared to ambient CO₂-grown plants. By 120 days of treatment the AGR was ~45% high in elevated CO₂- grown plants (~ 162 g plant⁻¹ day⁻¹) when compared with ambient CO₂-grown plants (~90 g plant⁻¹ day⁻¹). The above ground biomass was significantly high ($p < 0.001$) in elevated CO₂-grown plants compared

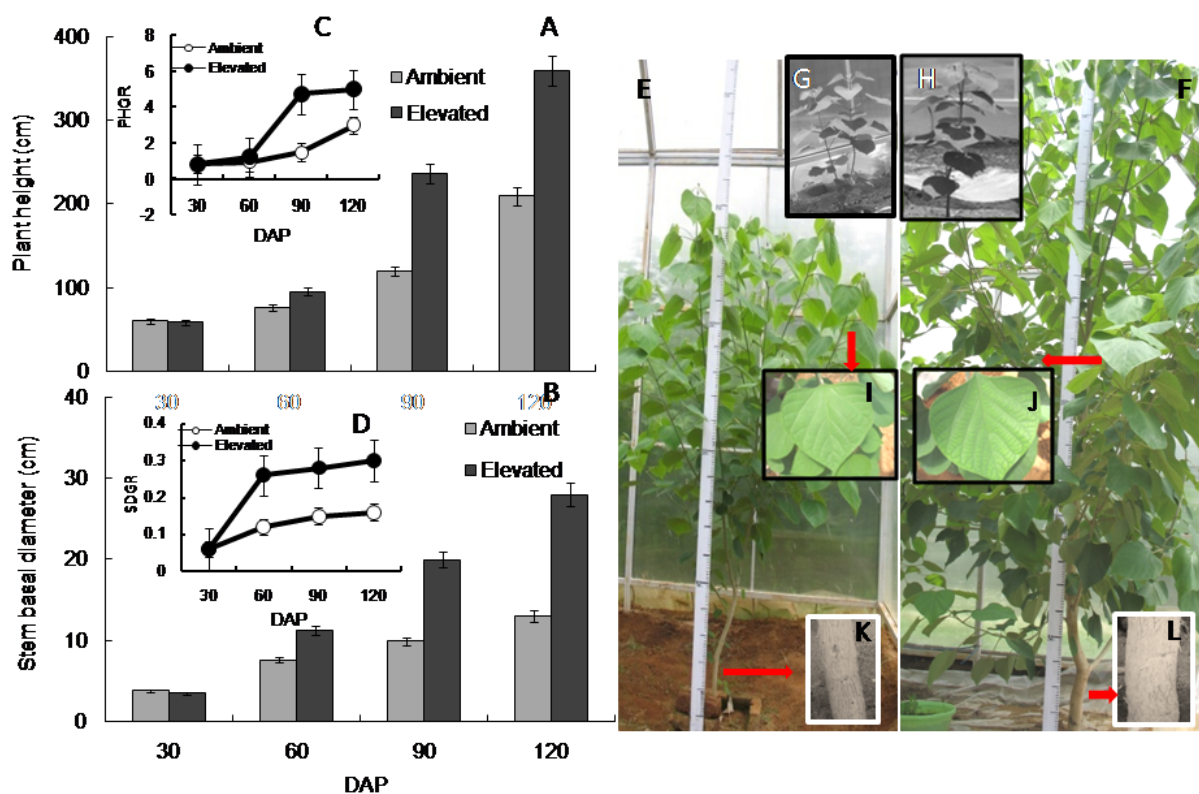


Fig.17 Comparative growth morphology of *Gmelina* grown in OTCs of ambient and elevated CO₂ atmosphere. Plant height (A) and basal stem diameter (B). Note the vigorous enhancement in plant height growth rate (C) and stem diameter growth rate (D) in elevated CO₂ - grown *Gmelina* compared to ambient. Five-months-old *Gmelina arborea* plants grown in open top chambers under Ambient (E) and Elevated (F) CO₂ concentrations. Inset G and H depict one – month-old *Gmelina* grown under ambient and elevated CO₂ respectively. Single leaf morphology of *Gmelina* grown under ambient (Inset I) and elevated CO₂ (Inset J). K and L depict the basal stem diameter in ambient and elevated CO₂-grown plants respectively.

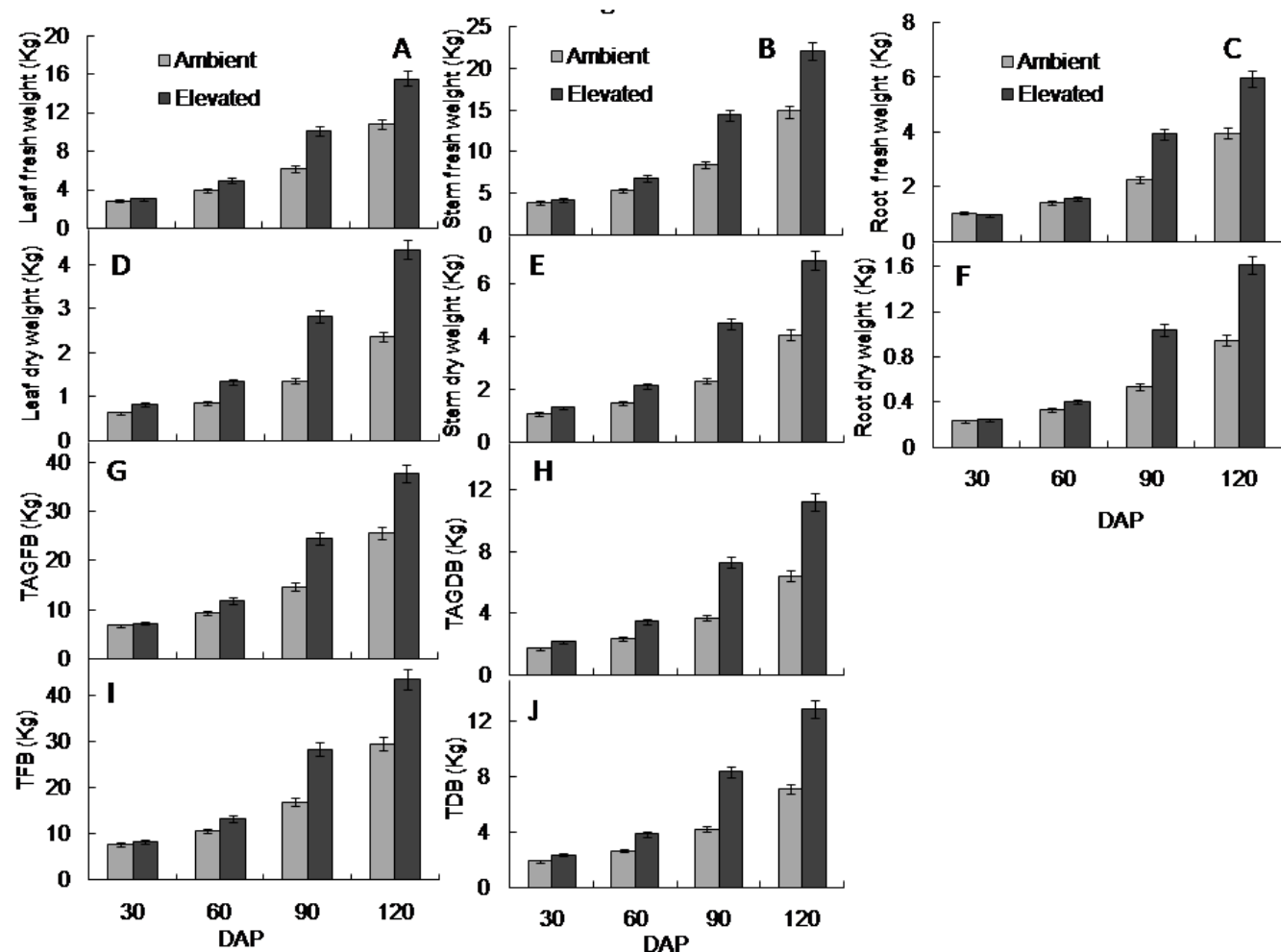


Fig. 18. Analysis of various growth and yield components of *Gmelina* grown under ambient and elevated CO₂ concentrations. The parameters investigated were (A) leaf fresh weight (kg), (B) stem fresh weight (kg), (C) root fresh weight (kg), (D) leaf dry weight (kg), (E) stem dry weight (kg), (F) root dry weight (kg), (G) Total Above Ground Fresh Biomass (TAGFB) (kg), (H) Total Above Ground Dry Biomass (TAGDB) (kg), (I) Total Fresh Biomass (TFB) (kg) and (J) Total Dry Biomass (kg). Values are mean \pm standard deviations.

Table 4 Effects of elevated CO₂ on the biomass of *Gmelina* during the growth period. Significance levels from ANOVA for CO₂, Time, Time x CO₂; *** p<0.001, **p<0.01, * p<0.05.

Source of variance	Time	CO ₂	Time x CO ₂
Height	**	***	***
Stem biomass	**	***	***
Leaf biomass	**	***	***
Root biomass	*	**	***
Total above ground biomass	*	**	***
Total biomass	**	***	***
Absolute growth rate	**	***	***

to ambient CO₂-grown plants (Fig. 19 B). ~1200 g of biomass was accumulated after 120 days of treatment in plants grown under elevated CO₂ atmosphere which is ~49% high compared to that of ambient counter parts (Fig. 19 B). ~ 2kg of CO₂ was sequestered per tree after 120 days of CO₂ treatment (Fig. 19 C). The efficiency of carbon sequestration was significantly high ($p < 0.001$) in elevated CO₂-grown plants when compared to ambient CO₂-grown plants (Fig. 19 C). After 90 days of treatment, the carbon sequestered in elevated CO₂-grown plants was ~ 1500g tree⁻¹ which increased to a level of ~ 2100 g tree⁻¹ after 120 days of treatment. During this period the ambient CO₂-grown plants could sequester ~ 1000g tree⁻¹ which was ~48% less when compared to the elevated CO₂ conditions (Fig. 19 C).

Pn in relation to TDB, AGR, stem dry weight and TAGDB

The relationships were established between *Pn*, TDB, AGR, stem dry weight and TAGDB to obtain productivity rates in relation to photosynthetic physiology in *Gmelina* grown under ambient and elevated CO₂-conditions (Fig 20). The Correlation coefficient of relationship between *Pn* and TDB was ~ 0.95 in elevated CO₂ grown plants which was significantly positive compared to ambient CO₂ grown plants ($r = 0.76$, $p < 0.01$) (Fig. 20 A). A strong positive correlation ($r = 0.92$, $p < 0.001$) was also observed in elevated CO₂ grown plants when *Pn* was related with AGR whereas, the ambient CO₂ grown plants showed only a weak correlation among them ($r = 0.78$) (Fig. 20 B). The correlation between TDB and AGR was significantly high in both ambient ($r = 0.95$, $p < 0.001$) and elevated CO₂ ($r = 0.91$, $p < 0.001$) grown plants (Fig. 20 C). The relationship between the stem basal diameter and stem dry weight showed a significant positive correlation in elevated CO₂ grown plants ($r = 0.97$, $p < 0.001$) compared to

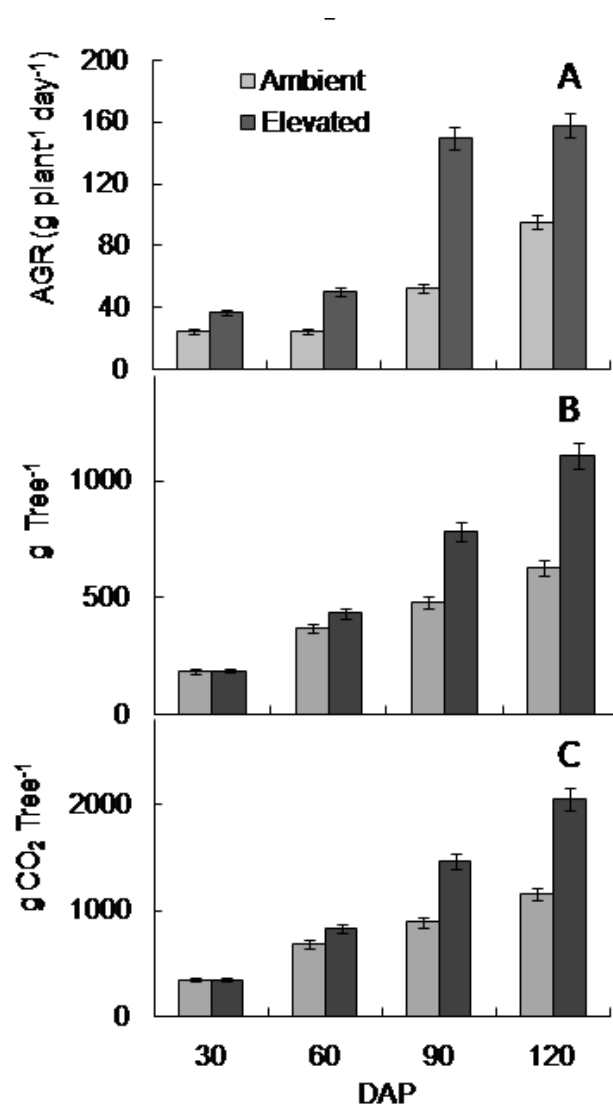


Fig.19. Absolute growth rate (AGR) (A), above ground biomass (g Tree⁻¹) (B) and CO₂ sequestered per tree (C) in *Gmelina* grown under ambient and elevated CO₂ atmosphere. Values are mean \pm standard deviations.

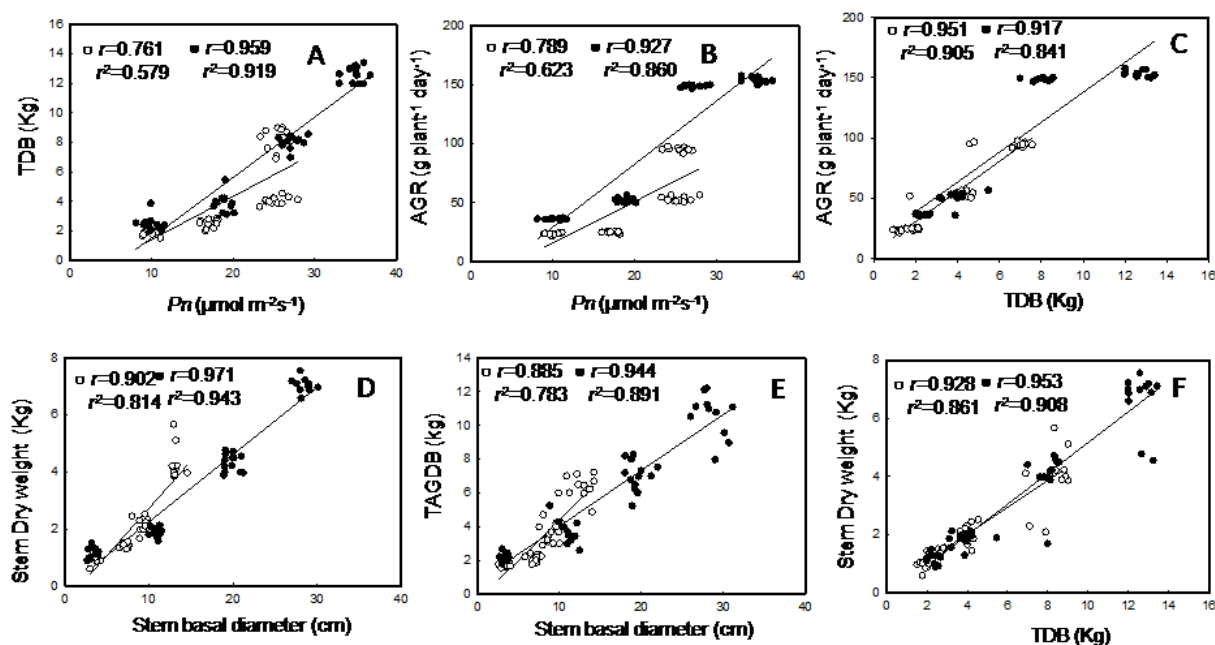


Fig. 20. Correlation analysis between (A) Total dry biomass (TDB) and photosynthetic rates (P_n), (B) Absolute growth rate (AGR) and P_n , (C) AGR and TDB, (D) stem dry weight and stem basal diameter, (E) total above ground dry biomass and stem basal diameter, (D) stem dry weight and TDB in *Gmelina* grown under ambient and elevated CO₂ conditions (○ ambient; ● elevated).

ambient CO₂ grown plants ($r = 0.90$, $p < 0.01$) (Fig. 20 D). Plants grown under elevated CO₂ atmosphere showed a significant positive correlation between stem basal diameter and TAGDB ($r = 0.94$; $p < 0.001$) (Fig. 20 E). The coefficient correlation between stem basal diameter and TAGDB was ~ 0.88 ($p < 0.010$) in ambient CO₂-grown plants (Fig. 20 E). The relationship between TDB and stem dry weight showed a strong correlation in both ambient ($r = 0.92$; $p < 0.001$) and elevated ($r = 0.95$; $p < 0.001$) CO₂ grown plants (Fig. 20 F).

Biomass allocation

Fresh biomass of stem accounted for an average of 50% (range 50-52%) of total fresh biomass in both ambient and elevated CO₂-grown plants (Fig. 21 A) while the biomass in root and foliage biomasses accounted to an average of 13.6% and 35.4 % respectively (Fig. 21 A). The dry biomass allocation also showed almost same pattern, where stem dry biomass accounted for 55.5% of total dry biomass. Root and leaf dry biomass accounted for 13 % and 33.6 % respectively (Fig. 21 B). The allocation strategy in different components of *Gmelina* grown under elevated and ambient CO₂ showed no significant variation. However, order of biomass allocation in different components at the end of two growing seasons was: stem>leaf>root (Fig. 21).

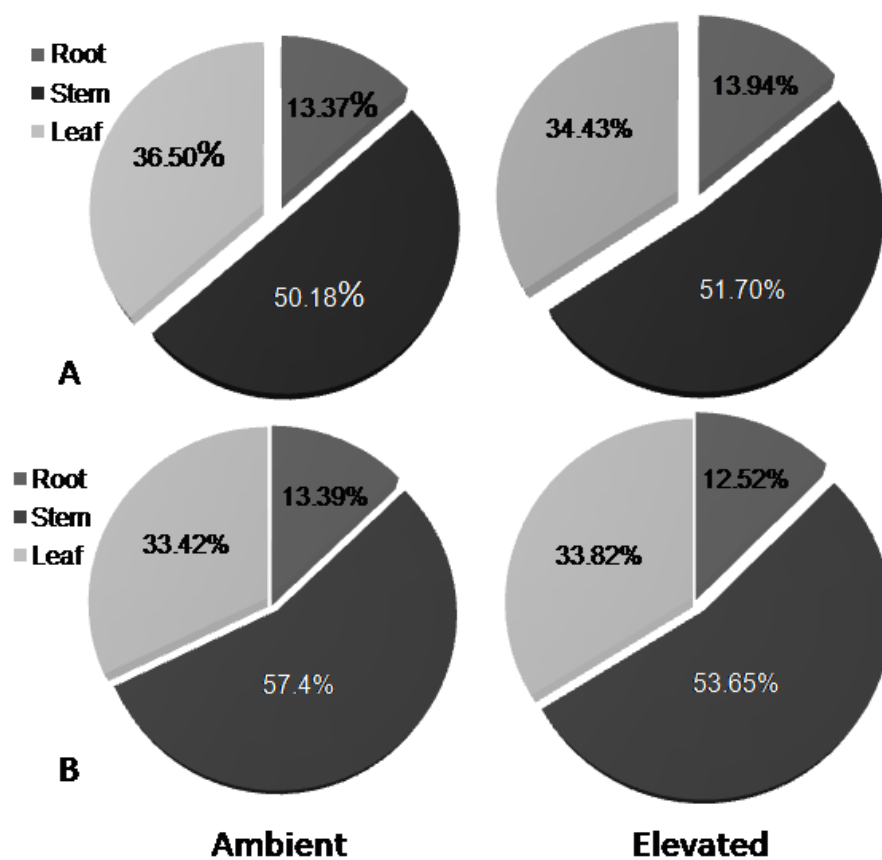


Fig. 21. Pie diagrams illustrating the percentage allocation of biomass in leaf, stem and root fresh weight (A) and dry weight (B) fractions of young *Gmelina* under ambient and elevated CO₂ conditions.

Discussion

The increasing levels of [CO₂] and its consequences on climate change prompted a renewed interest in increasing the size of carbon pools, especially in the tropics through planting fast growing trees. *Gmelina* is recognised as one among the potential tree species for effective carbon sequestration (Swamy *et al.*, 2003). In our study, the plant showed a positive growth response to elevated CO₂ throughout the experimentation. At the end of 120 days of high CO₂ treatment, *Gmelina* was ~ 42% taller and had 52% thicker stems in elevated CO₂ than those in ambient CO₂ (Fig. 17). Interestingly, the relative growth rates were also significantly high in elevated CO₂ grown plants after the initial period of 60 days (Fig. 17). Significant growth changes in plants grown under elevated CO₂ atmosphere can be attributed to increased availability of photosynthate leading to initiation of new sinks (Stitt, 1991).

Photosynthetic capacity of *Gmelina* progressively increased during the growth seasons under elevated CO₂ atmosphere. Coherently, the growth productivity was also enhanced indicating a sustained increase in carbon sinks under elevated CO₂. This increased growth under elevated CO₂ was also evidenced by significantly increased development of side shoots depicting the initiation of new sinks for better partitioning of carbohydrates. We noticed that increased number of branches resulted in greater crown size and structure of *Gmelina* under elevated CO₂ atmosphere. Profuse root growth and more number of secondary and tertiary roots in *Gmelina* under elevated CO₂ also showed the varied sink-source status of *Gmelina* plants. We attribute the positive correlation between photosynthesis and the morphological growth characteristics of *Gmelina* were due to its potential source-sink capacity. The extent to which sink metabolism responds to increased availability of carbohydrates will depend on genetic factors (Davey *et al.*,

2006) and age of the plant as suggested by Korner, (2006). Reduction in photosynthetic capacity under elevated CO₂ was not pronounced in young *Gmelina* which might be related to its fast and determinate juvenile growth pattern. In-turn, the high metabolic rates and storage sink activity in *Gmelina* might led to the sustained photosynthetic responses to elevated CO₂. Fast growing young tree species were found to be source-limited conjoined with high sink-strength (Davey *et al.*, 2006). The rapid growth of these plants could also effectively sequester CO₂ from the atmosphere through high foliar photosynthetic rates and store the additional carbohydrates for the enhanced growth and productivity as recorded in this study (Korner, 2006; Ainsworth and Rogers, 2007).

Elevated CO₂ atmosphere persistently enhanced the growth pattern in *Gmelina*. All the phenological characteristics including plant height, number of branches, internodes, internodal distance, aerial biomass and plant biomass increased significantly in the plants grown under elevated CO₂ suggesting that *Gmelina* plants have greater capacity for carbon sequestration and carbon accumulation. We believe that young *Gmelina* plants could act as sink for rising atmospheric CO₂ by fixing carbon through high photosynthetic rates and storing the excess carbon as biomass (Nowak and Crane, 2002; Jana *et al.*, 2009). Accordingly, *Gmelina* showed a significantly high carbon sequestration potential under elevated CO₂ atmosphere achieved through high absolute growth rate, effective CO₂ fixation and also through potent sink strength. *Gmelina* could store significantly high amount of carbon in the form of increased biomass. These results are very significant with respect to carbon sequestration studies. Our results clearly demonstrate that *Gmelina* had no acclimatory loss in the initial increase in photosynthetic rates under elevated CO₂, but had high biomass productivity. Fast growing coppice *Gmelina*

plantations could serve as a potential strategy to remove the CO₂ from the atmosphere and mitigate the global warming.

Conclusions

1. Elevated CO₂ atmosphere persistently enhanced the growth in *Gmelina*.
2. Profuse stem growth and more number of secondary and tertiary branches and roots in *Gmelina* under elevated CO₂ could serve as better sinks for more carbohydrates.
3. The substantial growth in *Gmelina* at elevated CO₂ concentrations was due to enhanced source activity in leaves and sufficient sink demand for photoassimilates.
4. The biomass allocation in *Gmelina* grown under elevated CO₂ atmosphere was high in the stem tissue compared to that of leaf or root tissues indicating that stem is the primary sink in *Gmelina*.
5. We conclude that *Gmelina* has greater potential for better sequestration of atmospheric carbon dioxide in a fast changing climate.

Chapter 5

Foliar proteomic changes in photosynthetic protein profile in response to elevated CO₂ concentrations

Chapter 5

Foliar proteomic changes in photosynthetic protein profile in response to elevated CO₂ concentrations

Introduction

Global atmospheric CO₂ is predicted to increase to 550 $\mu\text{mol mol}^{-1}$ by the end of this century (Prentice *et al.*, 2001), which could have a significant beneficial effect on plants as CO₂ assimilation could be enhanced under these condition. The morphological and physiological impacts of elevated CO₂ have been extensively studied in various plant species (Makino and Mae 1999; Long *et al.*, 2004). Photosynthesis was generally enhanced by elevated CO₂ and has also stimulated the growth and productivity in many crop plants (Ainsworth and Long, 2005). The net primary productivity of trees depends on the growth patterns, which in-turn are directly related to carbon fixation rates and energy production (Oren *et al.*, 2001; Schlensinger and Lichter, 2001; Victoria *et al.*, 2005). However, our current understanding of tree growth mechanisms that determine productivity and their responses to environmental changes is far from complete (Korner, 2003; Valledor *et al.*, 2008).

Plant adaptive strategies to changing climatic conditions were coordinated and fine-tuned by adjusting growth, development, cellular and molecular activities. Responses to these perturbations are usually accompanied by major changes in the plant transcriptome, proteome and metabolome (Bokhari *et al.*, 2007; Li *et al.*, 2008; Shulaev *et al.*, 2008; Chae *et al.*, 2009). Foliar protein content and composition are known to be the crucial factors for determining plant growth responses to environmental variables during ontogeny. In this context, Proteomics has become a powerful tool which is being successfully used in plant science research to investigate different biological processes including growth, development and responses to climate change (Jorge *et al.*, 2006).

Mass spectrometry (MS) is a potential analytical tool in proteomics to identify proteins by the analysis of peptides and correlation of resultant spectra with available database sequences (Yates, 2000; Griffin and Aebersold, 2001; Liska and Shevchenko, 2003; Mann *et al.*, 2007). In proteomic flowchart, such as two-dimensional electrophoresis (2-DE), followed by MS accomplishes peptide mass fingerprinting (PMF), which serves as a unique identifier or fingerprint of any protein. An accurate determination of peptide mass to charge (m/z) ratio using matrix- assisted laser desorption/ ionization time-of-flight (MALDI-TOF-TOF) mass spectrometer allows us to identify unknown proteins by matching the resulting peptide masses with the theoretical or existing peptide masses of proteins in databases (Senthil Kumar *et al.*, 2007).

Gmelina is very promising tree species due to its early establishment, rapid growth and promising wood characteristics. Interestingly, under elevated CO₂ atmosphere, *Gmelina* showed significant high photosynthetic activity conjoined with high growth and productivity as already depicted in previous chapters of this thesis (chapter 2, 3 &4). However, no information is available on either proteomic or molecular approaches to understand the growth and productivity of *Gmelina* for domestication programmes. As a first step to study the influence of elevated CO₂ on this agroforestry tree species, we extracted, separated and identified leaf proteins from *Gmelina* using 2-DE, MALDI-TOF-TOF, peptide mass fingerprinting and data base search, with particular emphasis on proteins involved in photosynthesis, using Mascot search engine against NCBI, SwissProt and Expressed sequence tags (EST) data bases. In the present study, we also aim to analyze the photosynthetic responses of *Gmelina* with respect to its leaf protein expression dynamics during elevated CO₂ treatment.

Methods

Protein extraction

Protein extraction from leaves was done according to Saravanan and Rose, (2004). Leaves (5 g fresh weight per sample) were ground to a fine powder with liquid nitrogen by using mortar and pestle. The powder was suspended in extraction buffer containing 0.5M Tris- HCl (pH 7.5), 0.7M sucrose, 0.1M KCl, 50mM EDTA, 2% β -mercaptoethanol and 1mM PMSF. Equal volumes of phenol saturated with Tris-HCl (pH 7.5) was added, mixed for 30 min at 4 °C and centrifuged at 5000 g for 30min at 4 °C. The phenolic phase was collected and the protein was precipitated with 0.5M ammonium acetate in methanol at -20 °C for overnight. The pellet was washed with methanol and acetone. Aliquots from the final pellet were vacuum dried and solubilised in 400 μ l of Iso-Electric Focussing (IEF) solubilising buffer containing 7 M w/v urea, 2 M Thiourea, 4 % w/v CHAPS, 18 mM DTT and 0.2 % v/v biolytes (Bio-Rad). Insoluble material was removed by centrifugation at 15 000 g for 15 min. The protein concentration was determined using the RC-DC Protein Assay (Bio-Rad, Hercules, CA, USA) with ovalbumin as a standard.

Two-dimensional gel electrophoresis

Two- dimensional gel electrophoresis was done according to Jorge *et al.*, (2005) with slight modifications. Active rehydration of protein (500 μ g) was done on immobilized pH gradient (IPG) strips (18 cm, 4-7 pH linear gradient; Amersham, GE) for 12 h at 50v. The strips were loaded onto Amersham GE IEF Cell system and proteins were electrofocused at 20 °C, the voltage setting for IEF was 500 V for 30 min, gradually increasing voltage of 500-10,000 V for 3 h and a step voltage up to 60,000 Vh. The strips were equilibrated for 30min under gentle shaking at room temperature in 10 ml equilibration solution (50 mM Tris-HCl buffer, pH 8.8, 6M urea, 30% (w/v) glycerol, 2% (w/v) SDS) containing 2% DTT and 4%

iodoacetamide respectively. Equilibrated strips were sealed on top of the second dimension gel with 0.5% low melting agarose solution. The second dimension (12% polyacrylamide gels) was performed over night in an Ettan Dalt6 chamber (GE Healthcare), using Laemmli's buffer system and 1mm thick polyacrylamide gels.

Staining and Image analysis

Gels were stained according to Wang *et al.*, (2007). Images were acquired with calibrated densitometric scanner (Amersham GE) and analysed using Image Master Platinum, image analysis software (Amersham GE). Intensities of spots were determined by number of pixels per area represented as normalised values of percent volume. Experimental *pI* was determined using a 4-7 linear scale over the total length of the IPG strip. *Mr* values were calculated by mobility comparisons with protein standard markers (Bangalore Genei, India). In order to correct the variability due to CBB-staining and to reflect the quantitative variations in the intensity of protein spots, the value of each spot was normalized as a percentage of the total volume in all of the spots present in the gel. The spots that were present on at least two gels of proteins from the leaves of high CO₂ treated or control plants, based on the image analysis, were identified as expressed protein spots. The identified protein spots were manually rechecked. The protein spots that changed more than 1.0-fold and passed the Student's t test ($p < 0.05$) were considered responsive to high-CO₂ treatment.

Gel Digestion of Proteins and MALDI Analysis

Stained protein spots from four reproducible gels were excised and pooled. The excised gels were destained by five washes at room temperature for 30 min each with 100 μ L of 50% acetonitrile (ACN) in 25mM ammonium bicarbonate followed by a wash with 50 μ L of ACN. The gel pieces were treated with 10mM DTT in 25mM ammonium bicarbonate and incubated

at 56 °C for one hour followed by treatment with 55mM iodoacetamide in 25mM ammonium bicarbonate at room temperature for 45min. The gel pieces were then washed with 25mM ammonium bicarbonate and ACN and were dried in a SpeedVac. The gel pieces were rehydrated in 20 μ L of 25 mM ammonium bicarbonate solution containing 12.5 ng/ μ L trypsin (Sequencing grade, Promega) and incubated on ice for 10 min and then overnight at 37 °C. The supernatant was collected and the peptides were extracted in 50 μ L of 1:1 ratio of 1% trifluoroacetic acid (TFA) and ACN, with frequent vortexing for 15 min and were concentrated in speed vac and stored at -20 °C until MS analysis. The samples were reconstituted in 5 μ l of 1:1 ratio of ACN and 0.1% TFA. 2 μ l of the sample was mixed with 2 μ l of freshly prepared α - cyano-4-hydroxy-trans-cinnamic acid (HCCA) matrix in 1:1 ratio of 50% ACN and 1% TFA and 1 μ l was spotted on target plate. The peptides were analyzed by autoflux III smart beam MALDI-TOF-TOF (Bruker Daltonics, Germany).

Protein identification

Protein identification was done by data base searches of corrected peptide masses of each spot by external calibration pepmix standard mix, employing Biotoools Software (Bruker Daltonics, Germany) and Mascot search engine for both peptide mass fingerprinting and MS/MS mass values. The similarity searches for mass values were done with existing digests and sequence information from NCBIInr, SwissProt and Expressed sequence tag (EST) database. The significant scores were considered for the identification.

Results

Separation of Gmelina leaf proteins

Proteomic analysis of *Gmelina* leaf was carried out using leaf extracts of four individual plants. Four biologically independent 2-DE images were obtained and a representative standard gel was constituted computationally (Fig 22 and 23). The proteins separated by 2-DE were visualised by modified Coomassie brilliant blue (CBB) staining which is MS compatible and allowed reproducible protein detection. The coomassie stained 2-DE gels (18cm) revealed that most of the spots were concentrated in the pH range of 4-7 and 16-97 kDa *Mr* range. Spot by spot validation was done for the match, spot volume, mean, SD and variance. The relationship between the intensities of protein spots and their quantitative variability was also established (Fig. 24). No significant correlation was found between the mean protein volume and standard deviation (SD) ($r = 0.41$, $p < 0.001$).

Identification of separated proteins

Although a large number of spots were noticed on the standard gel, only the high quality spots were used for spot qualification. A total number of 150 prominent and well resolved spots were excised from gels and digested with trypsin. These trypsin-digested proteins were analysed by MALDI TOF –TOF. Each spot was subjected to peptide sequence analysis by proteolytic cleavage and then subjected to MS/MS fragmentation. The amino acid sequences of the corresponding peptides were obtained from the differences in m/z ratios for a series of daughter ions. Subsequently, the sequence ions and the intact peptide masses were matched against protein databases using the biotools to confirm the identity of the proteins. As a representative, Figure 25 shows peptide finger print for the spot 64 which corresponds to rubisco large subunit and Figure 26 represents the MS/MS spectrum of 1465.88 peptide mass from the peptide finger print with detected sequence TFQGPPHGIQVQR matching

significantly with rubisco large subunit protein. Protein spots, which showed similar identities were represented by sequence with highest MS/MS scores (Table 5). Data in Table 5 include protein identity, accession number, experimental *Mr*, *pI*, significant peptide masses, peptide sequence, deviation, percent sequence coverage and significant MS/MS score. Putative protein functional classification was assigned based on similarity to understand the biological processes, encompassed by different proteins identified using the 2-DE proteomic approach. For interpreting the present proteomic expression data, proteins obtained through 2-DE were classified into 9 groups based on their corresponding biological functions (Fig. 27). Among the abundant proteins identified in the *Gmelina* leaf proteome, 37% were involved in photosynthesis and energy metabolism including rubisco large sub unit, rubisco activase, carbonic anhydrase, glyceraldehyde -3-phosphate dehydrogenase, triosephosphate isomerase, ferredoxin NADP reductase. About 12% of the identified proteins were involved in nitrogen fixation and amino acid metabolism which include cysteine synthase, phenylalanine ammonia lyase and glutamine synthetase. Other identified proteins were included in functions like protein translation, protein complex assembly, proteolysis and folding like elongation factor TU map kinase, ftsH like protein pftf precursor, chaperonin 30 beta subunit and stress related heat shock proteins. Proteins involved in electron transfer chain like ATP synthase beta subunit, vacuolar H⁺-ATPase subunitB, NADH dehydrogenase and putative transitional endoplasmic reticulum ATPase were accounted to 10% of the total spots identified. Additional identified protein spots involved in cellular redox maintenance include monodehydro ascorbate reductase, anionic peroxidase and 2-cys peroxiredoxin like protein (5%). Cytoskeleton and cell wall metabolism protein spots like actin1, glucanendo-1,3 beta -D- glucosidase and Early-responsive to dehydration (ERD4) related membrane proteins constituted to about 9%. Phytohormone metabolism proteins like putative 1-aminocyclopropane-1-carboxylic acid oxidase and putative 1-aminocyclopropane -1

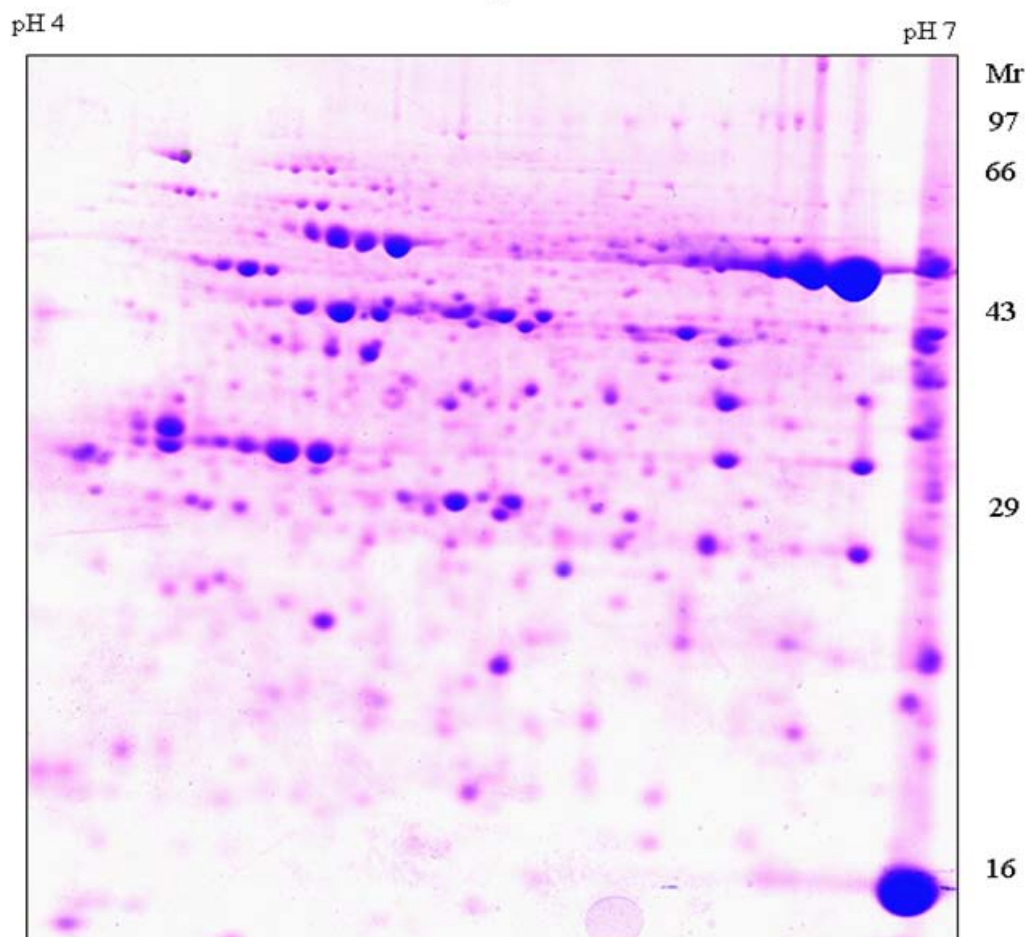


Fig. 22. 2- DE master gel of CBB stained leaf proteins from *Gmelina arborea*. Proteins were separated on first dimensional pH 4-7 linear IPG strips and second dimensional 12% vertical slab gels. The relative molecular masses of standard proteins are given on the right, while the pI range is given on the top of the figures.

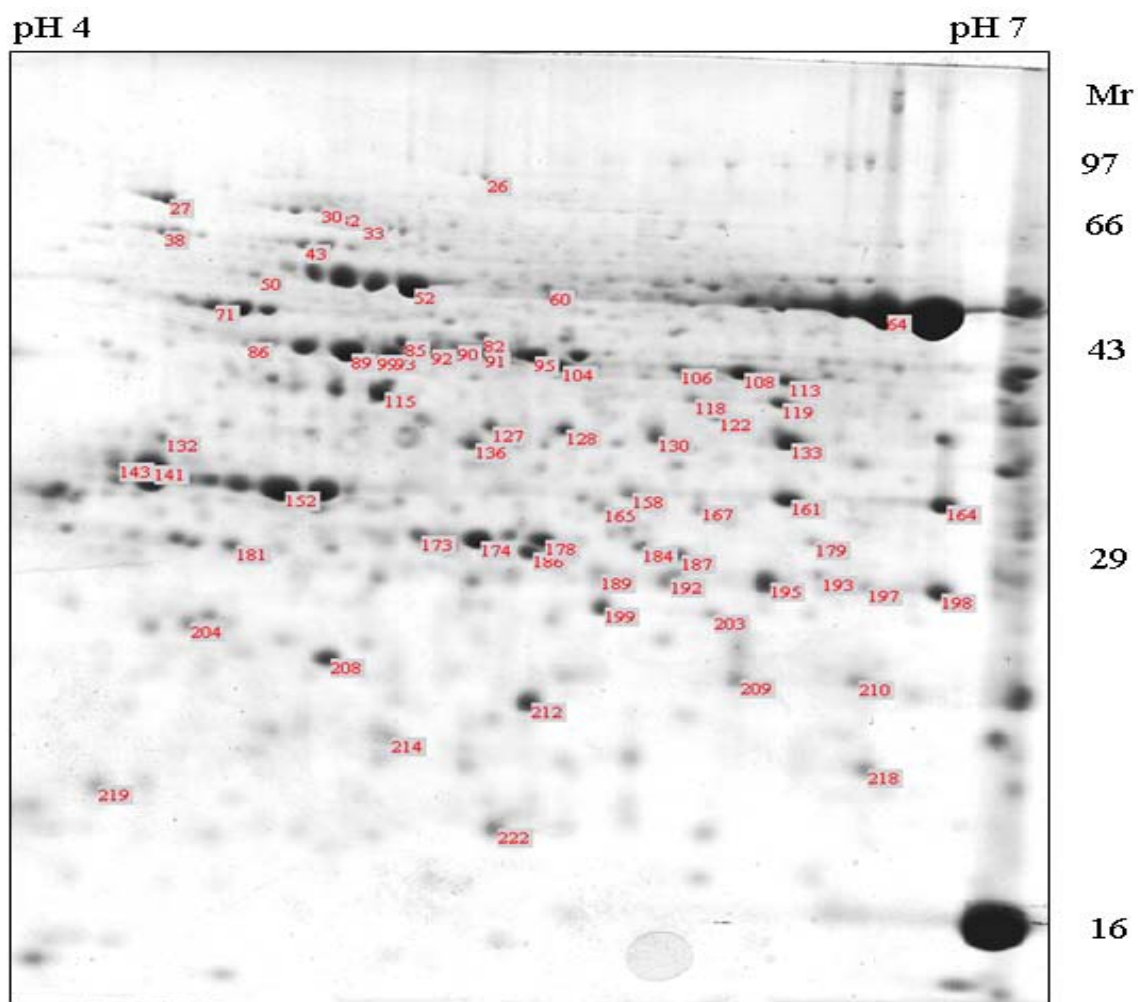


Fig. 23. 2-DE master gel of leaf proteins from *Gmelina arborea* illustrating seventy numbered spots which were chosen for protein identification and the derived data are presented in Table 5.

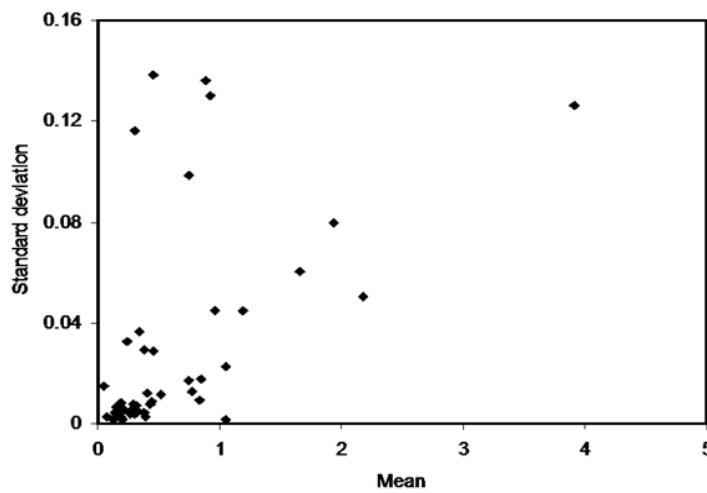


Fig.24. Analysis of the quantitative variation indicating relationship between the mean protein volume and standard deviation of the identified protein spots from four individual biologically variant 2-DE gels ($r = 0.41$, $p < 0.001$).

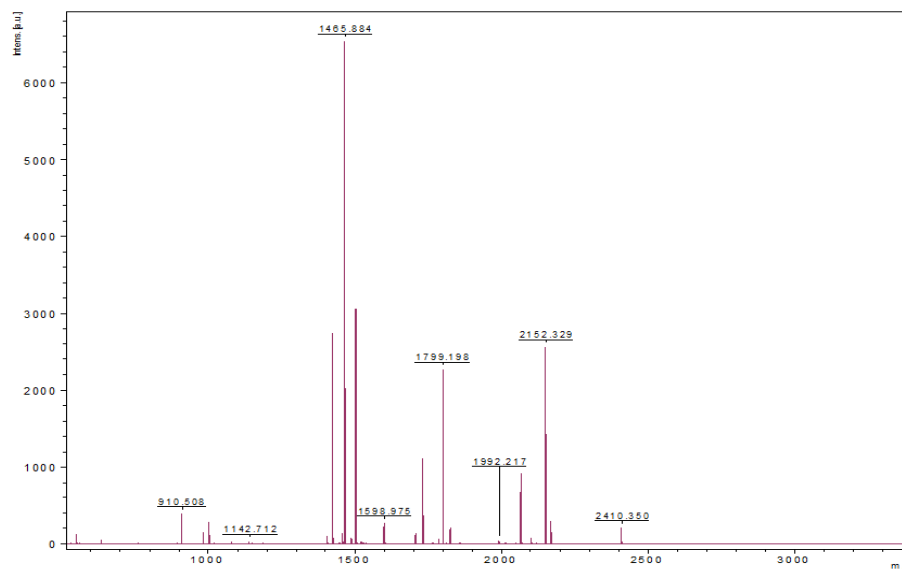


Fig.25. Peptide mass fingerprint of the spot 64, whose MS/MS spectrum for significant peptide mass matched for rubisco large subunit.

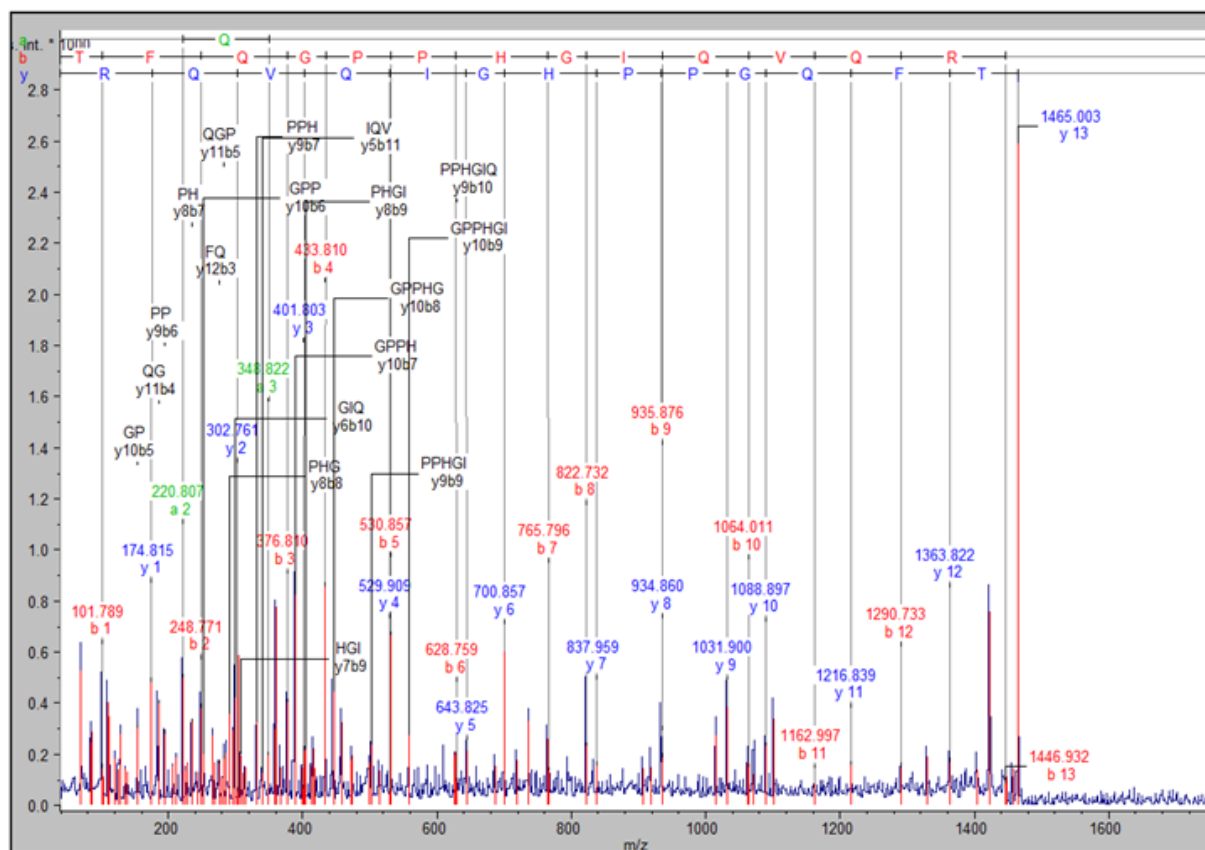


Fig.26. Representative MS/MS spectrum of one peptide of spot 64 (mass 1465.88). The annotated sequence TFQGPPHGIQVQR was matched by similar sequence search and protein was identified as rubisco large subunit.

Table 5 Proteins identified from the *Gmelina* leaf by MALDI TOF TOF. The data includes an assigned spot number, experimental molecular weight and pI; significant peptide mass; peptide sequence; deviation (Da); percent sequence coverage; MS/MS score; accession number. The assigned protein of the best matched was given with the accession number in which it has been identified.

Spot No.	Protein	Peptide Mass	peptide sequences matched	Dev. (Da)	Accession number	% Sequence coverage	Mr/pI	MS/M S Score
52, 165,167	ATP Synthase beta subunit	1921 1955	DALVYGQMNEPPGARMR IFNVLGEPVDNIGPVDTR	0.07	gi/16943741	7.07	52/5.3	152
43	Chaperonin 30 beta subunit	1701	AAVEEGIVVGGGCTLLR	0.10	gi/82589	10.8	60/5.0	150
91,95, 106,108	Glutamine synthetase	1028 1611 1627 1791 3489	KAILNLSLR HKEHIAAYGEGNER HKEHISAYGEGNER HETADISTFSWGVANR ITEQAGVVLSLDPKPIEGDWNGA GCHTNYSTK	0.15 0.23 0.29 0.21	gi/121348	26.9	42/5.7	124
38	Rubisco large subunit binding protein subunit alpha, chloroplast precursor	1755	AIELPDAMENAGAALIR	0.09	gi/464727	2.9	63/5.0	110

185,191, 195, 198,189	Carbonic anhydrase	1234 1263 1667 1701 1878 1994	FMVFACSDSR NIANMVPVFDK VENIVVIGHSACGGIK GQAPKFMVFFACSDSR EAVNVSLGNLLSYPFVR YEKNPALYGELSKGQAPK	0.088 0.212	gi/115472	27.5	29/5.6	109
64	Rubisco large subunit	1465 1799	TFQGGPHGIQVQR GHYLNATAGTCEDMMK	0.012 0.229	gi/33330923	6.6	49/6.6	90
50	Vacuolar H ⁺ - ATPase subunit B	1158 1286 1597 1716 1913 2178 2773	FVTQGAYDTR KFVTQGAYDTR QIYPPINVLPSLSR VTLFLNLADPTIER GYPGYMYTDLATIYER IPLFSAAGLPHNEIAAQICR AVVGEEALSSDLLYLEFLDKFER	0.22 0.19 0.21 0.23 0.25 0.28 0.27	gi/118721470	22.2	54/4.9	88
71,89,93, 186	Rubisco activase	1340 1869 2063 2089	FYWAPTREDR IVDSFPGQSIDFFGALR LLEYGNMLVQE QENVKR VPIIVTGNDFSTLYAPLIR	0.235 0.122 0.046 0.025	gi/10720247	13.7	43/4.9	83
204	2-Cys peroxiredoxin like protein	1502	SYGVLIPDQGIALR	0.03	gi/47027073	7.1	27/5.0	82
128,127, 136	Chloroplast cysteine synthase	1365	LITVVFPSPFGER	0.24	gi/59799343	3.1	37/5.7	81
85,92	Actin 1	1515 3152	IWHHTFYLELR TTGIVLDSDGDGVSHTVPIYEGYAL PHAILR	0.35 0.21	gi/113217	10.7	43/5.3	76

208	Putative transitional endoplasmic reticulum ATPase	1554	KSPIAADVDLNVLAK	0.11	gi/116000599	1.2	25/5.1	70
119,130	Fructose 1,6-bisphosphate aldolase	874 987 1115 1388 1623	EAAWGLAR TAKTVASPGR SAAYYQQGAR LASIGLENTEANR GILAMDESNATCGKR	0.072 0.225 0.60 0.181 0.33	gi/8272480	14.4	36/6.4	70
115	Phosphoribulokinase	2468	HFSPVYLFDEGSTISWIPCGR	0.170	gi/117296236	10.6	39/5.2	63
32	FtsH like protein pftf precursor	1199	FLEYLDKDR	0.09	gi/4325041	1.2	67/5.1	60
104	Phosphoglycerate kinase	999 1207 1689	FSLAPLVPR VILSSHLGRP VILSSHLGRP KGVTPK	0.151 0.218 0.253	gi/1177860	41.8		60
212	Pyruvate kinase	1661	QMLESMSVSNRPTR	0.09	gi/159485206	0.64	23/5.6	59
181,187	Triose phosphate isomerase	1388 1669 1824 2319	VIACIGETLEQR DLGCQWVILGHSE VATPAQAQEVHFE LAYALSQGVIA CIGELLEEF	0.012 0.180 0.02 0.20	gi/48773765	24.9	30/4.9	59
152	Oxygen evolving enhancer protein (OEE 1) 33KDa subunit	964 1236 1562 1760 2283	VPFLFTIK RLTFDEIQSK DVKIQQGIWYAQLE DGIDYAAVTVQLPGGER MAASLQAAATLMQPTKVG VAPAR	0.04 0.05 0.06 0.06 0.06	gi/11134054	21.3	33/5.0	58

173,174, 178	Putative 1-aminocyclopropane-1-carboxylic acid oxidase	1595	FVCEDYMKLYAR	0.26	gi/9188059	3.7	30/5.5	57
222	Putative polyprotein	1278	DILLGMPFLDK	0.31	gi/4775496	1.7	19/5.5	55
60	Phenylalanine ammonia lyase	1639	KTLSTNSNGHLHSAR	0.24	gi/159885624	2.9	51/5.7	55
141,143	Putative 1-aminocyclopropane-1-carboxylate	1405 2431	KICAELEEEER AGDHRTPGMHSGMWGSMAILDR	0.09	gi/116059293	7.4	55/5.0	53
113,132	Glyceraldehyde-3-phosphate dehydrogenase	1254 1382 1787	TFAEEVNAAFR KTFAEEVNAAFR VIAWYDNEWGYSQR	0.189 0.262 0.287	gi/66026	10.9	40/6.4	53
26,30	Heat shock cognate protein 70	1215 1358 1473 1680	DAGVIAGLNVMR NALENYAYNMR TPSYVAFTDSER NAVVTVPAYFNDQR	0.13 0.15 0.16 0.16	gi/41584275	7.8	69/5.1	52
193	Hypothetical protein	882	RSNAMCK	0.20	gi/147769397	2.5	27/6.4	52
184	Latex abundant protein	1942	SAEPGDLLFVHYSGHGTR	0.94	gi/4235430	3.5	30/6.0	51
82	Monodehydro ascorbate reductase	1472	LPGFHVCGSGGER	0.28	gi/15865451	2.9	44/5.5	43
214	Putative 3-deoxy-d-arabino heptulosonate-7-phosphate synthase	882	SDQFEEK	0.26	gi/76782186	2.5	22/5.3	43

99	Ferredoxin NADP reductase	713 1153 1281	VVKHSK AEQWNVEVY KAEQWNVEVY	0.339 0.086 0.325	gi/119905	6.9	42/5.2	42
209	P450	1165	VVCSKAMGVSK	0.22	gi/48526687	2.0	24/6.2	41
90	Elongation factor TU Map Kinase	1670	TLDQSVAGDENVGILLR	0.90	gi/11467799	3.9	43/5.4	35
158,161,164	Glucanend- 1,3-beta-D- glucosidase	2140	LLASTGAPLLANVYPYASYR	0.14	gi/104161966	5.9	33/6.4	35
199	Anionic peroxidase	1278	DEMRMGASLLR	0.17	gi/162459018	4.3	27/5.8	33
179	Stachyose synthase	920	REEAISSK	0.51	STSYN_PEA	0.9	30/6.4	31
118	Peptide transporter 1	1181	LRKPGGSPLTR	0.11	gi/115490708	11.8	39/6.1	26
210	ERD4 related membrane protein	1467	RAVALGAEEANLPR	0.19	gi/159488670	0.9	24/6.6	24
27	Heat shock protein – like protein	1851	DGSSPQNTKSPIPVVPTK	0.08	gi/28558784	4.6	70/4.9	20
218	Maturase K (Intron maturase)	1165 1449	YILRLSCIK QHDFLYPLIFR	0.16	gi/68052508	4.0	21/6.6	16
203	NADH dehydrogenase subunit	1382	RAFAYSSPDITR	0.29	gi/37779760	1.7	27/6.2	10

carboxylate constitute 7% of identified protein spots. Six protein spots of unknown biological functions constituted to about 9% of the total.

Protein expression profiling

To investigate the difference in photosynthetic protein expression patterns under elevated CO₂ conditions, leaf protein profiles of ambient and elevated CO₂-grown *Gmelina* were compared. Triplicate gels were obtained from three independent experiments and the representative gels for ambient and elevated CO₂ were illustrated in Figure 28. More than 150 spots were reproducibly detected in the colloidal coomassie stained gels with Image Master 2D Platinum software and all the gels showed highly similar distribution patterns in 2D image. A significant ($r = 0.94$, $p < 0.001$) positive correlation was observed in quantitative variation of ambient and elevated CO₂ grown *Gmelina* leaf protein spots (Fig. 29). Quantitative image analysis revealed that 30 protein spots of total 64 identified spots were significantly ($p < 0.05$) changed in their intensities in elevated CO₂ grown plants compared to ambient CO₂ grown plants (Table 6). These spots constitute 23 different proteins of the identified total of 40 proteins (Table 6). Among the 23 proteins which showed changes in their intensities, 9 proteins were significantly up-regulated (>1.0 fold) and 6 proteins were down-regulated in elevated CO₂-grown plants (Fig. 30). Induction factor results depict that photosynthetic proteins like rubisco large sub unit binding protein (Spot 15), rubisco large sub unit (spot 88), phosphoglycerate kinase (spot 100), rubisco activase (spot 102), triosephosphate isomerase (spot 195) and carbonic anhydrase (spot 234, 241 and 239) were significantly ($p < 0.05$) up-regulated in elevated CO₂ grown plants compared to ambient CO₂ grown plants (Table 6; Fig. 30). Phosphoribulokinase (spot 125) and Oxygen evolving enhancer protein (OEE 1) (spot 179) were down-regulated in elevated CO₂-grown plants in comparison to those in ambient CO₂-grown plants (Table 6; Fig. 30).

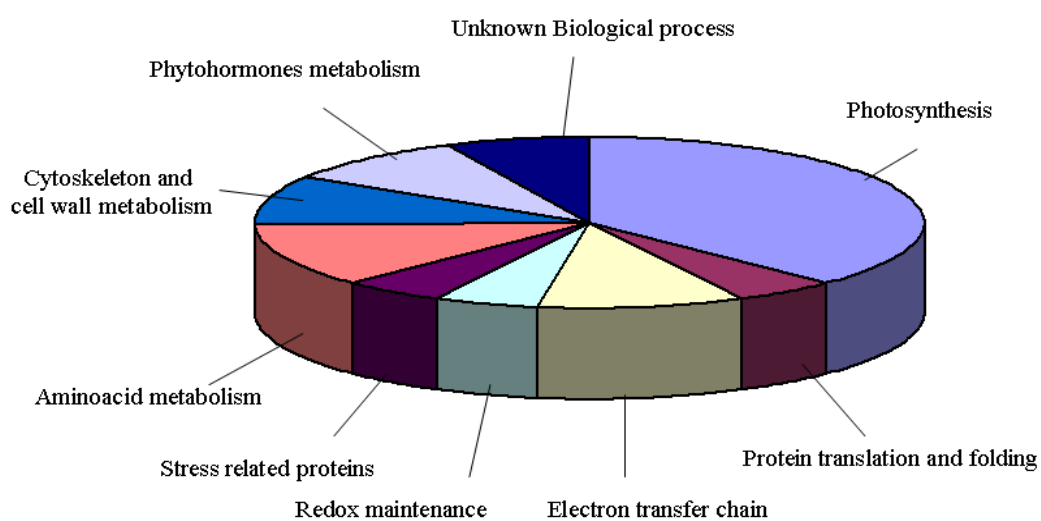


Fig.27. Distribution of proteins identified from the *Gmelina* leaf proteome depending on their functions or predicted functional domains. A total of 64 spots representing 9 different functional categories were classified.

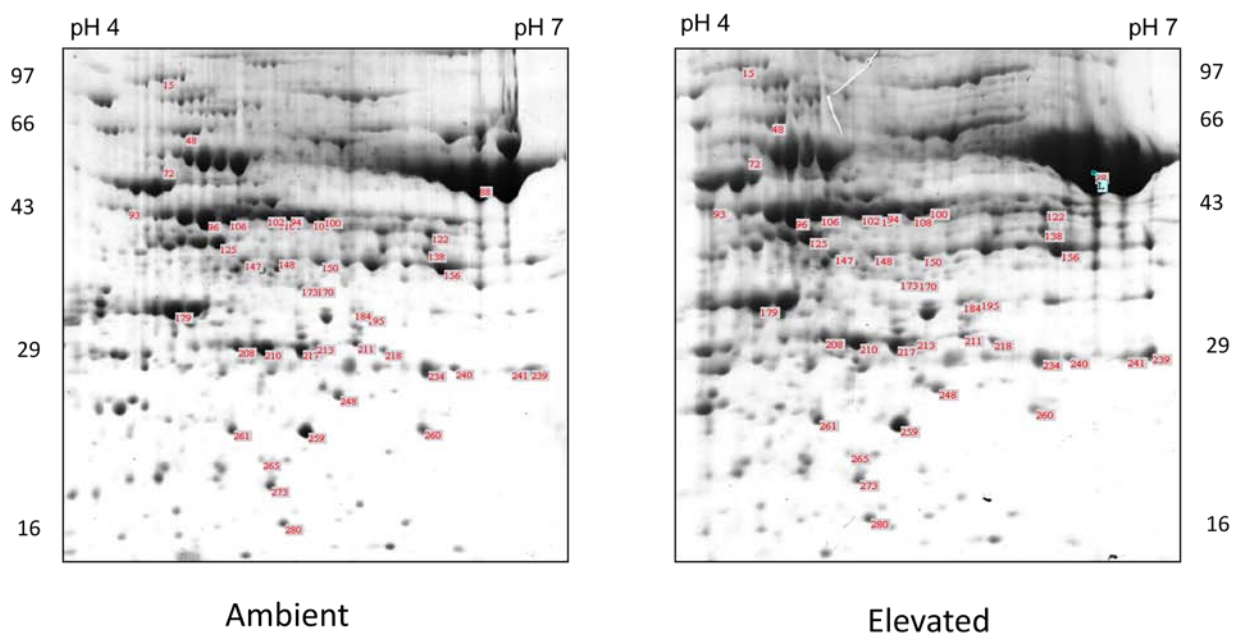


Fig. 28. Colloidal Coomassie-stained 2-D gels of proteins extracted from leaves of *Gmelina* grown under ambient (A) and Elevated CO₂ (B) illustrating thirty differentially expressed protein spots. 600 µg of protein was loaded on 18 cm IPG strip with a linear gradient of pH 4-7. 12% SDS-PAGE gels were used for the second dimension.

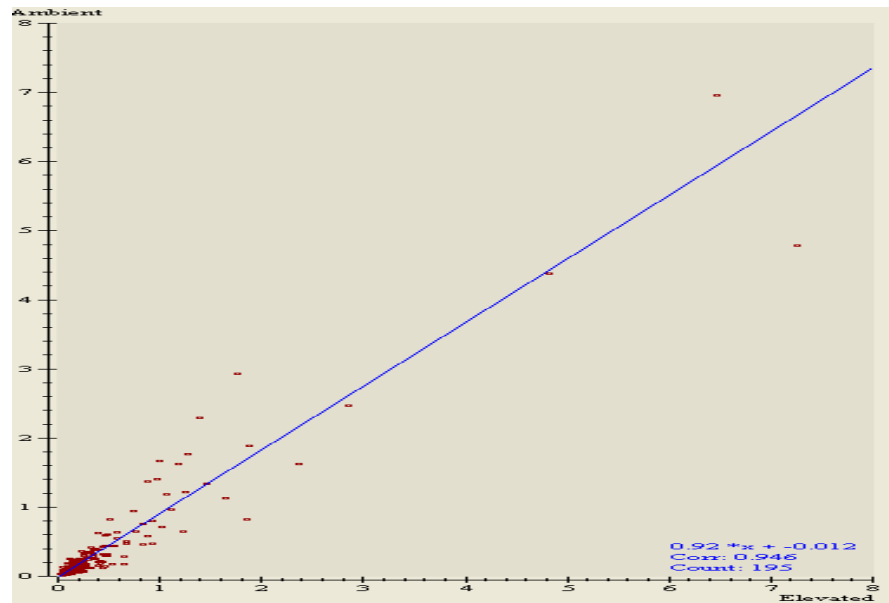
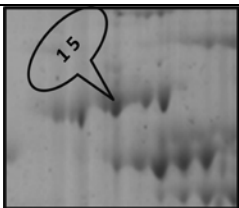
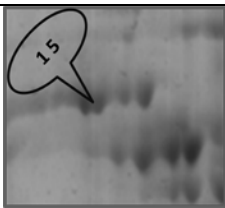
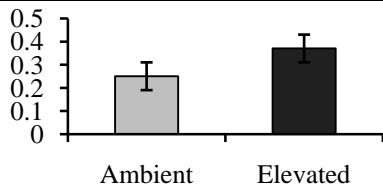
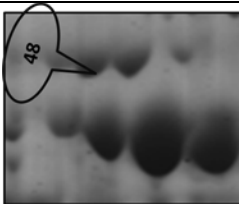
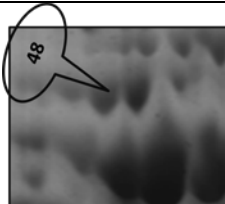
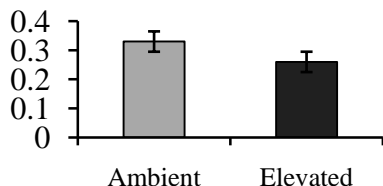
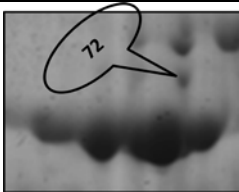
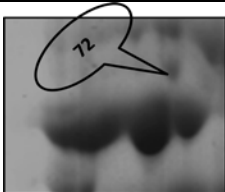
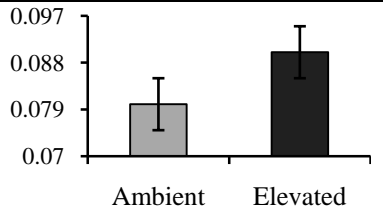
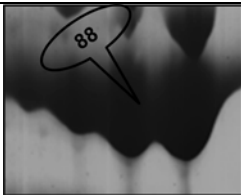
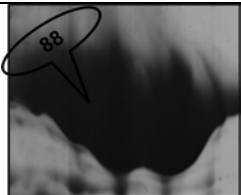
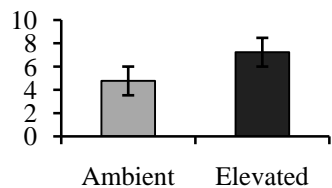
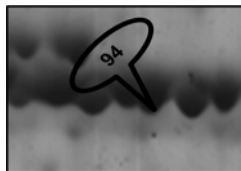
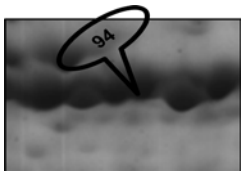
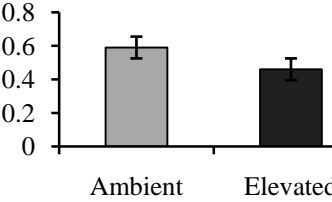
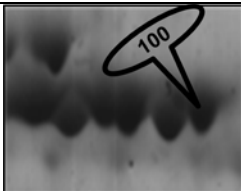
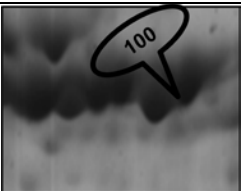
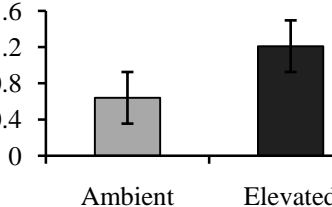
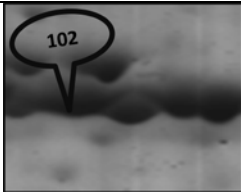
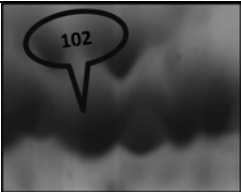
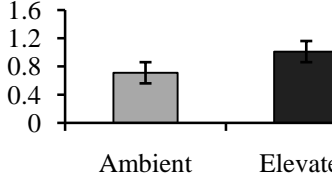
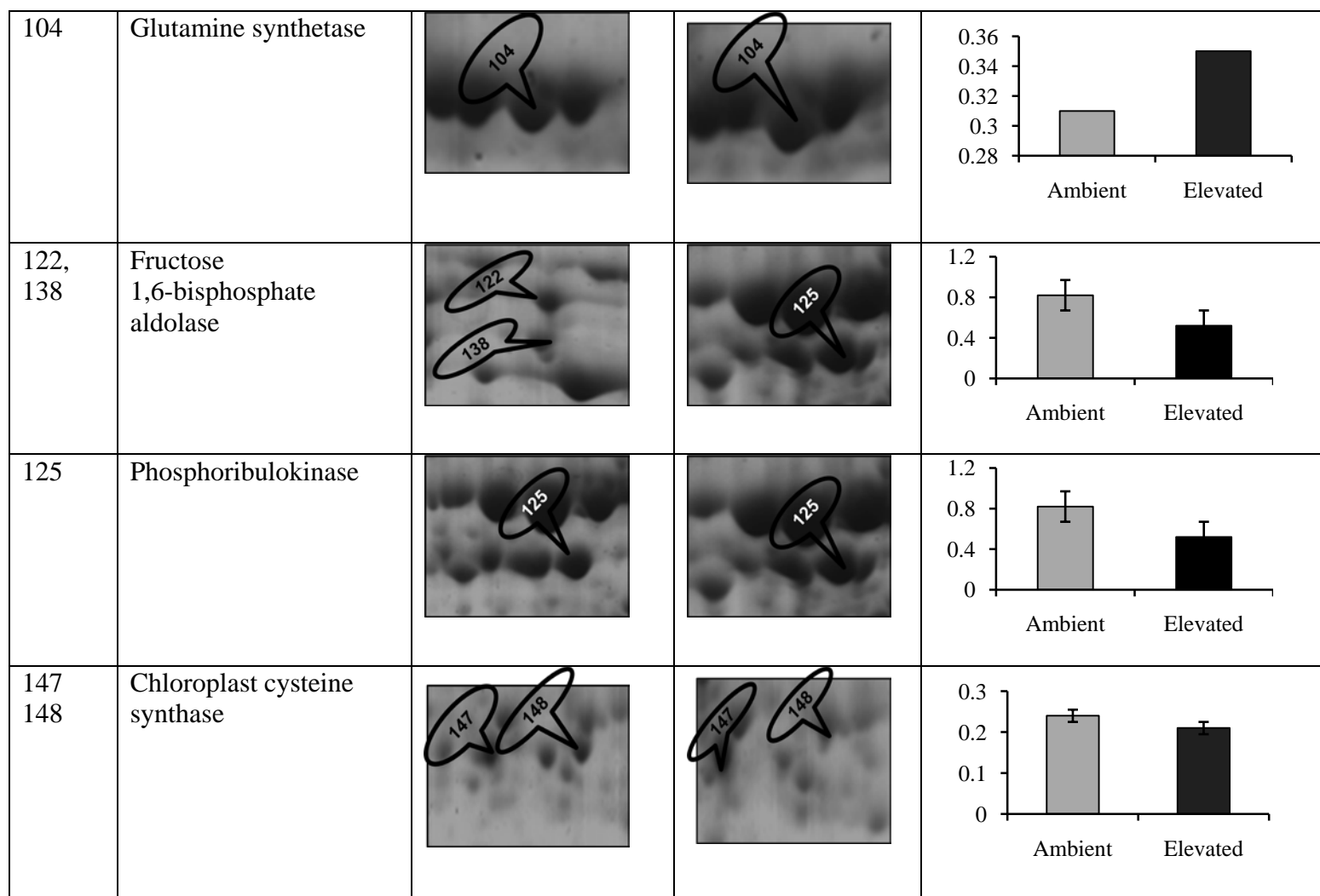



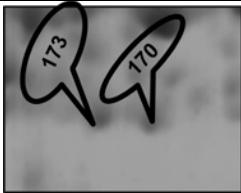
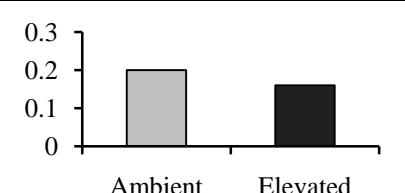
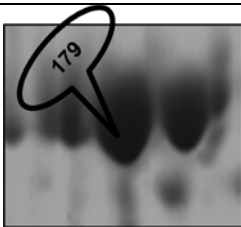
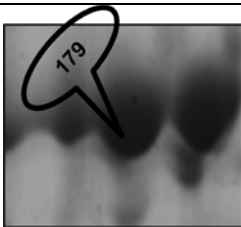
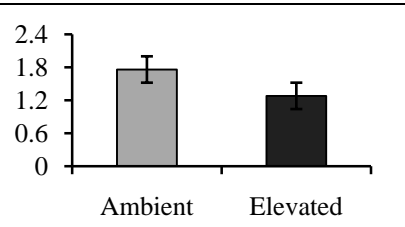
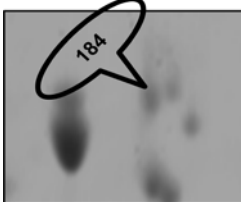

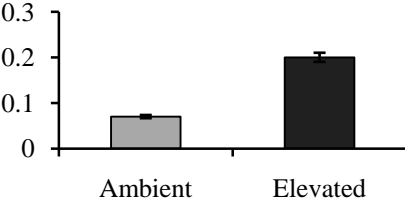
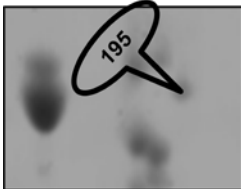
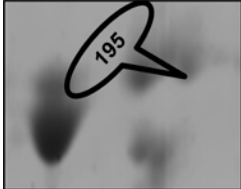
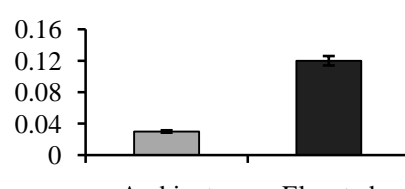
Fig. 29. Analysis of quantitative variation among the identified leaf protein spots from three individual biologically variant 2-DE gels of ambient and elevated CO₂-grown *Gmelina* ($r = 0.94$, $p < 0.001$).

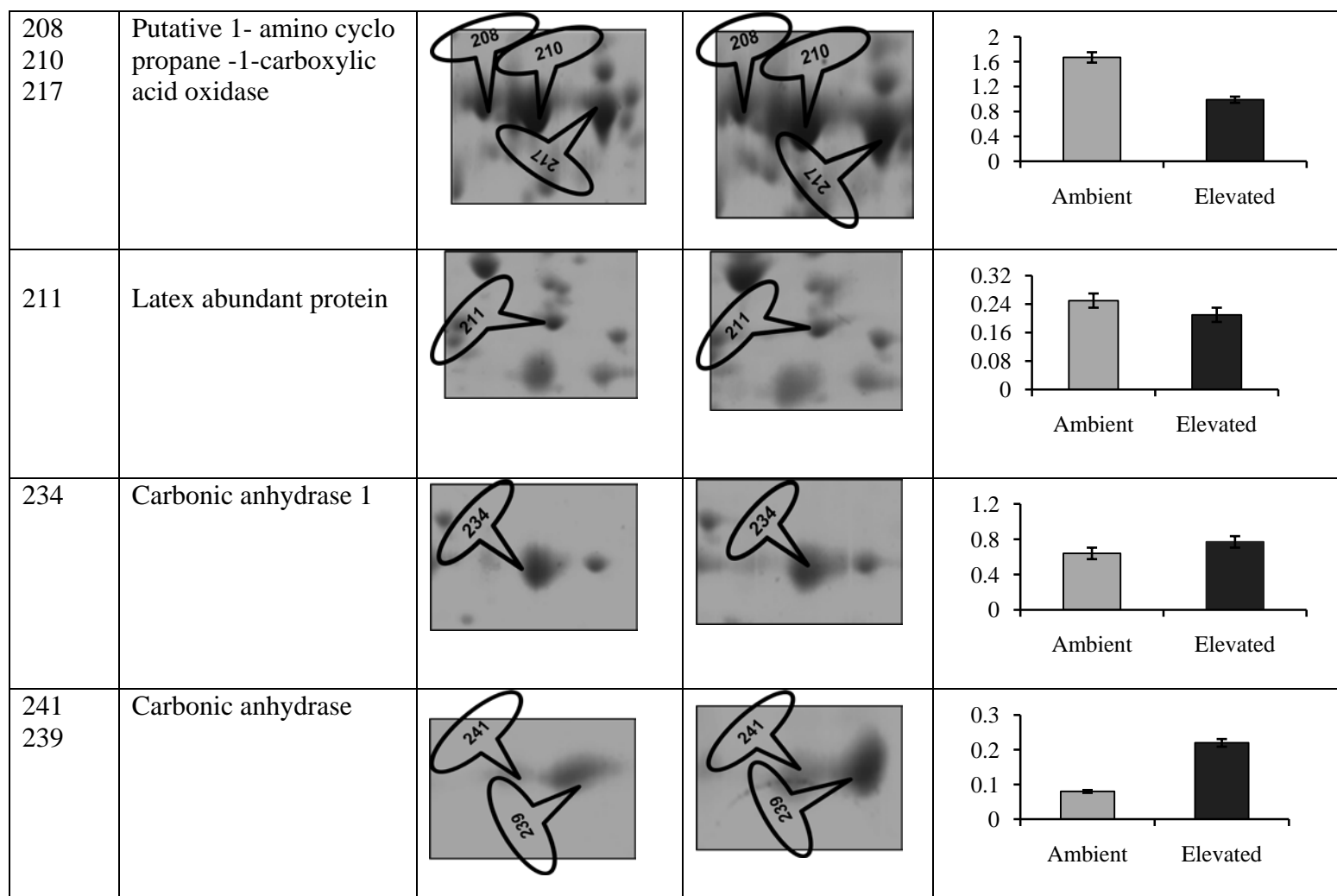
Table 6 Identification of major leaf proteins of *Gmelina* differentially expressed under ambient and elevated CO₂ atmosphere. Relative spot volumes for each spot were expressed as % Spot Vol, indicating the normalized values of the ratio of the individual spot to the total volume of all the spots in the gel.

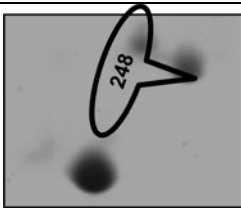
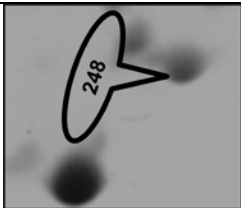
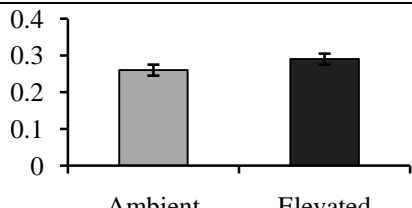
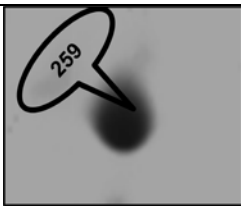
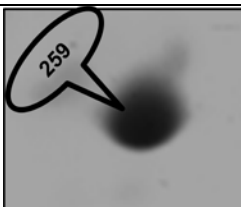
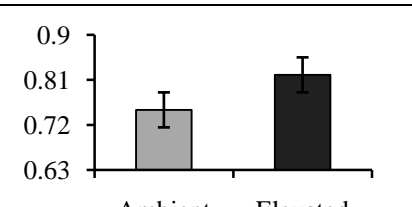

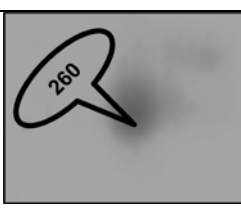
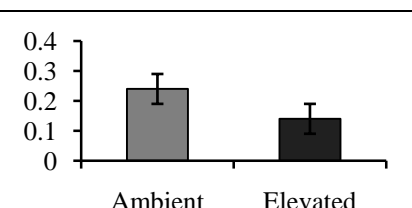
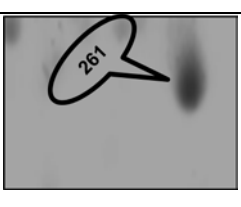
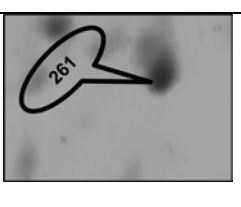
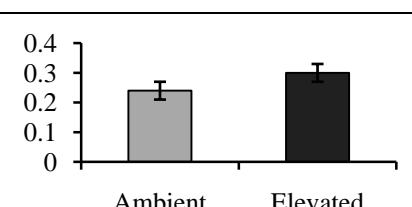
Spot No.	Protein	Ambient	Elevated	Relative spot volumes						
15	Rubisco large sub unit binding protein			 <table><tr><th>Condition</th><th>Relative spot volume</th></tr><tr><td>Ambient</td><td>0.25</td></tr><tr><td>Elevated</td><td>0.38</td></tr></table>	Condition	Relative spot volume	Ambient	0.25	Elevated	0.38
Condition	Relative spot volume									
Ambient	0.25									
Elevated	0.38									
48	Cheperonin 30 beta subunit			 <table><tr><th>Condition</th><th>Relative spot volume</th></tr><tr><td>Ambient</td><td>0.32</td></tr><tr><td>Elevated</td><td>0.25</td></tr></table>	Condition	Relative spot volume	Ambient	0.32	Elevated	0.25
Condition	Relative spot volume									
Ambient	0.32									
Elevated	0.25									
72	Vacuolar H ⁺ -ATPase Subunit B			 <table><tr><th>Condition</th><th>Relative spot volume</th></tr><tr><td>Ambient</td><td>0.079</td></tr><tr><td>Elevated</td><td>0.082</td></tr></table>	Condition	Relative spot volume	Ambient	0.079	Elevated	0.082
Condition	Relative spot volume									
Ambient	0.079									
Elevated	0.082									

88	Rubisco large subunit			 <table><tr><th>Condition</th><th>Relative Level</th></tr><tr><td>Ambient</td><td>~5.0</td></tr><tr><td>Elevated</td><td>~7.5</td></tr></table>	Condition	Relative Level	Ambient	~5.0	Elevated	~7.5
Condition	Relative Level									
Ambient	~5.0									
Elevated	~7.5									
94	Elongation factor TU map kinase			 <table><tr><th>Condition</th><th>Relative Level</th></tr><tr><td>Ambient</td><td>~0.6</td></tr><tr><td>Elevated</td><td>~0.48</td></tr></table>	Condition	Relative Level	Ambient	~0.6	Elevated	~0.48
Condition	Relative Level									
Ambient	~0.6									
Elevated	~0.48									
100	Phosphoglycerate kinase			 <table><tr><th>Condition</th><th>Relative Level</th></tr><tr><td>Ambient</td><td>~0.7</td></tr><tr><td>Elevated</td><td>~1.2</td></tr></table>	Condition	Relative Level	Ambient	~0.7	Elevated	~1.2
Condition	Relative Level									
Ambient	~0.7									
Elevated	~1.2									
102	Rubsico activase			 <table><tr><th>Condition</th><th>Relative Level</th></tr><tr><td>Ambient</td><td>~0.75</td></tr><tr><td>Elevated</td><td>~1.05</td></tr></table>	Condition	Relative Level	Ambient	~0.75	Elevated	~1.05
Condition	Relative Level									
Ambient	~0.75									
Elevated	~1.05									



170 173	ATP synthase beta subunit			 <table><tr><th>Condition</th><th>Relative Level</th></tr><tr><td>Ambient</td><td>0.2</td></tr><tr><td>Elevated</td><td>0.15</td></tr></table>	Condition	Relative Level	Ambient	0.2	Elevated	0.15
Condition	Relative Level									
Ambient	0.2									
Elevated	0.15									
179	Oxygen evolving Enhancer protein (OEE 1)			 <table><tr><th>Condition</th><th>Relative Level</th></tr><tr><td>Ambient</td><td>1.8</td></tr><tr><td>Elevated</td><td>1.2</td></tr></table>	Condition	Relative Level	Ambient	1.8	Elevated	1.2
Condition	Relative Level									
Ambient	1.8									
Elevated	1.2									
184	Glucanend-1,3-beta D-glucosidase			 <table><tr><th>Condition</th><th>Relative Level</th></tr><tr><td>Ambient</td><td>0.07</td></tr><tr><td>Elevated</td><td>0.2</td></tr></table>	Condition	Relative Level	Ambient	0.07	Elevated	0.2
Condition	Relative Level									
Ambient	0.07									
Elevated	0.2									
195	Triose phosphate isomerase			 <table><tr><th>Condition</th><th>Relative Level</th></tr><tr><td>Ambient</td><td>0.03</td></tr><tr><td>Elevated</td><td>0.12</td></tr></table>	Condition	Relative Level	Ambient	0.03	Elevated	0.12
Condition	Relative Level									
Ambient	0.03									
Elevated	0.12									



248	Anionic peroxidase			 <table><tr><th>Condition</th><th>Relative Level</th></tr><tr><td>Ambient</td><td>0.26</td></tr><tr><td>Elevated</td><td>0.29</td></tr></table>	Condition	Relative Level	Ambient	0.26	Elevated	0.29
Condition	Relative Level									
Ambient	0.26									
Elevated	0.29									
259	Pyruvate kinase			 <table><tr><th>Condition</th><th>Relative Level</th></tr><tr><td>Ambient</td><td>0.74</td></tr><tr><td>Elevated</td><td>0.82</td></tr></table>	Condition	Relative Level	Ambient	0.74	Elevated	0.82
Condition	Relative Level									
Ambient	0.74									
Elevated	0.82									
260	P450			 <table><tr><th>Condition</th><th>Relative Level</th></tr><tr><td>Ambient</td><td>0.25</td></tr><tr><td>Elevated</td><td>0.15</td></tr></table>	Condition	Relative Level	Ambient	0.25	Elevated	0.15
Condition	Relative Level									
Ambient	0.25									
Elevated	0.15									
261	Putative transitional endoplasmic reticulum ATPase			 <table><tr><th>Condition</th><th>Relative Level</th></tr><tr><td>Ambient</td><td>0.24</td></tr><tr><td>Elevated</td><td>0.30</td></tr></table>	Condition	Relative Level	Ambient	0.24	Elevated	0.30
Condition	Relative Level									
Ambient	0.24									
Elevated	0.30									

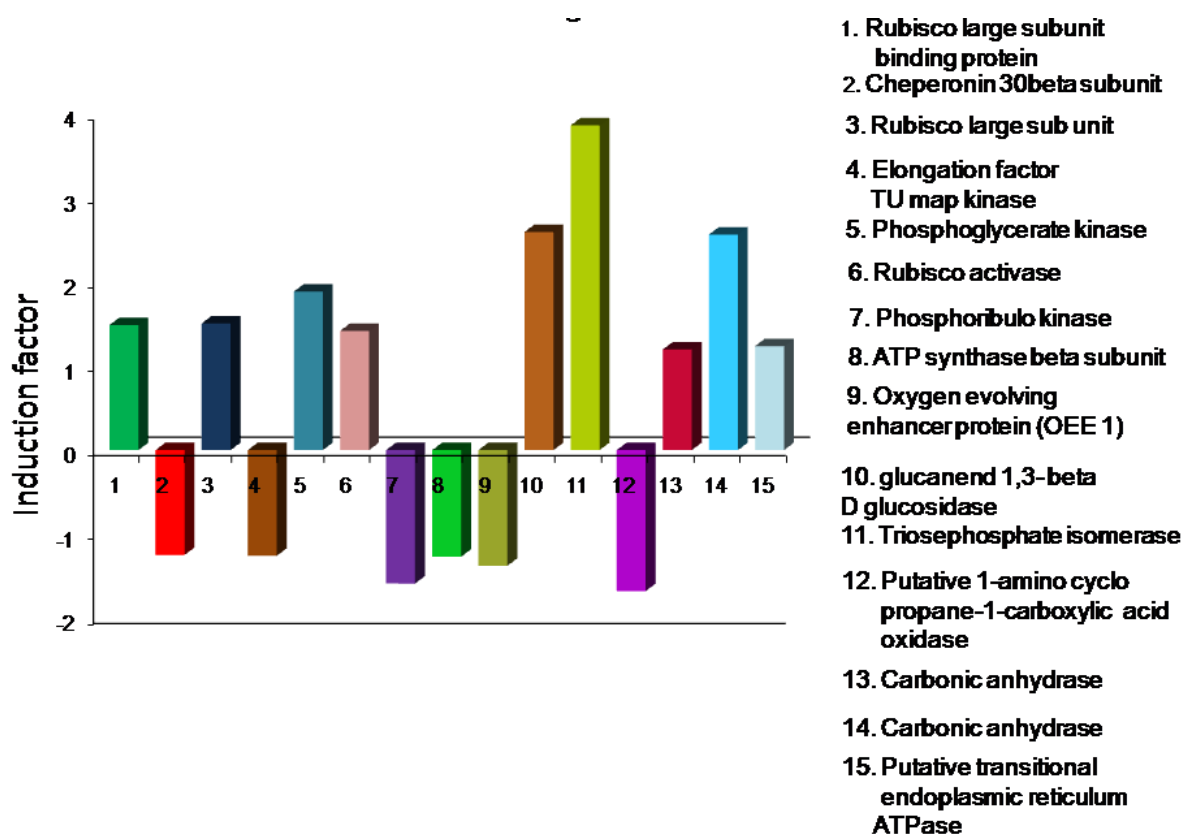


Fig. 30. Induction factors of fifteen differentially expressed protein spots in elevated CO₂-grown *Gmelina* compared to ambient CO₂-grown plants. The protein spots that changed more than 1.0-fold and passed the Student's t test ($p < 0.05$) were considered responsive to high-CO₂ treatment.

Discussion

The present study identified proteins related to different biological functions in *Gmelina arborea*. Identification of these leaf proteins laid a baseline to study the protein expression differences between ambient and elevated CO₂ grown plants. The highlight of this chapter is that we have optimized an efficient protocol for analysis of *Gmelina* leaf proteome, which minimized the presence of interfering compounds including polyphenols, pigments, polysaccharides and terpenes. The most critical step in proteomic study in trees is sample preparation as tree leaves have relatively low protein content and rich in proteases and oxidative enzymes. Polyphenols will co-purify with proteins resulting in horizontal and vertical streaking, smearing and a reduction in the number of distinctly resolved protein spots in 2-DE (Saravanan and Rose, 2004). *Gmelina* leaf proteins which were solubilised in phenol and subsequently precipitated with methanol and ammonium acetate, resulted in qualitatively good effective protein extracts with minimum contamination. 2-DE technique has been criticized for its low reproducibility when a direct comparison of different gels from different sources was performed (Hunt *et al.*, 2005; Ruebelt *et al.*, 2006). The linear correlation between the mean and SD for different individual leaf spots from our study showed no significant correlation ($p < 0.001$, $r = 0.41$) indicating that the abundant protein spots are not showing much variation in all the four 2-DE gels from four individual tree protein extracts (Fig. 29).

Our study also showed a dynamic distinct range of different proteins, despite the presence of predominant rubisco large subunit protein. Certain spots shared the identified peptides with one or more other spots. For example in Figure 23, spot no. 52 (ATP synthase beta subunit) shared certain identified peptides like that of 165 and 167, which were also identified as ATP synthase beta subunit. In our study, 12 proteins have multiple spots: rubisco activase (71, 89,

93,186); glyceraldehyde-3-phosphate dehydrogenase (113,132); ATP synthase beta subunit (165, 167, 52); CA (185,191,195,198,189); triose phosphate isomerase (181,187); fructose 1,6 biphosphate aldolase (119,130); glutamine synthetase (91,95,106,108); chloroplast cysteine synthase (128,127,136), actin (85,92); glucanendo-1,3-D- beta glucosidase (158,161,164); heat shock cognate protein 70 (26,30); putative 1-aminocyclopropane-1-carboxylic acid oxidase (173,174,178) and putative 1-aminocyclopropane-1-carboxylate (141,143). Several factors may be responsible for the presence of multiple spots as the protein migration in a 2-DE gel is very sensitive to small structural differences. These spots appear to be different isoforms with small amino acid sequence differences which was previously shown by the presence of multiple isoforms of CA in leaf tissues (Lazova *et al.*, 2004).

Gmelina grown under elevated CO₂ conditions showed a significant upsurge in photosynthesis, growth and productivity when compared to ambient CO₂-grown plants. Interestingly, the 2-DE leaf protein profile of *Gmelina* was also dominated by photosynthetic enzymes. The relatively high concentrations of the abundant photosynthetic enzymes in the leaves demonstrate their biological importance in effective energy harvesting, conversion and storage of photoassimilates (Watson *et al.*, 2003). Photosynthesis is mainly mediated by rubisco, which is the most abundant enzyme in nature and constitutes more than 50% of the total soluble proteins in leaves (Gutteridge and Gatenby, 1987). Accordingly, in our study rubisco large sub unit was the prominent spot with very high quality MS/MS spectra and score. In *Gmelina*, unlike the other C₃ plants, increase in [CO₂] resulted in a steady progressive increase in rates of photosynthesis. This was also observed in the differential protein expression patterns in elevated CO₂-grown plants. The proteins involved in photosynthesis showed an overall positive response when compared to ambient CO₂-grown plants. Photosynthetic proteins like rubisco large sub unit, rubisco activase and CA were

significantly ($p < 0.05$) up-regulated in elevated CO_2 grown plants compared to ambient CO_2 grown plants. The most important protein among the photosynthesis group was rubisco large subunit. Many studies have given much attention to the levels of rubisco because the enzyme limits the photosynthetic CO_2 assimilation rate at current CO_2 level. However, the reduction of rubisco under elevated CO_2 was also observed in many plant species (Nakano *et al.*, 1997, Long *et al.*, 2004, Fukayama *et al.*, 2009). Our results indicate that the significant increase in the rubisco large sub unit protein expression in *Gmelina* depicts that the photosynthetic machinery is amply equipped to accommodate a rise in $[\text{CO}_2]$ by adjusting activities and expression of the enzymes involved.

The role of rubisco activase is to maintain rubisco activity by removing inhibitory sugars from the active site of carbamylated and uncarbamylated enzymes (Portis, 2003, Bokhari *et al.*, 2007). It is a nuclear encoded chloroplastic protein which also enables rubisco to function efficiently under varying physiological conditions (Crafts-Brandner and Salvucci, 2000). Increasing the CO_2 concentration resulted in a significant ($p < 0.05$) up- regulation of rubisco and rubisco activase protein expression in *Gmelina* and these results were well correlated with dynamic photosynthetic rates observed in these plants under elevated $[\text{CO}_2]$. Another important photosynthetic enzyme CA, which provides adequate levels of inorganic carbon to acceralate carbon assimilation (Li *et al.*, 2004), was prominently recorded as five different spots in this study. CA activity was significantly high in elevated CO_2 grown *Gmelina*, which was also well correlated with protein expression patterns. In Figure 28, three protein spots (Spot no. 234, 239 and 241) corresponding to CA were significantly expressed in elevated CO_2 -grown *Gmelina* compared to ambient CO_2 -grown plants. Although the protein composition was largely unchanged, key photosynthetic proteins were differentially expressed under elevated CO_2 in *Gmelina* with an exception of phosphoribulo kinase and oxygen evolving enhancer protein, which showed a less significant decrease. The changes in

OEE indicate that increased [CO₂] may not result in any significant changes in the light harvesting complex (Logothetis *et al.*, 2004). However, it is hard to explain this effect with the current proteomic data, where most of the proteins isolated were of soluble proteins. Our data clearly demonstrate that elevated CO₂ significantly affected the photosynthetic protein profile in the leaves of *Gmelina*. Increased expression of protein spots associated with key photosynthetic enzymes were well correlated with the foliar photosynthetic data as already shown in previous chapters of this thesis.

Conclusions

1. The relatively high concentrations of the abundant photosynthetic enzymes in the leaves as observed in 2-DE protein profile demonstrate their biological importance like energy harvesting, conversion and storage of photoassimilates.
2. Enhanced CA expression under elevated CO₂ might catalyse the rapid equilibration of inorganic carbon species across the stroma towards Rubisco.
3. Rubisco plays a major role in determining the rate of photosynthesis under elevated CO₂ as recorded by its increased induction factor.
4. Proteomic data also suggest that rubisco activase, phosphoglyceratekinase, trisophosphate isomerase also play significant role in the regulation of CO₂ fixation under elevated CO₂ atmosphere.
5. *Gmelina* leaf protein profile elucidates that *Gmelina* positively responds to elevated CO₂ atmosphere at the protein level, which provide a clue to improve photosynthesis and productivity in tree species.

Chapter 6

Summary and Conclusions

Chapter 6

Summary and Conclusions

Sequestering atmospheric carbon and storing it in the terrestrial biosphere is one of the options which have been proposed to mitigate green house gas emissions. Young fast growing tree species are believed to be a major potential sinks and could absorb large quantities of CO₂. The ongoing enrichment of the atmosphere with CO₂ found to stipulate a positive effect on tree species due to increasing availability of carbon. The present study dissects out the CO₂ fertilization effects on photosynthetic gas exchange characteristics, key responses of photosynthetic enzymes consorted with overall plant growth performance in a fast growing tree species, *Gmelina arborea* Roxb (*Verbenaceae*).

Gmelina plants were grown under ambient (360 $\mu\text{mol mol}^{-1}$) and CO₂-enriched conditions (460 $\mu\text{mol mol}^{-1}$) in open top chambers (OTCs) and investigated the effects of high CO₂ on plant growth and productivity during two marked growth seasons. *Gmelina* showed high photosynthetic rates under [CO₂] despite of decrease in the stomatal density and conductance. Previous reports indicates an acclimatory down-regulation of photosynthesis under elevated CO₂ which was linked with factors like maintenance of *Ci*, photosynthetic capacity, light intensity, rubisco activity and source-sink carbohydrate relations or sinks strength. In our study, decrease in stomatal conductance was observed in *Gmelina* under elevated CO₂, mainly due to increase in the *Ci* and due to decrease in stomatal density. In-spite of this, photosynthetic rates were significantly high in *Gmelina* was presumed to be due to better maintenance of *Ci/Ca* ratio, patchiness of stomata and due to efficient photosynthetic machinery. In tropical climate conditions, high light intensities also play a major role in maintaining the photosynthetic rates. Diurnal fluorescence studies on *Gmelina* under ambient and elevated CO₂ showed

photoinhibition during the peak irradiance but the plants grown under elevated CO₂ mitigated the photoinhibition through enhanced electron transport rates and through efficient photosynthetic biochemical reactions.

Photosynthesis in several C₃ plants was found to be sensitive to increases in [CO₂], because the present [CO₂] is insufficient to saturate rubisco, and also because CO₂ inhibits the competing process of photorespiration. Interestingly, the activity of rubisco showed a significantly high activity in *Gmelina* grown under elevated CO₂ which was also conjoined by significantly high activities of other key photosynthetic enzymes including CA, FBPase, hexokinase and SPsynthase. The correlation between photosynthetic rates (P_n) and biochemical variables led to localize bottlenecks for enhanced photosynthesis. CA activity showed significant positive linear correlation with P_n and RUBPcase activity indicating that CA might play a major role in regulating the photosynthesis under elevated CO₂. The P_n as a function of CA and g_s also suggests that significantly high CA activity might prevent acclimation of photosynthesis due to limitation in stomatal conductance and C_i saturation. Photosynthetic down regulation in *Gmelina* grown under elevated CO₂ was not observed though there was significant high accumulation of total carbohydrates and starch. We believe that fast growing tree species are source-limited and can utilize the additional carbohydrates for growth enhancement. Our results also suggest that *Gmelina* was able to escape the photosynthetic down-regulation through high source capacity which was associated significantly with high sink strength.

In the present study, we have been able to describe the enhanced gas exchange physiology and foliar biochemistry by examining the effects of elevated CO₂ on growth and yield performance of young *Gmelina*. Photosynthetic down regulation was not observed in *Gmelina* plants grown under elevated CO₂ and we believe that this lack of down regulation was due to greater sink

demand. *Gmelina* showed significant increase in the plants growth under high CO₂, suggesting that *Gmelina* plants have greater capacity for carbon accumulation along with greater source strength. Morphological changes during the growth in *Gmelina* under elevated CO₂ positively correlated to increased availability of photosynthate, leading to initiation of new sinks and their development. This increased development of news sinks like lateral shoots and roots indicate better partitioning of carbohydrates and in-turn preventing the photosynthetic acclimation in plants. Our results also suggest that elevated CO₂ increased the biomass of *Gmelina* significantly which consequently led to a profound increment in carbon stock and carbon sequestration potential under elevated CO₂.

Plants conform to [CO₂] by adjusting transcriptome, proteome and metabolome. These adaptations can be observed through foliar protein content. The composition of proteome was known to be the crucial factors for determining plant growth and responses to environmental variables. To investigate the differences in photosynthetic protein expression patterns under elevated CO₂, leaf protein profiles of *Gmelina* grown under ambient and elevated CO₂ were compared. Overall analysis of all the gels revealed that, out of the matched photosynthetic protein spots, proteins corresponding to rubisco large sub unit, rubisco activase and carbonic anhydrase were significantly up-regulated in response to increased atmospheric CO₂. Increased net photosynthetic rates and accelerated growth in *Gmelina* would have triggered due to significant increase in activity and expression of rubisco and other photosynthetic proteins like carbonic anhydrase, phosphoglycerate kinase.

In conclusion, we demonstrate a strong and sustained photosynthetic enhancement in *Gmelina* plants grown under CO₂-enrichment. Our data also propound that *Gmelina* can be a potent tree species for efficient carbon sequestration corresponding to its rapid growth and high sink

demand with no acclimatory responses. *Gmelina* plants showed a consistent increase in the photosynthetic activity conjoint with biochemical responses in two growing seasons and CA was found to play a pivotal role in preventing the photosynthetic acclimatory responses under elevated CO₂ atmosphere. We also recommend that *Gmelina* can certainly be considered for high biomass production through large scale tree planting as well as to mitigate the rapid rising levels of CO₂ in the atmosphere

Major conclusions

1. Our data suggest that *Gmelina* showed a potent photosynthetic capacity by combining a high source strength and high sink demand.
2. Elevated CO₂ treatment also mitigated midday depression of photosynthesis through enhanced PS II photochemistry and thus limiting down regulation of photosynthesis in *Gmelina*.
3. The increase activities of CA, RuBPcase, FBPase and SPsynthase might play a pivotal role in preventing the photosynthetic acclimation in *Gmelina* under elevated CO₂ atmosphere.
4. The 2-DE profile of *Gmelina* provides a reference map to identify different proteins associated with tree growth and development with particular emphasis on carbon metabolism.
5. Our data clearly demonstrate that *Gmelina arborea* should be well suited for afforestation projects aimed to increase carbon sequestration in future elevated CO₂ environment.

Chapter 7
Literature cited

Chapter 7

Literature cited

Ainsworth EA, Davey PA, Bernacchi CJ, Dermody OC, Heaton EA, Moore DJ, Morgan PB, Naidu SL, RA HSY, Zhu XG, Curtis PS, Long SP (2002) A meta-analysis of elevated [CO₂] effects on soybean (*Glycine max*) physiology, growth and yield. *Global Change Biology* **8**, 695–709.

Ainsworth EA, Rogers A, Blum H, Nosberger J, Long SP (2003) Variation in acclimation of photosynthesis in *Trifolium repens* after eight years of exposure to Free Air CO₂ Enrichment (FACE). *Journal of Experimental Botany* **54**, 2769–2774.

Ainsworth EA, Long SP (2005) What have we learned from 15 years of free-air CO₂ enrichment (FACE)? A meta-analytic review of responses to rising CO₂ in photosynthesis, canopy properties and plant production. *New Phytology* **165**, 351–372.

Ainsworth EA, Rogers A, Nelson R, Long SP (2004) Testing the “Source-Sink” hypothesis in elevated CO₂ in the field with single gene substitutions in *Glycine max*. *Agricultural and Forest Meteorology* **122**, 85-94.

Ainsworth EA, Rogers A (2007) The response of photosynthesis and stomatal conductance to rising [CO₂]: molecular mechanisms and environmental interactions. *Plant Cell and Environment* **30**, 258-270.

Albert KR, Mikkelsen TN, Ro-Poulsen H (2005) Effects of ambient versus reduced UV-B radiation on high arctic *Salix arctica* assessed by measurements and calculations of chlorophyll-a-fluorescence parameters from fluorescence transients. *Physiologia Plantarum* **124**, 208-226.

Allakhverdiev SI, Kreslavski VD, Klimov VV, Los DA, Carpentier R, Prasanna M (2008) Heat stress: an overview of molecular responses in photosynthesis. *Photosynthesis Research* **98**, 541-550.

- Ammerlaan FHM, de Visser AJC (1993)** Effect of CO₂ enrichment on photosynthesis and carbohydrate utilisation: consequences of regrowth of *Lolium perenne*. In: van de Geijn SC, Goudriaan J, Berendse F (Eds) *Agrobiologische Themas 9. Climate Change; Crops and Terrestrial Ecosystems*, CABO-DLO, Wageningen, pp. 1–22.
- Anderson LJ, Maherali H, Johnson HB, Polley HW, Jackson RB. 2001.** Gas exchange and photosynthetic acclimation over sub ambient to elevated CO₂ in a C₃-C₄ grassland. *Global Change Biology* **7**, 693-707.
- Aranjuelo I, Erice G, Norgues S, Morales F, Irigoyen JJ, Sanchez-Diaz M (2008)** The mechanism(s) involved in the photoprotection of PSII at elevated CO₂ in nodulated alfalfa plants. *Environmental Experimental Botany* **64**, 295-306.
- Assmann SM (1999)** The cellular basis of guard cell sensing of rising CO₂. *Plant Cell and Environment* **22**, 629-637.
- Badger MR, Price GD (1994)** The role of carbonic anhydrase in photosynthesis. *Annual Review of Plant Physiology and Plant Molecular Biology* **45**, 369-392.
- Beedlow PA, Tingey DT, Phillips DL, Hogsett WE, Olszyk DM (2004)** Rising atmospheric CO₂ and carbon sequestration in forests. *Frontiers in Ecology and the Environment* **2**, 315-322.
- Bernacchi CJ, Calfapietra C, Davey PA et al. (2003)** Photosynthesis and stomatal conductance responses of poplars to free-air CO₂ enrichment (PopFACE) during the first growing cycle and immediately following coppice. *New Phytologist* **159**, 609–621.
- Bokhari SA, Wan XY, Yang YW, Zhou L, Tang WL, Liu JY (2007)** Proteomic Response of Rice Seedling Leaves to Elevated CO₂ Levels. *Journal of Proteome Research* **6**, 4624–4633.
- Bowes G (1991)** Growth at elevated CO₂: photosynthetic responses mediated through Rubisco. *Plant Cell and Environment* **14**, 795–806.

- Bradford MM (1976)** A rapid and sensitive method for the quantitation of microgram quantities of protein utilizing the principle of protein-dye binding. *Analytical Biochemistry* **72**, 248-254.
- Canadell JG, Pataki D, Gifford R, Houghton RA, Lou Y, Raupach MR, Smith P, Steffen W (2007)** Terrestrial Ecosystems in a Changing World In: Canadell JG, Pataki D, Pitelka L, eds. *International Geosphere–Biosphere Programme Series*. Springer, Berlin.
- Chae L, Sudat S, Dudoit S, Zhu Tand Luan S (2009)** Diverse transcriptional programs associated with environmental stress and hormones in the *arabidopsis* receptor-like kinase gene family. *Molecular Plant* (2009) **2**, 84-107.
- Cheng L, Fuchigami LH (2000)** Rubisco activation state decreases with increasing nitrogen content in apple leaves. *Journal of Experimental Botany* **51**, 1687-1694.
- Clark AJ, Landolt W, Bucher JB, Strasser RJ (2000)** Beech (*Fagus sylvatica*) responses to ozone exposure assessed with a chlorophyll *a* fluorescence performance index. *Environmental Pollution* **110**, 1-7.
- Coleman JR (2000)** Carbonic anhydrase and its role in photosynthesis. In: Leegood RC, Sharkey TD, von Caemmerer S eds. *Photosynthesis: Physiology and metabolism*. The kluwer Academic, Netherlands.
- Crafts-Brandner SJ, Salvucci ME (2000)** Rubisco activase constrains the photosynthetic potential of leaves at high temperature and CO₂. *Proceedings of the National Academy of Science USA* **97**, 13430-13435.
- Davey PA, Olcer H, Zakhleniuk O, Bernacchi CJ, Calfapietra C, Long SP, Raines CA (2006)** Can fast-growing plantation trees escape biochemical down-regulation of photosynthesis when grown throughout their complete production cycle in the open air under elevated carbon dioxide? *Plant Cell and Environment* **29**, 1235–1244.

- DeLucia EH, George K, Hamilton JG (2002)** Radiation-use efficiency of a forest exposed to elevated concentrations of atmospheric carbon dioxide. *Tree Physiology* **22**, 1003–1010.
- Drake BG, Gonzàlez-Meler MA, Long SP (1997)** More efficient plants: a consequence of rising atmospheric CO₂? *Annual Review of Plant Physiology and Molecular Biology* **48**, 609–39.
- Dyson FJ (1977)** Can we control the carbon dioxide in the atmosphere? *Energy* **2**, 287-91.
- Dyson T (2005)** On development, demography and climate change: The end of the world as we know it? *Population and Environment* **27**, 117-149.
- Escobar-Gutiérrez AJ, Combes D, Rakocevic M, de Berranger C, Eprinchard-Ciesla A, Sinoquet H, Varlet-Grancher C (2009)** Functional relationships to estimate morphogenetically active radiation (MAR) from PAR and solar broadband irradiance measurements: the case of a sorghum crop. *Agricultural and Forest Meteorology* **149**, 1244-1253.
- Evans JR, Poorter H (2001)** Photosynthetic acclimation of plants to growth irradiance: the relative importance of specific leaf area and nitrogen in maximizing carbon gain. *Plant Cell and Environment* **24**, 755-767.
- Farquhar GD, Sharkey TD (1982)** Stomatal conductance and photosynthesis. *Annual Reviews in Plant Physiology and Plant Molecular Biology* **33**, 317-345.
- Farquhar GD, von Caemmerer S, Berry JA (1980)** A biochemical model of photosynthetic CO₂ assimilation in leaves of C₃ species. *Planta* **149**, 78-90.
- Flexas J, Ribas-Carbo M, Diaz-Espejo A, Galmés J, Medrano H (2008)** Mesophyll conductance to CO₂: current knowledge and future prospects. *Plant Cell and Environment* **31**, 601–621.

- Fukayama H, Fukuda T, Masumoto C, Taniguchi Y, Sakai H, Cheng W, Hasegawa T, Miyao M (2009)** Rice plant response to long term CO₂ enrichment: Gene expression profiling. *Plant Science* **177**, 203–210.
- Geider RJ, DeLucia EH, Falkowski PG et al. (2001)** Primary productivity of planet earth: biological determinants and physical constraints in terrestrial and aquatic habitats. *Global Change Biology*, **7**, 849–882.
- Greenep H, Turnbull MH, Whitehead D (2003)** Response of photosynthesis in second-generation *Pinus radiata* trees to long-term exposure to elevated carbon dioxide partial pressure. *Tree Physiology* **23**, 569–576.
- Griffin TJ, Aebersold R (2001)** Advances in proteome analysis by mass spectrometry. *Journal Biological Chemistry* **276**, 45497–45500.
- Gunderson CA, Sholtis JD, Wullschleger SD, Tissue DT, Hanson PJ, Norby RJ (2002)** Environmental and stomatal control of photosynthetic enhancement in the canopy of a sweetgum (*Liquidambar styraciflua* L.) plantation during 3 years of CO₂ enrichment. *Plant, Cell and Environment*, **25**, 379–393.
- Gunderson CA, Wullschleger SD (1994)** Photosynthetic acclimation in trees to rising atmospheric CO₂: a broader perspective. *Photosynthesis Research* **39**, 369–388.
- Gutteridge S, Gatenby AA (1987)** The molecular analysis of the assembly, structure and function of Rubisco. In: Mifflin BJ, eds. *Oxford Surveys of Plant Molecular and Cell Biology*. Oxford University Press, Oxford.
- Herrick JD, Maherali H, Thomas RB (2004)** Reduced stomatal conductance in sweet gum (*Liquidambar styraciflua*) sustained over long-term CO₂ enrichment. *New Phytologist* **162**, 387–396.

- Herrick JD, Thomas RB (2001)** No photosynthetic down-regulation in sweet gum trees (*Liquidambar styraciflua* L.) after three years of CO₂ enrichment at Duke Forest FACE experiment. *Plant Cell and Environment* **24**, 53-64.
- Hetherington AM, Woodward FI (2003)** The role of stomata in sensing and driving environmental change. *Nature* **424**, 901–908.
- Hoang CV, Chapman KD (2002)** Biochemical and molecular Inhibition of plastidial carbonic anhydrase reduces the incorporation of acetate into lipids in cotton embryos and tobacco cell suspensions and leaves *Plant Physiology* **128**, 1417 - 1427.
- Hodge JE, Hofreiter BT (1962)** In: Whistler RL and Be Miller JN, eds. *Methods in carbohydrate chemistry*. Academic Press, New York.
- Huber SC (1981)** Interspecific variation in the activity and regulation of leaf sucrose phosphate synthase. *Plant Physiology* **102**, 443-450.
- Hunt SMN, Thomas MR, Sebastian LT, Pedersen SK, Harcourt RL, Sloane AJ, Wilkins MR (2005)** Optimal Replication and the Importance of Experimental Design for Gel-Based Quantitative Proteomics. *Journal of Proteome Research* **4**, 809-819.
- Hymus GJ, Baker NR, Long SP (2001)** Growth in elevated CO₂ can both increase and decrease photochemistry and photoinhibition of photosynthesis in a predictable manner. *Dactylis glomerata* growth in two levels of nitrogen nutrition. *Plant Physiology* **127**, 1204-1211.
- Hymus GJ, Ellsworth DS, Baker NR, Long SP (1999)** Does free-air carbon dioxide enrichment (FACE) affect photochemical energy use by evergreen trees in different seasons? A chlorophyll fluorescence study of mature loblolly pine. *Plant Physiology* **120**, 1183-1191.
- Intergovernmental Panel on Climate Change (IPCC) (2007)** In: Metz B, Davidson OR, Bosch PR, Dave R, Meyer LA, Eds. *Climate Change Mitigation. Contribution of Working*

Group III to the Fourth Assessment Report of the Intergovernmental Panel on Climate Change. Cambridge University Press, Cambridge, United Kingdom and New York, USA.

Intergovernmental Panel on Climate Change (IPCC) (2000) In: Watson R, Noble IR, Bolin B, Ravindranath NH, Verardo DJ, Dokken DJ, Eds. *Land use, Land-use Change, and Forestry: A Special Report*. Cambridge University Press, Cambridge, UK.

Intergovernmental Panel on Climate Change (IPCC) (2001) In: McCarthy JJ, Canziani OF, Leary NA, Dokken DJ, White KS, Eds. *Impacts, Adaptations and Vulnerability. Contribution of Working Group II to the Third Assessment Report of the Intergovernmental Panel on Climate Change*. Cambridge University Press, Cambridge, UK and New York, USA.

Jana KB, Biswas S, Majumder M, Roy PK, Mazumdar A (2009) Carbon sequestration rate and aboveground biomass carbon potential of four young species. *Journal of Ecology and the Natural Environment* **1**, 015–024.

Jensen RG (2000) Activation of Rubisco regulates photosynthesis at high temperature and CO₂. *Proceedings of the National Academy of Sciences USA* **97**: 12937-12938.

Jorge I, Navarro- Cerrillo RM, Lenz C, Ariza D, Porras C, Jorriin J (2005) The Holm Oak leaf proteome: Analytical and biological variability in the protein expression level assessed by 2-DE and protein identification tandem mass spectrometry de novo sequencing and sequence similarity searching. *Proteomics* **5**, 222- 234.

Jorge I, Navarro-Cerrillo RM, Lenz C, Ariza D, Jorriin J (2006) Variation in the holm oak leaf proteome at different plant developmental stages, between provenances and in response to drought stress. *Proteomics* **6**: S207-S214.

Kautsky H, Hirsch A (1931) *Neue Versuche Zur Kohlensäureassimilation* **48**, 964.

Kitajima K, Hogan KP (2003) Increases of chlorophyll a/b ratios during acclimation of tropical woody seedlings to nitrogen limitation and high light. *Plant Cell and Environment* **26**, 857-865.

- Körner C (2003)** Carbon limitation in trees. *Journal of Ecology* **91**, 4–17.
- Korner C (2006)** Plant CO₂ responses: an issue of definition, time and resource supply. *New phytologist* **172**, 393-411.
- Lazova GN, Naidenova T, Velinova K (2004)** Carbonic anhydrase activity and photosynthetic rate in the tree species *Paulownia tomentosa* Steud. effect of dimethylsulfoxide treatment and zinc accumulation in leaves. *Journal of Plant Physiology* **161**, 295-301.
- Leakey ADB, Xu F, Gillespiea KM, McGratha JM, Ainsworth EA, Ort DR (2009).** Genomic basis for stimulated respiration by plants growing under elevated carbon dioxide. *Proceedings of the National Academy of Sciences USA* **106**, 3597-3602.
- Lee SK, Jeon JS, Bornke F, Voll L, Cho JI, Goh CH, Jeong SW, Park YI, et al. (2008)** Loss of cytosolic fructose-1,6-bisphosphase limits photosynthetic sucrose synthesis and causes severe growth retardations in rice (*Oryza sativa*). *Plant Cell and Environment* **31**, 1851-1863.
- Lemus R, Lal R (2005)** Bioenergy crops and carbon sequestration. *Critical Reviews in Plant Sciences* **24**, 1-21.
- Li B, Wei A, Song C, Li N, Zhang J (2008)** Heterologous expression of the *TsVP* gene improves the drought resistance of maize. *Plant Biotechnology Journal* **6**, 146–159.
- Li MH, Xiao WF, Shi P, Wang SG, Zhong YD, Liu XL, Wang XD, Cai XH, Shi ZM (2008)** Nitrogen and carbon source–sink relationships in trees at the Himalayan tree lines compared with lower elevations. *Plant, Cell and Environment* **31**, 1377–1387.
- Li X, Hou J, Bai K, Yang X, Lin J, Li Z, Kuang T (2004)** Activity and distribution of carbonic anhydrase in leaf and ear parts of wheat (*Triticum aestivum* L.) *Plant Science* **166**, 627-632.
- Liska AJ, Shevchenko A (2003)** Expanding the organismal scope of proteomics: cross-species protein identification by mass spectrometry and its implications. *Proteomics* **3**, 19-28.

- Liu SR, Barton C, Lee H, Jarvis PG, Durrant D (2002)** Long-term response of Sitka spruce (*Picea sitchensis* (Bong.) to CO₂ enrichment and nitrogen supply. Growth, biomass allocation and physiology. *Plant Biosystems* **136**, 189-198.
- Logothetis K, Dakanali S, Ioannidis N, Kotzabasis K (2004)** The impact of high CO₂ concentrations on the structure and function of photosynthetic apparatus and the role of polyamines. *Journal of Plant Physiology* **161** 715–724.
- Long SP, Ainsworth EA, Rogers A, Ort DR (2004)** Rising atmospheric carbon dioxide: plants face the future. *Annual Review of Plant Biology* **55**, 591–628.
- Ma CC, Gao YB, Guo HY, Wang JL (2004)** Photosynthesis, transpiration and water use efficiency of *Caragana microphylla*, *C. intermedia* and *C. korshinskii*. *Photosynthetica* **42**, 65-70.
- Maherali H, Reid CD, Polley HW, Johnson HB, Jackson RB (2002)** Stomatal acclimation over a subambient to elevated CO₂ gradient in C₃/C₄ grassland. *Plant Cell and Environment* **25**, 557-566.
- Majeau N, Coleman JR (1996)** Effect of CO₂ concentration on carbonic anhydrase and ribulose-1,5-bisphosphate carboxylase/oxygenase expression in pea. *Plant Physiology* **112**, 569–574.
- Makino A, Mae T (1999)** Photosynthesis and plant growth at elevated levels of CO₂. *Plant and Cell Physiology* **40**, 999–1006.
- Malone S, Mayeux H, Johnson H, Polly H (1993)** Stomatal density and aperture length in four plant species grown in subambient CO₂ gradient. *American Journal of Botany* **80**, 1413-1418.
- Mann K, Olsen JV, Maček B, Gnad F, Mann M (2007)** Identification of new chicken egg proteins by mass spectrometry-based proteomic analysis. *Proteomics* **16**, 209-218.
- Martinez-Barajas E, Randall DD (1998)** Purification and characterization of fructokinases from developing tomato (*Lycopersicon esculentum* Mill.) fruits. *Planta* **199**, 451-458.

- Maxwell K, Johnson GN (2000)** Chlorophyll fluorescence-a practical guide. *Journal of Experimental Botany* **51**, 659-668.
- Mehta P, Jajoo A, Mathur S, Bharti S (2009)** Chlorophyll *a* fluorescence study revealing effects of high salt stress on Photosystem II in wheat leaves. *Plant Physiology and Biochemistry* **48**, 16-20.
- Messinger SM, Buckley TN and Mott KA (2006)** Evidence for the involvement of photosynthetic process in the stomatal responses to CO₂. *Plant Physiology* **140**, 771-778.
- Nakano H, Makino A, Mae T (1997)** The effect of elevated partial pressures of CO₂ on the relationship between photosynthetic capacity and N content in rice leaves, *Plant Physiology* **115**, 191–198.
- Negi JDS, Manhas RK, Chauhan PS (2003)** Carbon allocation in different components of some tree species of India: A new approach for carbon estimation. *Current Science* **85**, 101-104.
- Newbould PJ (1967)** Methods for estimating the primary production of forests. IBP Handbook No. 2. International Biological Programme, Oxford.
- Noormets A, Sôber A, Pell EJ, Dickson RE, Podila GK, Sôber J, Isebrands JG, Karnosky DF (2001)** Stomatal and non-stomatal limitation to photosynthesis in two trembling aspen (*Populus tremuloides* Michx.) clones exposed to elevated CO₂ and/or O₃. *Plant Cell and Environment* **24**, 327 – 336.
- Norby RJ, Todd DE, Fults J, Johnson DW (2001)** Allometric determination of tree growth in a CO₂-enriched sweetgum stand. *New Phytologist* **150**, 477-487.
- Nowak DJ, Crane DE (2002)** The urban forest effects (UFORE) model: Quantifying urban forest structure and functions. In: *Proceedings of the 2nd international Symposium on Integrated Tools for Natural Resources Inventories in the 21st Century*. Gen. Tech. Rep. NC-212, USDA Forest Service, North Central Forest Experiment Station, St. Paul, MN.

- Oquist G, Huner NPA (1993)** Cold-hardening-induced resistance to photoinhibition of photosynthesis in winter rye is dependent upon an increased capacity for photosynthesis. *Planta* **189**, 150–156.
- Oren R, Ellsworth DS, Johnsen KH. et al. (2001)** Soil fertility limits carbon sequestration by forest ecosystems in a CO₂-enriched atmosphere. *Nature* **411**, 469–472.
- Oren R, Ellsworth DS, Johnsen KH, Phillips N, Ewers BE, Maier C, Schäfer KVR, McCarthy H, Hendrey G, McNulty SG, Katul GG (2001)** Soil fertility limits carbon sequestration by forest ecosystems in a CO₂-enriched atmosphere. *Nature* **411**, 469–472.
- Paoletti E, Grulke NE (2005)** Does living in elevated CO₂ ameliorate tree response to ozone? A review on stomatal responses. *Environmental Pollution* **137**, 483–493.
- Pastenes C, Santa-Maria E, Infante R, Franck N (2003)** Domestication of the Chilean guava (*Ugni molinae* Turcz.) a forest understorey shrub, must consider light intensity. *Scientia Horticulturae* **98**, 71–84.
- Patterson BD, Atkins CA, Graham D, Wills RBH (1971)** Carbonic anhydrase A new method of detection on polyacrylamide gels using low-temperature fluorescence. *Analytical Chemistry* **44**, 388–391.
- Pego JV, Kortstee AJ, Huijser G, Smeekens SGM (2000)** Photosynthesis, sugars and the regulation of gene expression. *Journal of Experimental Botany* **51**, 407–416.
- Porra RJ, Thompson WA, Kriedelman PE (1989)** Determination of accurate extraction and simultaneously equation for assaying chlorophyll a and b extracted with different solvents: verification of the concentration of chlorophyll standards by atomic absorption spectroscopy, *Biochimica et Biophysica Acta* **975**, 384–394.
- Portis AR Jr. (2003)** Rubisco activase- Rubisco's catalytic chaperone. *Photosynthesis Research* **75**, 11–27.

- Possell M, Hewitt CN (2009)** Gas exchange and photosynthetic performance of the tropical tree *Acacia nigrescens* when grown in different CO₂ concentrations. *Planta* **229**, 837-846.
- Prentice IC, Farquhar GD, Fasham MJR, Goulden ML, Heimann M, Jaramillo VJ, Kheshgi HS, LeQuere C, Scholes RJ, Wallace DWR, et al. (2001)** The carbon cycle atmospheric carbon dioxide. In: Houghton JT, Ding Y, Griggs DJ, Noguer M, Van der Linder PJ, Dai X, Maskell K, Johnson CA, eds. *Climate Change 2001: The Scientific Basis. Contributions of Working Group I to the Third Assessment Report of the Intergovernmental Panel on Climate Change*. New York: Cambridge University Press.
- Radford PJ (1967)** Growth analysis formulae - their use and abuse. *Crop Science* **7**, 171-175.
- Rajput SS, Shukla NK, Gupta VK, Jain JD (1996)** "Timber Mechanics: Strength Classification and Grading of Timber". *ICFRE-Publication-38, New Forest*, Dehradun.
- Rey A, Jarvis PG (1998)** Long-term photosynthetic acclimation to increased atmospheric CO₂ concentration in young birch (*Betula pendula*) trees. *Tree Physiology* **18**, 441-450.
- Reynolds JF, Kemp PR, Acock B, Chen JL, Moorhead DL (1996)** Progress, limitations and challenges in modeling the effects of elevated CO₂ on plants and ecosystems. In: Koch GW and Mooney HA eds. *Carbon dioxide and terrestrial ecosystems*. Academic Press, New York, USA.
- Rogers A, Ellsworth DS (2002)** Photosynthetic acclimation of *Pinus taeda* (loblolly pine) to long-term growth in elevated pCO₂ (FACE). *Plant Cell and Environment* **25**, 851-858.
- Ruebelt MC, Lipp M, Reynolds TL, Schmuke JJ, Astwood JD, DellaPenna D (2006)** Application of two-dimensional gel electrophoresis to interrogate alterations in the proteome of genetically modified crops, 3-Assessing unintended effects. *Journal of Agriculture and Food Chemistry* **54**, 2169-2177.
- Sage RF (2002)** How terrestrial organisms sense, signal and respond to carbondioxide. *Integrative and Comparative Biology* **42**: 469-480.

- Sage RF (1994)** Acclimation of photosynthesis to increasing atmospheric CO₂; the gas exchange perspective. *Photosynthesis Research* **39**, 351--368.
- Saravanan RS, Rose JKC (2004)** A critical evaluation of sample extraction techniques for enhanced proteomic analysis of recalcitrant plant tissues. *Proteomics* **4**, 2522-2532.
- Schapendonk Ad HCM, van Oijen M, Dijkstra P, Pot CS, Jordi WJRM, Stoopen GM. (2000)** Effects of elevated CO₂ concentration on photosynthetic acclimation and productivity of two potato cultivars in open-top chambers. *Australian Journal of Plant Physiology* **27**, 1119-1130.
- Schlesinger W, Lichter J (2001)** Limited carbon storage in soil litter of experimental forest plots under increased atmospheric CO₂. *Nature* **411**, 466-469.
- Senthil kumar D, Wood TD, Nagarajan P, Rabin RA (2007)** Evaluating peptide mass fingerprinting-based protein identification. *Genomics Proteomics and Bioinformatics* **5**: 3-4.
- Sholtis JD, Gunderson CA, Norby RJ, Tissue DT (2004)** Persistent stimulation of photosynthesis by elevated CO₂ in a sweetgum (*Liquidambar styraciflua* L.) forest stand. *New Phytologist* **162**, 343-354.
- Shulaev V, Cortes D, Miller G, Mittler R (2008)** Metabolomics for plant stress response. *Physiologia Plantarum* **132**, 199–208.
- Sicher RC, Kremer DF, Rodermeier SR (1994)** Photosynthetic acclimation to elevated CO₂ occurs in transformed tobacco with decreased ribulose-1,5-bisphosphate carboxylase/oxygenase content. *Plant Physiology* **104**, 409–415.
- Solomon S, Qin D, Manning RB et al. (2007)** Technical summary. In: Solomon S, Qin D, Manning M, Chen Z, Marquis M, Averyt KB, Tignor M, Miller HL, eds. *Climate Change 2007: The Physical Science Basis. Contribution of Working Group I to the Fourth Annual Assessment Report of the Intergovernmental Panel on Climate Change*. Cambridge, UK/New York, NY, USA: Cambridge University Press.

- Špunda V, Kallian J, Urban O, Luis VC, Sibisse I, Puértolas J, Šprtova M, Marek MV, (2005)** Diurnal dynamics of photosynthetic parameters of Norway spruce trees cultivated under ambient and elevated CO₂: the reasons of midday depression in CO₂ assimilation. *Plant Science* **168**, 1371-1381.
- Stitt M (1991)** Rising CO₂ levels and their potential significance for carbon flow in photosynthetic cells. *Plant Cell and Environment* **14**, 741–762.
- Strasser BJ, Strasser RJ (1995)** Measuring fast fluorescence transients to address environment questions: the JIP-test, In: P. Mathis, eds. *Photosynthesis: from Light to Biosphere*, Kluwer Academic, Dordrecht-Boston –London.
- Strasser RJ, Govindjee (1992)** The *F_o* and O-J-I-P fluorescence rise in higher plants and algae, In: Argyroudi-Akoyunoglou JH, eds. *Regulation of Chloroplast Biogenesis*, Plenum Press, New York.
- Strasser RJ, Tsimilli-Micheal M, Srivastava A (2000)** The fluorescence transient as a tool to characterize and screen photosynthetic samples, In: M. Yunus, U. Pathre, P. Mohanty, eds. *Probing Photosynthesis: Mechanisms, Regulation and Adaptation*. Taylor & Francis, London.
- Streck C, Scholz SM (2006)** The role of forests in global climate change: whence we come and where we go. *International Affairs* **82**, 861-879.
- Stylinski CD, Oechel WC, Gamon JA, Tissue DT, Miglietta F, Raschi A (2000)** Effects of lifelong CO₂ enrichment on carboxylation and light utilization of *Quercus pubescens* Wild. examined with gas exchange, biochemistry and optical techniques. *Plant cell and environment* **23**, 1353-1362.
- Swamy SL, Mishra A, Puri S (2003)** Biomass production and root distribution of *Gmelina arborea* under an agrisilviculture system in sub-humid tropics of Central India. *New Forests* **26**, 167-186.

- Upriety DC, Sunita K, Neeta D, Rajat M (2000)** Effect of elevated CO₂ on growth and yield of rice. *Indian Journal of Plant Physiology* **5**, 11-16.
- Upriety DC, Dwivedi N, Jain V, Mohan R (2002)** Effect of elevated carbon dioxide concentration on the stomatal parameters of rice cultivars. *Photosynthetica* **40**, 315-319.
- Upriety DC, Garg SC, Bisht BS, Maini HK, Dwivedi N, Paswan G, Raj A, Saxena DC (2006)** Carbon dioxide enrichment technologies for crop response studies. *Journal of Scientific and Industrial Research* **65**, 859-866.
- Valledor L, Castillejo MA, Lenz C, Rodriguez R, Canal MJ, Jorriin J (2008)** Proteomic analysis of *Pinus radiata* Needles: 2-DE Map and protein identification by LC/MS/MS and substitution-tolerant database searching. *Journal of Proteome Research* **7**, 2616-2631.
- van Heerden PDR, Strasser RJ, Krüger GHJ (2004)** Reduction of dark chilling stress in N₂-fixing soybean by nitrate as indicated by chlorophyll *a* fluorescence kinetics, *Physiologia Plantarum* **121**, 239-249.
- Van Oosten JJ, Besford RT (1994)** Sugar feeding mimics effect of acclimation to high CO₂: rapid downregulation of RuBisCO small subunit transcripts, but not of the large subunit transcripts. *Journal of Plant Physiology* **143**, 306-312.
- Victoria EW, Bernacchi CJ, Zhu XZ, Calfapietra C, Ceulemans R, Deangelis P, Gielens B, Miglietta F, Morgan PB, Long SP (2005)** Gross primary production is stimulated for three *Populus* species grown under free-air CO₂ enrichment from planting through canopy closure. *Global Change Biology* **11**, 644-656.
- von Caemmerer S, Farquhar GD (1981)** Some relationships between the biochemistry of photosynthesis and the gas exchange of leaves. *Planta* **153**, 376-387.
- von Caemmerer S, Quick PW (2000)** Rubisco, physiology *in vivo*. In: Leegood RC, Sharkey TD, von Caemmerer S, eds. *Photosynthesis: Physiology and Metabolism*. Kluwer Academic Publishers, Dordrecht, The Netherlands.

- Vu JCV, Gesch RW, Pennanen AH, Allen Jr LH, Boote KJ, Bowes G (2001)** Soybean photosynthesis, Rubisco, and carbohydrate enzymes function at supra optimal temperatures in elevated CO₂. *Journal of Plant Physiology* **158**, 295–307.
- Wang KY, Kellomaki S, Li C, Zha T (2003)** Light and water-use efficiencies of pine shoots exposed to elevated carbon dioxide and temperature. *Annals of Botany* **92**, 53-64.
- Wang X, Li X, Li Y (2007)** A modified coomassie brilliant blue staining method at nanogram sensitivity compatible with proteomic analysis. *Biotechnology Letters* **29**, 1599-1603.
- Warren CR, Adams MA (2004)** Evergreen trees do not maximize instantaneous photosynthesis. *Trends in Plant Science* **9**, 270-274.
- Watson BS, Asirvatham VS, Wang L, Sumner LW (2003)** Mapping the proteome of barrel medic (*Medicago truncatula*). *Plant Physiology* **131**, 1104-1123.
- Webber AN, Nie GY, Long SP (1994)** Acclimation of photosynthetic proteins to rising atmospheric CO₂. *Photosynthesis Research* **39**, 413-425.
- Werner C, Motyka V, Laucou V, Smets R, Van Onckelen H, Schmulling T (2003)** Cytokinin-deficient transgenic Arabidopsis plants show multiple developmental alterations indicating opposite functions of cytokinins in the regulation of shoot and root meristem activity. *Plant Cell* **15**, 2532-2550.
- Wilbur KM, Anderson NG (1948)** Electrometric and colorimetric determination of carbonic anhydrase. *Journal of Biological Chemistry* **176**, 147-154.
- Winjum JK, Lewis DK (1993)** Forest management and the economics of carbon storage: the nonfinancial component. *Climate Research* **3**, 111-119.
- Wolfe DW, Gifford RM, Hilbert D, Luo Y (1998)** Integration of photosynthetic acclimation to CO₂ at the whole-plant level. *Global Change Biology* **4**, 879–893.
- Yates JR (2000)** Mass spectrometry. From genomics to proteomics. *Trends in Genetics* **16**, 58-60.

Zimmerman G, Kelly GE, Latzko E (1978) Purification and properties of spinach leaf cytoplasmic fructose 1,6-bisphosphatase. *Journal of Biological Chemistry* **253**, 5952-5956.

Appendix

List of publications

Research papers published

Girish Kumar Rasineni Madhurarekha Chinnaboina Attipalli Ramachandra Reddy (2010) Proteomic approach to study leaf proteins in a fast-growing tree species, *Gmelina arborea* Linn. Roxb. *Trees* 24:129–138.

Attipalli R. Reddy, **Girish Kumar Rasineni**, Agepati S. Raghavendra (2010) The impact of global elevated CO₂ concentration on photosynthesis and plant productivity. *Current Science* 99:46-57.

Anirban Guha, **Girish Kumar Rasineni** and Attipalli R. Reddy (2010) Drought tolerance in mulberry (*Morus* Spp.): A physiological approach with insights into growth dynamics and leaf yield production. *Experimental Agriculture* 46: 1-18.

Anirban Guha, Debashree Sengupta, **Girish Kumar Rasineni**, Attipalli Ramachandra Reddy (2010) An integrated diagnostic approach to understand drought tolerance in mulberry (*Morus indica* L.) *Flora* 205:144-151.

Girish Kumar Rasineni, Dayananda Siddavattam, Attipalli R Reddy (2009) Free radical quenching activity and polyphenols in three *Coleus* species. *Journal of Medicinal Plants Research* 10:285-291.

Kolluru Viswanatha Chaitanya, **Girish Kumar Rasineni**, Attipalli Ramachandra Reddy (2009) Drought stress-induced proline metabolism in different mulberry (*Morus alba*.L) cultivars *Acta Physiologiae Plantarum* 31:437-443.

K. Sumithra, **Girish Kumar Rasineni** and Attipalli R. Reddy (2007) Photosynthesis and Antioxidative Metabolism in Cow Pea Grown under Varying Water Deficit Regimes *Journal of Plant Biology* 34:57-65.
